LASER SPECTROSCOPY: TDLAS INSTRUMENTATION AND NIR ANALYSIS OF SOME ORGANIC MATERIALS

Thesis Submitted to
Cochin University of Science and Technology
for the award of the degree of
DOCTOR OF PHILOSOPHY

BY
Shibu M Eappen

Department of Physics
Cochin University of Science and Technology
Cochin 682 022 India.

April 2003

Not on my merits… but on His grace…

Dedicated to my parents and brother……

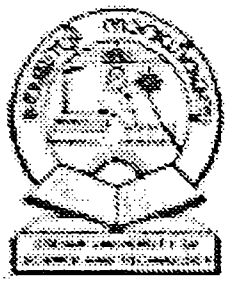

Department of Physics
Cochin University of Science and Technology
Cochin 682 022

CERTIFICATE

Certified that the work presented in this thesis entitled " Laser Spectroscopy: TDLAS instrumentation and NIR analysis of some organic materials" is based on the bonafide research work done by Mr. Shibu M Eappen under my guidance in the Department of Physics Cochin University of Science and Technology Cochin 682 022, and has not been included in any other thesis submitted previously for the award of any degree.

K.P Rajappan Nair

Cochin- 22

4-04-03

Prof. K.P Rajappan Nair

(Supervising guide)

DECLARATION

Certified that the work presented in this thesis entitled " **Laser Spectroscopy: TDLAS instrumentation and NIR analysis of some organic materials**" is based on the original work done by me under the guidance of Prof. K.P Rajappan Nair Dean Faculty of Science, Cochin University of Science and Technology, Cochin 682 022, and has not been included in any other thesis submitted previously for the award of any degree.

Cochin- 22

04-04-03

Shibu M Eappen

Acknowledgement

Cusat has been a profound experience. I feel I am at the end of my epic journey. Through out this endeavor number of people have impacted my life, adding richness, flavor and often meaning to education. To all those people I offer my deepest thanks.

With great pleasure I express my deepest gratitude to my guide Dr. K.P.Rajappan Nair, Dean Faculty of sciences Cochin University of science and technology for his excellent guidance and constant encouragement.

My sincere thanks are not less to Dr. T.M Abdul Rasheed, Reader, Dept. of Physics, Cochin University of science and technology for his valuable suggestions and directions during this course of work.

I am thankful to Prof K.P Vijay Kumar, Head, Dept. of Physics, Cochin University of Science and Technology and Prof. M. Sabir, Prof. Elizabeth Mathai former Heads of the department and Dr. M.K Jayaraj for providing the necessary facilities. And I thank all the teaching and non-teaching staff of the Dept. of physics for their sincere co-operation.

I have had a wonderful fortune of sharing lab space with very talented people. My first couple of years overlapping with Mr. Shaji. S helped expedite my progress on an initially imposing apparatus. After a year Ms. Jyotsna Ravi joined our two men army. Her enthusiasm and shrewdness helped in developing the lab and her acumen always kept the atmosphere lively. It is said that a common motivation for teaching is desire to touch people's lives. I felt it myself during these years when I did work along with Mr. Sunny Kuriakose, Mr. K.K Vijayan, Mr. Thomas P Zacharia, Mrs. Syamala Kumari, Ms. T Nandini, Mrs. Usha John and. Mr. K Ravindranath. I remember all the M.Sc project students, Sudheer, Manju, Dinish, Rajmohan, Vinod, Pramod,

Denny Mathew, V. Pai, Shanavas and Lekshmi who extended their sincere help to me.

I thank Ms. Bindu .K, Mr. Thomas Lee, Mr. S. Saravanan, Mr. Sebu Thomas, Mr. Anish kumar, Mr. Vinod Kumar P.P, Mr. Aldrin Antony and Mr. Manoj R for their timely help and I acknowledge all my contemporary research scholars who offered their help for the successful completion my work.

I thankfully acknowledge the financial assistance from Department of Science and Technology (DST) Govt. of India and CUSAT, and I would like to acknowledge the helps offered by the staff of USIC during the fabrication of our setup.

Thanks are due to Prof. H.P Rudolph, University of Ulm, Germany for allowing my supervisor for recording the microwave spectra in his stark modulated microwave spectrometer and I thank Prof. V Unükrishnan Nayar, Kerala University, for helping us to record the laser Raman spectrum

I would like to note my thanks to my bosom friends Anil and Alex who are "always there"

Shibu

CONTENTS

Preface

Tunable diode laser absorption spectroscopy (TDLAS) is a highly selective and versatile technique for measuring many trace atmospheric constituents with detection sensitivities in the sub-parts-per-billion (ppbv) concentration range. Because of the versatility, selectivity, and sensitivity of TDLAS, numerous laboratory, ground-based, aircraft, and balloon-borne studies employ this technique.

Near-infrared spectroscopy can be a workhorse technique for materials analysis in industries such as agriculture, pharmaceuticals, chemicals and polymers. A near-infrared spectrum represents combination bands and overtone bands that are harmonics of absorption frequencies in the mid-infrared. Near-infrared absorption includes a combination-band region immediately adjacent to the mid-infrared and three overtone regions.

All four near-infrared regions contain "echoes" of the fundamental mid-infrared absorptions. For example, vibrations in the mid-infrared due to the C-H stretches will produce four distinct bands in each of the overtone and combination regions. As the bands become more removed from the fundamental frequencies they become more widely separated from their neighbors, more broadened and are dramatically reduced in intensity. Because near-infrared bands are much less intense, more of the sample can be used to produce a spectra and with near-infrared, sample preparation activities are greatly reduced or eliminated so more of the sample can be utilized. In addition, long path lengths and the ability to sample through glass in the near-infrared allows samples to be measured in common media such as culture tubes, cuvettes and reaction bottles. This is unlike mid-infrared where very small amounts of a sample produce a strong spectrum; thus sample preparation techniques must be employed to limit the amount of the sample that interacts with the beam.

In the present work we describe the successful the fabrication and calibration of a linear high resolution linear spectrometer using tunable diode laser and a 36 m path length cell and measurement of a highly resolved structure of OH group in

methanol in the transition region $\Delta v = 3$. We then analyse the NIR spectrum of certain aromatic molecules and study the substituent effects using local mode theory. The whole work is described in six chapters as discussed below.

Chapter I gives a brief review of the area of laser spectroscopy, giving a general introduction and recent trends in the same field. The laser light, first generated about forty years ago, has now become an important tool in various fields of science and technology. The area of spectroscopy is most benefited from the developments in the field of lasers. Most of the methods of atomic and molecular spectroscopy require that the laser radiation frequency coincide with the frequency of a definite quantum transition between two energy levels of the atom or molecule. The revolutionary influence of the laser on optical spectroscopy is based on a combination of unique characteristics of laser radiation such as high power density, high monochromaticity and tunability.

Chapter II describes the successful setting up and calibration of a high-resolution spectrometer using a commercial near infrared tunable diode laser as the source, a 32-meter multipass cell as the sample holder and a solid state balanced detector. The chapter further demonstrates the utility of this spectrometer in recording the second overtone band of the -OH group in methanol molecule, where the highly resolved rotational structure of P, Q and R branches were identified.

Chapter III discusses an outline of the local mode theory, which has been used as a tool to analyze the vibrational overtone transitions in molecules containing X-H oscillators (X=C, N, O....) in the NIR and visible spectral range.

Chapter IV and V discuss in detail The NIR overtone spectroscopic analysis using local mode model, with emphasis on substituent effects, in ortho and meta isomers of chlorotoluene, meta and para isomers of fluorotoluene, ortho, meta and para isomers of

nitrotoluene, ortho, meta and para isomers of hydroxytoluene (cresols or methylphenol), and 1- hydroxynaphthalene.

Chapter VI gives a comparative analysis of the laser Raman and microwave spectral analysis of o-chlorotoluene. The low-lying vibrational levels were identified using the laser Raman technique.

The summary and conclusions of the present study are given towards the end of the thesis.

CHAPTER I

Laser Spectroscopy an Overview

1.1 Introduction

The lasers created a quarter of century ago have received much recognition today in various fields of Science and Technology [1]. The application of laser light has proved unexpectedly successful in the field of medicine, material processing, isotope separation etc. In conventional fields such as spectroscopy meteorology and photochemistry, the use of laser is found to be very promising from the beginning. Most of the methods of atomic and molecular spectroscopy except Raman spectroscopy require that the laser radiation frequency should coincide with the frequency of a definite quantum transition between two energy levels of the atom or molecule. But the first pulsed and continuous wave lasers operated at a limited number of discreet frequencies of visible and NIR ranges. Late in the 1960s various methods of generating coherent light with a tunable frequency began to develop rapidly [2-12].

Lasers are line sources that emit high-intensity electromagnetic radiation over a very narrow frequency range. Typically, light from a tunable laser (such as a dye laser, semiconductor diode laser, or free-electron laser) is directed into the sample under study just as the more traditional light sources are used in absorption or emission spectroscopy. For example, in fluorescence emission spectroscopy, the frequency and amount of light scattered by the sample is measured as the frequency of the laser light is varied. There are many advantages to using a laser as a light source: (1) the light from

lasers are highly monochromatic. As the light is tuned across the frequency range of interest and the absorbance or fluorescence is digitized, extremely narrow spectral features can be measured. Modern tunable lasers can easily resolve spectral features less than 1 million hertz wide, while the highest-resolution grating spectrometers have resolutions that are hundreds of times worse. Atomic lines as narrow as 30 hertz out of a transition frequency of 6×10^{14} hertz have been observed with laser spectroscopy (2) because the laser light in a given narrow frequency band is much more intense than virtually all broadband sources of light used in spectroscopy, the amount of fluorescent light emitted by the sample can be greatly increased. Laser spectroscopy is sufficiently sensitive to observe fluorescence from a single atom in the presence of 1×10^{20} different atoms.

The resolution of classical methods of atomic and molecular spectroscopy in the gas phase was usually limited by the instrumental resolution of the spectrometer. Tunable lasers with narrow radiation line particularly injection IR lasers and dye Lasers in the visible region have realized the ultimate spectral resolution of linear spectroscopy which is determined by the real absorption spectrum of the sample without any external influence by the spectral instrument. [9-11,13].

The high monochromaticity has made it possible to elaborate quite new methods of Doppler free non-linear spectroscopy of atoms and molecules in the gas phase [14-15]. The creation of ultra short pulse laser which employ the effect of synchronization of a great number of modes of wide spectral range laser has culminated in rapid

progress in methods of laser Pico second resolution spectroscopy [16]. Later further progress has been made in generating sub pico-second pulses [17].

The development of tunable lasers and its use in spectroscopy has materially increased the sensitivity of all known methods of spectroscopy both for atoms and molecules. Quite new methods have been developed like multistep photoionization of atoms and molecules [18], intra cavity absorption [19] and coherent antistokes Raman scattering [20,21].

In analyzing a real sample selectivity is also of critical importance. That is the ability to detect the presence of atoms or molecules of definite sort in mixtures. The use of laser radiation made it possible in some cases to simplify the optical spectra of molecules for example the fluorescence spectra of molecules in low temperature matrix. [22] and has increased the selectivity of analysis.

Laser beam can induce fluorescence or scattering in a remote region thus the application of laser to study the composition of matter of non-radiative objects has been developed [23-25]. The spatial coherence of laser radiation enables it to be focused onto an area with minimum dimensions of the order of light wavelengths. This property has formed the basis for micro-spectral emission analysis of atoms [26] and local mass spectral analysis of molecule [27]. The use of laser pulse in micro sample spectral analysis was demonstrated soon after the advent of laser [28].

In the regions of a spectrum where a tunable laser is available it may be practicable to use it in the way that a tunable klystron or backward wave oscillator is

used in the microwave or millimeter wave spectroscopy. Attenuation of the source radiation as a function of frequency produces the absorption spectrum. This technique is employed with a tunable diode laser to produce IR absorption spectrum. When electronic transitions are being studied greater sensitivity is usually achieved by monitoring secondary process, which follow, and are directly related to the absorption, which has occurred. Such process follows the absorption of one or more additional photons or ionizations. This happens in fluorescence, dissociation and predisposition techniques. The spectrum resulting from these processes resembles very closely the absorption spectrum [29].

High monochromaticity of lasers has made it possible to investigate atoms and molecules in the gas phase by methods of Doppler free non-linear spectroscopy of [1]. The temporal resolution in pre-Laser kinetic spectroscopy was at best about 10^{-8} s due to the use of pulsed flash lamps and Kerr-cell shutter.

The three most widely used spectroscopic techniques used for analytical purpose are

(i) absorption method

(ii) optoacoustic method and

(iii) fluorescence method

The method of measuring transmission is particularly useful in the case of lines, which are sufficiently intense when the absorbed intensity is a measurable fraction of the incident one. Intra-cavity absorption technique, laser spectroscopy of magnetic resonance, optoacoustic, optothermal, optogalvanic, fluorescence, Raman scattering are

the most widely used linear techniques to measure the spectrum. Laser radiation can induce various non-linear effects in matter. Nonlinear resonance effects arising during excitations of atoms and molecules form the basis of non-linear spectroscopy The non-linear spectroscopy can be classified into three

(i) absorption saturation

(ii) multi-step excitation and

(iii) multi-quantum excitation

The absorption saturation effect means a significant change in the initial distribution of level population for the quantum transition understudy. This effect is useful for spectroscopy when monochromatic laser radiation interacts with an in homogeneously broadened spectral line since it changes line shape and make it possible to reveal the structure of spectra screened by inhomogeneous broadening.

The effect of multistep excitation of high-lying quantum levels takes place when a particle is excited subsequently at several quantum transitions under the action of multi-frequency laser radiation. Such a method of strong excitation provides the production of highly excited particles, which can be detected very easily by their ionization. The methods of multistep laser spectroscopy are characterized by a very high sensitivity and high selectivity since it is possible to detect a multidimensional absorption spectrum at subsequent quantum transitions.

The effect of multiquantum excitation differs from the effect of multistep excitation by the fact that the radiation frequency need not be in resonance with

intermediate quantum levels [30,31]. The resonance conditions for two quantum transitions in a two-frequency laser field have the form

$$\hbar\omega_1 + \hbar\omega_2 = E_{exc} - E_0$$

$$\hbar\omega_1 - \hbar\omega_2 = E_{exc} - E_0$$

where ω_1 and ω_2 ($\omega_1 > \omega_2$) are the laser radiation frequencies, E_{exc} and E_o are the energies of initial and final quantum states respectively.

1.2 Tunable Diode laser Absorption Spectroscopy

The advent of highly monochromatic laser radiation has stimulated the field of optical spectroscopy. Better accuracy in the measurement of frequency are achieved by eliminating the Doppler broadening of spectral lines. Non-linear spectroscopy techniques using high intensity laser source permits Doppler free observations of a simple gas sample.

Unique advantages of tunable diode lasers are [1].

(1) The line widths of absorbing molecules at low pressures ($\leq$ 1 torr) are (1-5) $\times 10^{-1}$ Therefore the use of diode lasers with emission line widths of 10^{-4}-10^{-5} cm^{-1} does not distort the spectrum recorded

(2) The TDL can be easily tuned and modulated, for example by changing temperature or bias current.

(3) The TDL is a coherent device and have high spectral brightness. This allows higher degree of spatial resolution for long path length measurements.

1.3 Semiconductor diode lasers

(a) Principle of operation and characteristics

TDL consists of a small crystal lead salt chip installed in a copper package. This package is mount on a cryogenic system. Lasing takes place when a forward bias current is applied. Emission in TDLS is due to the thermal electron hole recombination across the energy gap E_g between conduction and valance band of the semi conductor. Thus the laser emission frequency is partially determined by alloy composition. The diode laser cavity is a Fabry-Perrot resonator formed by crystal cleaving. The coherent radiation frequency of the cavity resonance ν_q

$$\nu = \nu_q = \frac{1}{2n^* L} q$$

where q is the index of axial mode, $n^* = [1+ (\nu/n)(\partial n/\partial \nu)]$ index of refraction of laser material and L is the length of the cavity

(b) Wave length Tuning

The most important property of a TDL is the possibility of considerable wave length tuning when the operating conditions are changed. In TDL the gain curve position is determined by the band gap energy E_g Thus all methods of changing E_g ca be used for coarse frequency tuning.

1.4 Advances in Tunable Diode Laser Absorption Spectroscopy

Tunable diode laser absorption spectroscopy (TDLAS) is a highly selective and versatile technique for measuring many trace atmospheric constituents with detection

sensitivities in the sub-parts-per-billion (ppbv) concentration range. As the name implies, this technique utilizes a tunable diode laser source which emits in the mid-infrared spectral region between 3 and 30 m. Individual lasers, which are comprised of tertiary or quaternary salts of lead, are tailor made to access specific regions of the mid-infrared spanning tens to several hundred cm^{-1} in width. The lasers are cooled cryogenically to a temperature between 10-120 K. By adjusting the laser conditions, generally the temperature and/or injection current, the output wavelength of individual devices can be tuned continuously in small intervals of several cm^{-1} throughout the entire tuning width. Although each continuous interval is separated by several cm^{-1}, one can sometimes gain access to the gaps by further adjustments in laser temperature and current.

The mid-infrared spectral region accessed by diode lasers is extremely attractive for detecting many atmospheric species with high selectivity. Many trace gases of atmospheric importance exhibit moderate to strong absorptions in this region while the major constituents, oxygen and nitrogen, do not. Furthermore, absorption lines in this region, which result from vibrational-rotational transitions, predominantly appear as sharp discrete features for small molecules when the sampling pressure is in the 1 to 50 torr range. Under such conditions, the spacing between individual absorption features generally exceeds typical absorption linewidths, which for most atmospheric molecules are in the 0.001 cm^{-1} range. Tunable diode laser (TDL) linewidths by contrast, are typically in the 10^{-4} to 10^{-5} cm^{-1} range. These conditions result in the high resolution, and hence high selectivity, inherent in TDLAS. This is in contrast to spectroscopic

measurements in the visible and ultraviolet regions where many atmospheric species exhibit broad and non-structured absorption features which can overlap. Figure 1.1. Schematically shows a general setup which is fundamental to all lead salt tunable diode laser systems [32]

The sample of interest is drawn into the cell at reduced pressure. Most frequently, a multipass absorption cell based on the design of White or Herriott is employed as the sampling cell. Using base paths of 0.3 to 1.5 meters, such cells result in total absorption pathlengths ranging between 10 and 200 meters. The transmitted light is recorded with a solid state detector as the laser wavelength is repetitively scanned through absorption features of the analyte gas. Wavelength scanning is generally accomplished by applying a ramp signal (typically a sawtooth ramp) to the quiescent injection current at frequencies of 10 - 100 Hz.

Fig.1.1 Schematic representation of a TDLA spectrometer

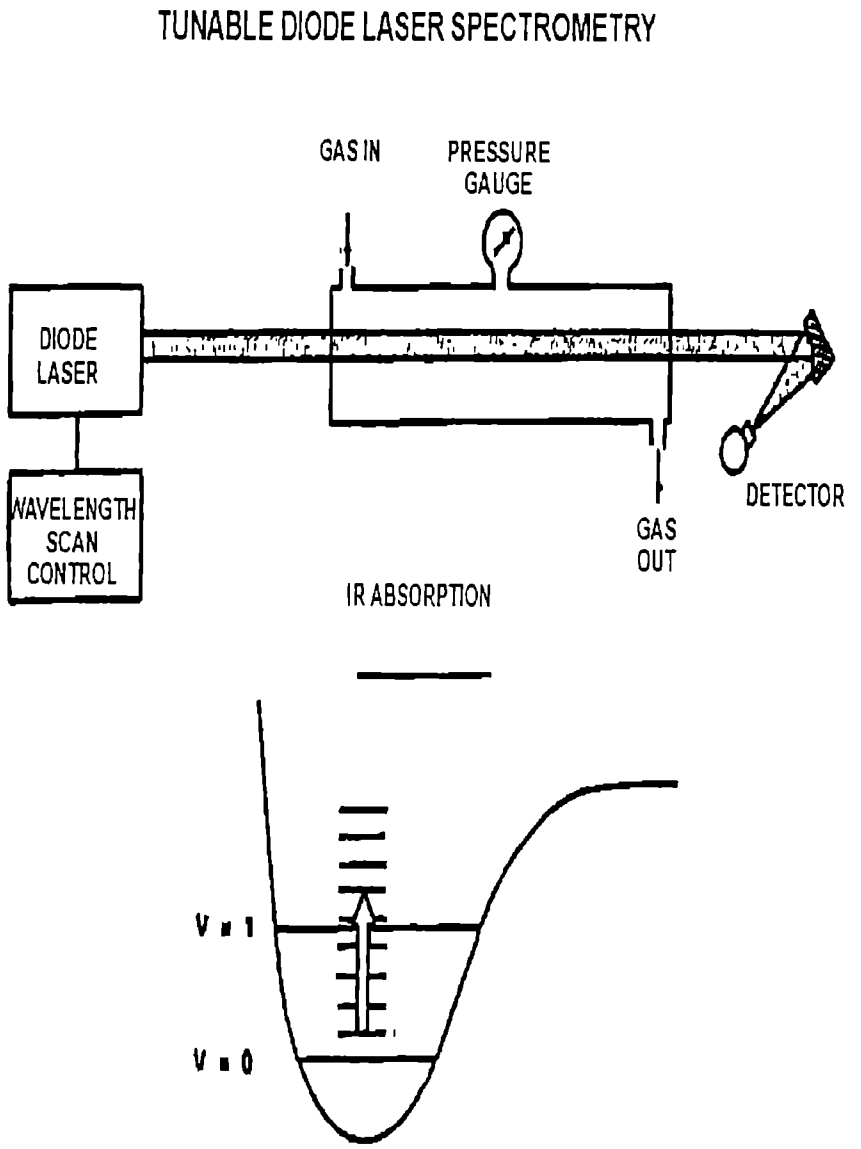

Quantitative information is obtained using the Beer-Lambert Law. However, since the diode laser source is scanned over an entire absorption feature, including the baseline off the feature, the sample gas in this case does not have to be removed to obtain the incident intensity (I_o). One uses the transmitted intensity at line center, together with measurements of pressure, path length, and absorption cross section, to obtain a concentration. Alternatively, one frequently integrates over the entire absorption feature using the integrated absorption cross section to obtain a concentration. This procedure, although requiring more work to accurately calibrate the frequency scale and baseline position, does not suffer from a potential systematic error due to a laser "slit function." This arises from the small but finite laser line width relative to the absorption feature under study. Both methods are direct absorption approaches, which yield absolute concentration determinations based solely on photometric and cross section measurements, without the need for calibration standards. In fact, this approach has been used to independently determine the concentration of various calibration standards with absolute accuracies in the 1 to 10% range. This aspect of absolute calibration sets spectroscopic techniques in general, and TDLAS specifically, apart from other measurement approaches.

In addition to direct absorption, TDL measurements are frequently carried out using the technique of harmonic detection. Most frequently, second harmonic detection is employed. In this mode, an external modulation waveform in the kilohertz frequency domain is simultaneously superimposed on the diode laser scanning current. A lock-in amplifier is used to detect the resultant frequency-modulated absorption synchronously.

In most instances, the second harmonic frequency (detection at twice the modulation frequency) is chosen.

Figure 1.2 illustrates the direct, first, and second harmonic absorption line shapes. As shown, second harmonic detection produces a zero baseline signal, thus eliminating the necessity of measuring small differences between two large intensities, I and I_o, as is the case for direct absorption. Further advantages of second harmonic detection over direct absorption are: (1) the elimination of a strongly sloping background often present in direct absorption; (2) reduced susceptibility to low frequency noise due to the kHz detection regime; and (3) enhanced discrimination against signals that do not have a strong wavelength dependence such as the broad absorption tails of ambient H_2O vapor. Employing second harmonic detection, minimum detectable absorbances ($ln\ I_o/I$) of 10^{-5} to 10^{-6} are frequently obtained in TDLAS systems using total pathlengths around 100 m. This corresponds to minimum detectable concentrations ranging between a few parts-per-trillion (pptv) to parts-per-billion (ppbv), depending upon the absorption cross section.

Figure 1.2 Direct, First and Second harmonic line shapes

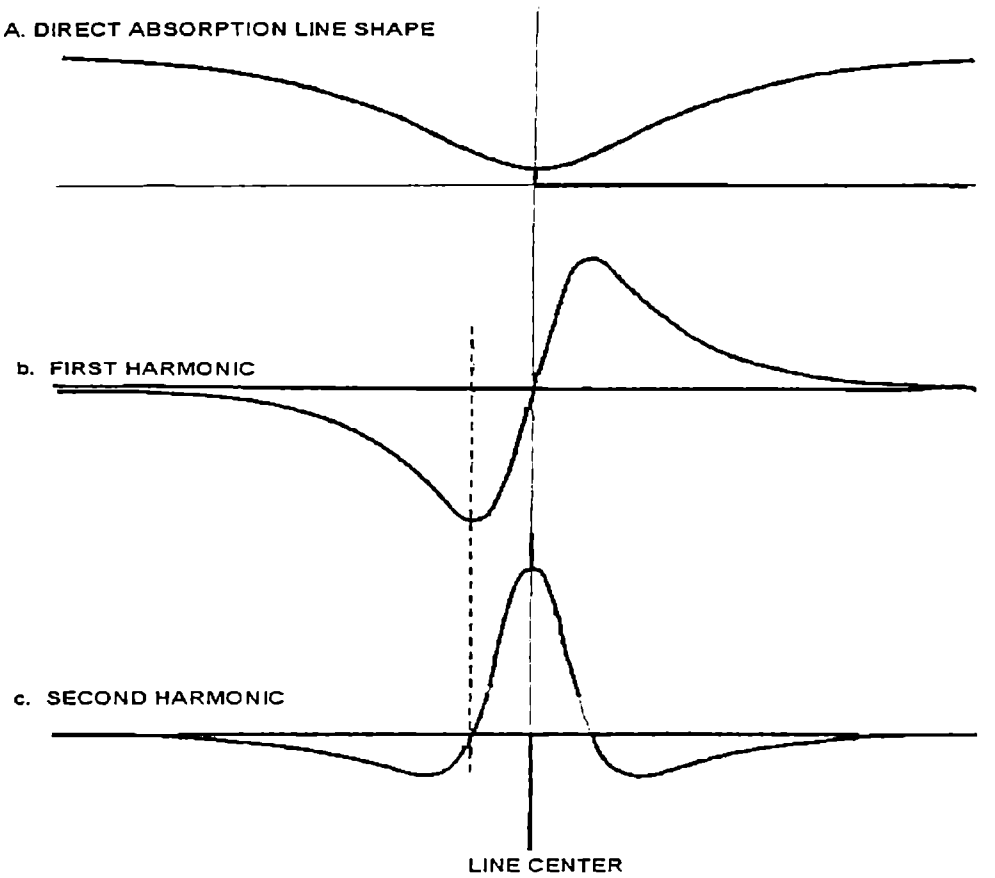

Molecules such as carbon disulfide CS, CO_2, and carbonyl sulfide (OCS), which have very high cross sections, are examples of the former sensitivity range, while H_2S represents the latter. Unlike direct absorption, many instrument and experiment-dependent factors must be taken into account when deducing absolute concentrations from the measured second harmonic response. As a result, accurate quantitative analysis employing second harmonic detection is most frequently accomplished using calibration standards.

1.5 Applications of TDLAS

Because of the versatility, selectivity, and sensitivity of TDLAS, numerous laboratory, ground-based, aircraft, and balloon-borne studies employ this technique. Although many such examples can be cited, two recent applications of this technique:

(1) ground-based measurements of long-lived gases and

(2) airborne measurements of carbon monoxide (CO) and methane (CH_4)

Long-lived trace atmospheric gases such as CO_2, CH_4, OCS, and nitrous oxide (N_2O), to name a few, have received considerable attention in recent years. The ambient fluctuations of these gases contain important information about sources, sinks, and potential secular trends. In air not directly influenced by local sources, such fluctuations can be quite small, typically less than a few percent. Extracting ambient information thus requires comparable measurement precision, which can be achieved by TDLAS. This, however, necessitates extreme care in both TDL system design and operation. A versatile TDL system has been developed at NCAR which addresses the major factors

affecting TDL precision. This system, which is being employed in measuring the important sulfur gas *OCS*, can be used to measure any of the above gases with a precision around 0.1 - 0.2%.

Up to four high temperature operation diode lasers (80 K) are mounted on a temperature controlled stage housed in a liquid nitrogen dewar. The emerging infrared radiation from the selected laser, which is emitted downward, is collected and imaged into a 1.5-m base path multipass White cell. The total pathlength typically employed ranges between 90 and 150 meters and the cell pressure is around 25 Torr.

In the second application, a TDL system has been used to measure *CO* and CH_4 on an aircraft platform to achieve all the advantages discussed previously in addition to broad spatial coverage Although fundamentally similar to the NCAR system, the airborne spectrometer known as DACOM uses two independent laser channels to access simultaneously the absorption lines from *CO* and CH_4 in the 4.7 and 7.6 μ regions, respectively. These airborne measurements are extremely useful in characterizing the geographical distribution of both gases, detecting the chemical signature of biomass plumes conveyed by long range transport, identifying air mass changes and their potential origins, and in studying vertical transport.

1.6 Analytical techniques

(a) Sensitivity limits

The sensitivity limits of absorption method depends on the ability of the recording system to detect small variations of Laser power. In the laser shot noise limit the minimum change in the laser power which can be detected by an ideal detector is

$$\Delta P_{min} = (2P_s h\nu \Delta f)^{1/2}$$

where P is the laser power in absence of absorption, $h\nu$ is the photon energy and Δf the band width of detection system [1].

1.7 TDLA spectrometer Calibration Techniques

According to Beers law, the signal due to absorption is linearly proportional to the number of absorbing molecules and the power of the laser beam for small optical depths. Several methods are employed to determine the frequency of laser light. The major techniques are outlined below.

(1) Using Michleson scanning interferometer and by counting the number of interference maxima [33,34].

(2) Method of internal standard in which the frequency is determined from a value of absorption line width under Doppler limited conditions [35].

(3) Calibration with a Fabri-Perrot etalon and reference lines.

(4) Optical heterodyne techniques, when the frequency stabilized CO_2 or CO laser is used as a local oscillator

The simplest method is that in which the laser frequency dependence on tuning parameter is determined by measurement of Fabri-Perrot etalon transmission spectrum

and the absolute calibration of this dependence is performed using frequency calibration standards.[36,37,38]

The important aspects in wave number calibration can be summarized as below.

(1) The reproducibility of the entire tuning curve from scan to scan could not be worse than 1×10^{-4} cm $^{-1}$ and the producer of spectra recording over a single mode frequency range takes only a few seconds. The acquisition should in the sweep integration method. The band widths of detectors and amplifiers used, should not higher than 1MHz.

(2) Digital data rerecording and processing with the help of microcomputers is advantageous [39]. Baseline correction would be made using subtraction or dividing the transmission spectra of the studied gases and the etalon point by point by the background one. Analog or digital filtering are also effective for background elimination.

(3) To exclude systematic errors a set of spectral recordings (background, reference gas, the studied gas and fringes of the Fabri-Perrot etalon) should be made more than once at different tuning parameters.

1.8 Calibration of analytical signal

The important problem for qualitative analysis is to establish the functional dependence of a gas analyzer signal on the concentration of molecules detected and to calibrate these dependence. A very sharp spectral line of a TDL ensures the validity of Beer's law. The linear dependence exists not only if the direct transmission signal is detected but also when harmonic integration or correlation methods are used the non

linearity may be caused by optical effects such as a parasitic etalon fringes, baseline slope, interference absorption lines or by molecular process such as adsorption on cell walls or chemical reaction in the mixture. The calibration in PPB range in the optical absorption method can be performed using standard mixtures with high concentrations. this can be achieved by placing a short cell containing a calibrated mixture with relatively higher concentration, in the laser beam sequentially with the multipass cell. Because the absorption is linearly proportional to the concentration path length product this method enables to simulate an absorption signal equivalent to that from mixtures with extremely low concentration [40].

1.9 Line Broadening Mechanisms

The width and shape of spectroscopic transitions will affect the ability to extract qualitative and quantitative information from a spectrum. The line shapes of spectroscopic transitions depend on the broadening mechanisms of the initial and final states, and include, natural broadening, collision broadening, power broadening and Doppler broadening. Natural, collisional, and power broadening are homogeneous mechanisms and produce Lorentzian lineshapes, and Doppler broadening is a form of inhomogeneous broadening and has a Gaussian lineshape. The general form of Lorentzian and Gaussian lineshapes are shown in fig.1.3. Combinations of Lorentzian and Gaussian lineshapes can be approximated by a Voigt profile.

Collisions broaden spectroscopic linewidths by shortening the lifetime of the excited states. Pressure broadening occurs by shortening the lifetime of the excited state due to stimulated emission. Doppler broadening is due to the distribution of atomic

velocities (speed and direction), which each have a Doppler shift with respect to an observer.

Fig.1.3 Typical Gaussian and Lorentzian profile

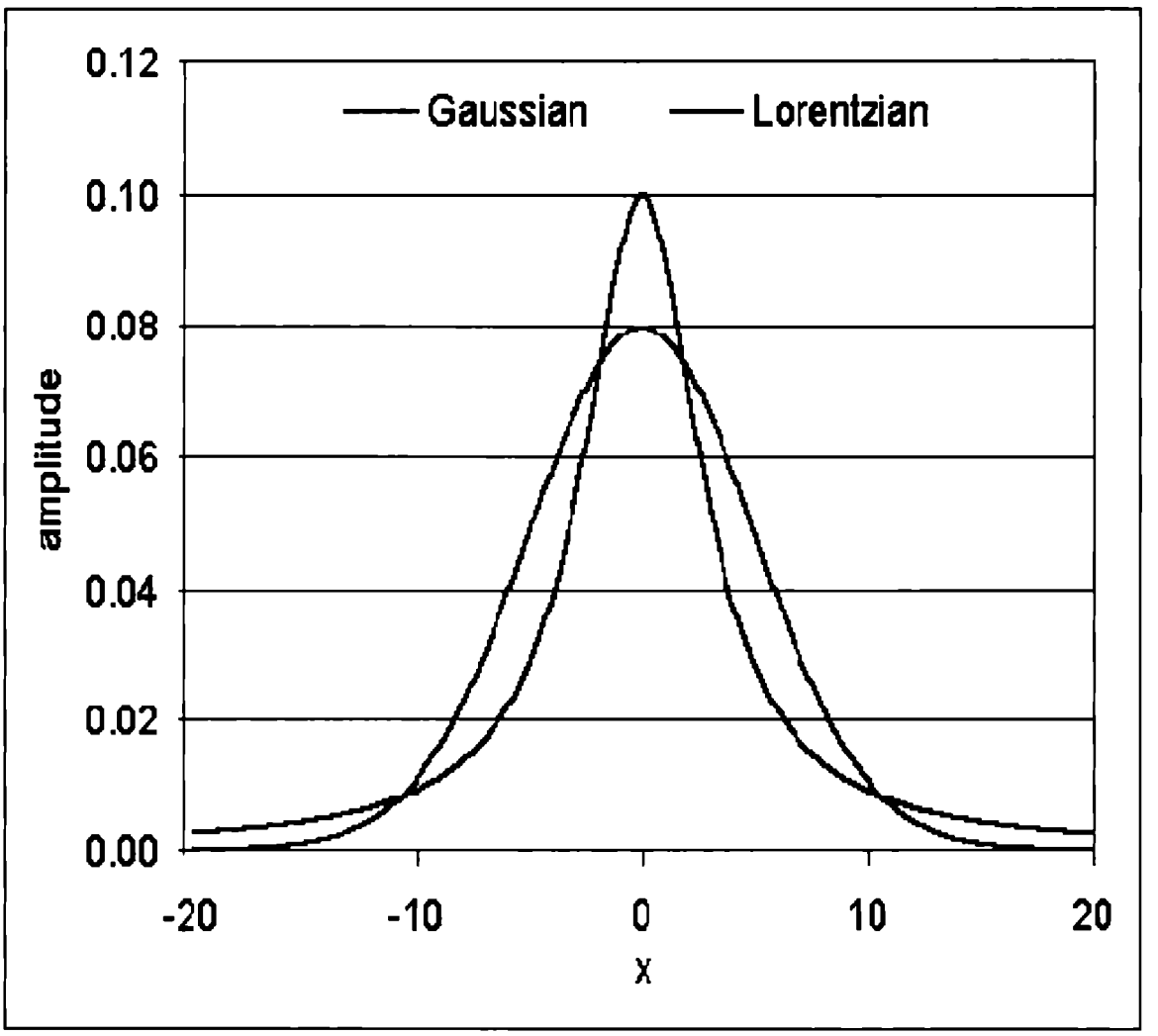

1.10 High Resolution Spectroscopy

High-resolution spectroscopy requires the narrow-bandwidth excitation sources that are only achievable with lasers studies in the visible spectral region typically use a

tunable dye laser and studies in the near-ultraviolet and near-infrared are becoming more common as frequency-doubling and wave-mixing methods improve. Near-infrared diode lasers are also used for high-resolution vibrational spectroscopy

(i) Molecular Methods

High-resolution studies require cooling of the molecules to remove spectral congestion and to reduce the Doppler width of the transitions. Gas-phase studies use free-jet expansions or molecular beams to cool molecules to very low temperatures. Large molecules are commonly dissolved in a suitable solvent and cooled to cryogenic temperatures to form a glass or crystalline matrix.

The Major application of TDLS is high resolution recording of vibrational rotational spectra of molecules in the gas phase. The major uses are summarized below.

(i) investigation and analysis of fundamental and vibrational-rotational bands of chemically stable molecules, line assignments, determination of precise spectroscopic constants and molecular structure;

(ii) study of rotational fine structure of molecular spectra;

(iii) investigation of individual line parameters- profiles, intensities widths and also coefficients of broadening and shifts.

(iv) Spectroscopy of transient species, in particular, free radicals and molecular ions;

(v) Investigation of absorption by molecules in excited states;

(vi) Study of dynamic molecular process

In our work we have fabricated a high-resolution spectrometer, using a tunable diode laser and a multipass sample holder 36m effective path length.

References

1 V.S Letokhov, "Laser Analytical Spectrochemistry", IOP publishing Ltd, 1986

2. S.Haroche, J.C Pebay-Peyroula, T.W Hansch and S.E Harris, "Laser Spectroscopy" (Lecture note in Physics vol.43), Berlin: Springer, 1975 ed.

3. J.L Hall and J.L Carlsten. *Laser Spectroscopy III Springer Series in Optical sciences, Berlin: Springer* vol.7, 1977 ed.

4. H Walther and K.W Rothe, *Laser Spectroscopy IV Springer Series in Optical sciences, Berlin: Springer.* vol.21, 1979 ed.

5. A.R.W McKellar, T Oka and B. P Stoicheff, *Laser Spectroscopy V Springer Series in Optical sciences, Berlin: Springer.* vol.30, 1981 ed.

6. H.P Weber and W Luthy, *Laser Spectroscopy VI Springer Series in Optical sciences Berlin: Springer.*, vol.40, 1983 ed.

7 M.S Field, A Javan and N.A Kurnit, Fundamental and Applied laser Physics, New York: Wiley, 1973

8. A Mooradian, T Jager and P.Stokeseth, *Tunable lasers and their Applications, Springer Series in Optical sciences, , Berlin: Springer.* vol.3, 1976 ed.

9. A.H Zewail, *Advances in Laser Chemistry Springer Series in Chemical Physics, Berlin: Springer.* vol.3 1978 ed.

10. H. Walther, *Laser Spectroscopy, of atoms and Molecules, Springer Series in Topics in applied Physics, Berlin: Springer*, vol.2,. 1976 ed.

11. W Demtröder, *Laser Spectroscopy, Springer Series in Chemical Physics, Berlin: Springer*, vol.5, 1981 ed.

12. N.Omenetto, "Analytical Laser Spectroscopy", New York Wiley 1979ed.

13. D.S Kliger Ultrasensitive Laser Spectroscopy", New York Academic, 1983ed.

14. K.Shimoda *"High resolution Laser Spectroscopy" Springer series Topics in applied Physics*, vol.13, 1976, Berlin: Springer

15. V.S Lokhov, V.P Chebotayev, *Non-linear Laser Spectroscopy, Springer Series in Optical sciences*, vol.4, Berlin: Springer. 1977 ed.

16. S.L Shapiro, *"Ultra short Light Pulses" Springer series Topics in applied Physics*, vol.18, 1977, Berlin: Springer.

17 K.B Eisenthal, R.M Hochstrasser, W.Kaiser and A.Laubereau, *"Pico second Phenomena III" Springer series Topics in Chemical Physics*, vol.23, 1982, Berlin: Springer.

18. R.V Ambartzumian and Lekhotov V.S *Appl. Opt.* 11, 354, 1972.

19. N.C Peterson, M.J Kurylo, W.Braun, A.M Bass and K.A Keller, *J.Opt. Soc. Am.* 61 746, 1971.

20. P.D Maker, R.W Terhune, *Phys. Rev.* A137, 801, 1965.

21. J.A Giordamine and W.Kaiser *Phys.Rev.* A144, 676, 1966.

22. R.I Personov, E.I Al'shitz and L.A Bykovskaya, *Opt.Commun.* 6, 169, 1972.

23. M.R Bowman, A.J Gibson, M.C.W Sandford, *Nature*, 221, 456,1969

24. E.D Hinkley, *Laser monitoring of atmosphere, Springer series Topics in Applied Physics,* vol.14, 1976, Berlin: Springer.

25. D.K Killinger and A. Mooradian, Optical and Laser Remote Sensing, *Springer series Topics in Optical sciences,* vol.39, 1983, Berlin: Springer.

26. H.Moenke and L Moenke, Laser Microspectrochemical Analysis, Adam Hilger-London, 1973.

27 F.Hillenkamp, E.Unsöld, R.Kaufmann, and R.N Ntische, *Appl.Phys,* 8, 341, 1975.

28. F.Brech, L.Cross, *Anal.Spectrosc.*, 16, 59, 1962.

29. J.Michael Hollas, "High Resolution spectroscopy" John Wiley & Sons, II ed. 1998.

30. J.A Giodmaine and W Kaiser *Phys rev.* A144 676 1966.

31. M.D Levenson " Introduction to Nonlinear Spectroscopy" Academic Press , New York, 1982

32. www. Asp.ucar.educolloquium/1992/part2/node9.html

33. Nagai.K, Kawaguchi.K Yamada .C, Hyakawa.K, Takagi.Y Hirota E. *J. Mol. Spectra*. 80, 197, 1980.

34. Shubin M.V *Sov. J.Opt.Technology* 12,, 46, 1983

35. Chang T Y, Morris R.N and Yeung E.S *Appl.Spect*. 35, 587, 1981.

36. Kauppinen.J, Jolma.K and Homeman *Appl.Optics* 21 3332, 1982,

37 Jolma.K, Kauppinen.J, and Homeman *J Mol.Spect*. 101, 300, 1983,

3 8. Jolma.K, Kauppinen.J, and Homeman, *J.Mol Spectro*. 101 278, 1983

39 Davis P.B, Hamilton. P.A, Lewis Bevan.W and Okumura .M *J Phys E. Sci.Instr*. 16, 289, 1983

40. Reid.J, Shewchun,J, Garside, B.K and Ballik E.A *Appl.Opt*. 17, 300 1978

CHAPTER 2

High-Resolution Spectrometer Instrumentation

2.1 Introduction

The major application of Tunable Diode Laser (TDL) is high-resolution recording of vibrational rotational spectra of molecule in the gas phase. Diode lasers have high spectral brightness and are coherent devices. These features allow the use of Tunable Diode Laser for long path length measurements, with high degree of spatial resolution. The most important property of Tunable Diode Laser is the probability of considerable emission frequency tuning with operating conditions changed. Since the gain curve position ν_s is determined by band gap energy E_g, all methods of changing Eg can be used for coarse frequency tuning. E_g can be tuned by varying the temperature T of the semiconductor crystal by applying pressure or a magnetic field H [1]. The tuning range of a laser can be significantly widened with the help of simultaneous temperature and pressure tuning [2]. Fine frequency tuning, which is used for high resolution spectroscopy is performed by shifting the frequency of effective cavity optical length mainly through index of refraction [3].

In measurements of trace gases by laser absorption spectroscopy, the absorption signal strength is proportional to the product of oscillator strength of the absorption transition and the number of molecules in the path of the laser beam. Hence at very low concentrations, long path length is required for generating detectable absorption signals [3].

The effective path length can be increased by using multi pass cell. The multipass optical system limits the beam divergence and provides large path length and facilitates operation at low pressure and thus broadening of spectral lines can be avoided.

2.2 Spectrometer Instrumentation

The major components of the spectrometer are (i) source- tunable diode laser, (ii) sample holder -a multipass cell and (iii) detector

2.2.1 Source

The source used in the present setup is a tunable diode laser (Model no.6321, New Focus Inc.) The maximum output power is up to 150 mW The tuning laser tuning range is from 935nm to 975nm. The operating temperature is 20°C. Out put power can be varied by adjusting the current. The grating spectral filter used in the laser head is narrow enough to force the laser to operate in a single longitudinal mode.

The laser cavity is shown in fig.2.1 A high reflection coating on one end of the diode laser forms one end of the cavity and a high reflecting tuning mirror forms the other starting from the diode the beam in the cavity passes through a collimating lens and then strikes a diffraction grating at near grazing incidence. The beam is diffracted toward the tuning mirror, which reflects the light back on itself for the reverse path. Part of the light from the diode is reflected, not refracted by the grating. This portion forms the output beam.

The grating functions as a narrow spectral filter. Its pass band is only a few giga hertz wide. The high wavelength selectivity results because many lines of the grating are illuminated by the grazing incidence beam and because the beam is diffracted by the grating twice in each round trip through the cavity. The grating spectral filter is narrow enough to face the laser to operate in a single longitudinal mode.

Different wavelength diffract off the grating at different angles. However only one wavelength leaves the grating in a direction that is exactly perpendicular to the surface of the tuning mirror forming the resonant laser cavity. This is the lasing wavelength because it is the only one that will survive for many cavity round trips. Thus the tuning can be achieved by changing the angle of the tuning mirror

Fig.2.1 Laser Cavity

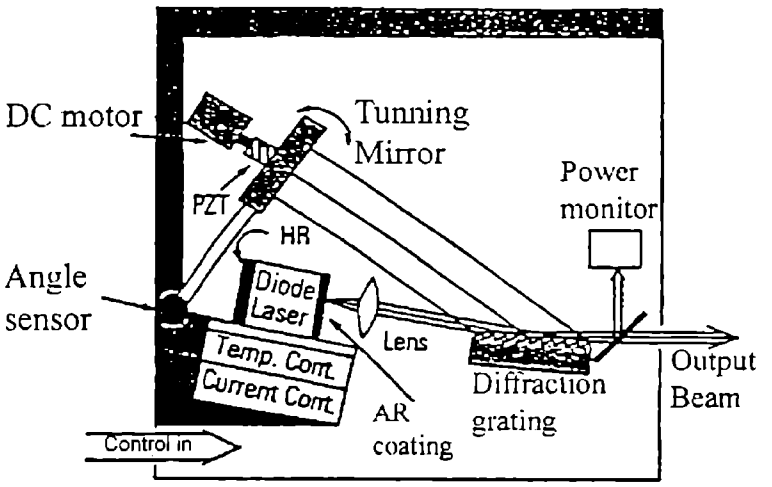

The number of waves in the cavity is maintained by having the tuning mirror rotate around a specific pivot point. The pivot point creates a relationship between the cavity length and the laser wavelength. The laser wavelength is set by the standard law of refraction of light off a grating

$\lambda = \Lambda (\mathrm{Sin}\theta_I + \mathrm{Sin}\theta_d)$

Λ is the spacing between the grooves in the grating while θ_I and θ_d refer to incident and diffracted angles of the laser beam measured from a line normal to the surface of grating. The cavity length divided by the wavelength gives the total number of waves in the cavity

2.2.2 Multipass cell

The multipass cell is divided into six main parts, base plate glass tube, two housings and two mirrors. The base plate is a piece of anodized aluminum with three slots for mounting on optical tables. The glass tube is made of borosilicate glass and the tube is sealed to the housings with an O-ring that is held in place by an anodized aluminum O-ring retainer. The two housings are made of nickel coated aluminum aside from the aluminum mirrors and the housings, the remaining metal parts inside the cell are made of stainless steel.

There are three couplings in the front and back plates for various applications such as sample intake, pressure checking etc.. the mirrors are made of a nickel-

plated aluminum substrate that is polished into desired toroidal shape. A protected silver coating is deposited onto its surface. The flat surface on the edge of the mirror is approximately aligned with one of the mirror is approximately aligned with one of the mirrors toroidal axes. A schematic representation of the multipass cell is given in fig.2.2

2.2.2.1 Multipass cell Theory:

The multipass cell employs astigmatic or toroidal mirrors, that is along the two orthogonal axes, the mirrors have radii of curvature at differ by about 10% in the multipass cell the mirrors are separated by nearly this radius of curvature and an optical beam is coupled into the cell through a hole in front mirror. The beam enters the cell in the horizontal plane at an angle to the axis of the cell and then bounces back and forth a number of times between the mirrors if the cell is aligned correctly, the beam will travel along a re entrant path which closes itself at the coupling hole after a finite number of passes. Then the beam exits the cell through the original coupling hole.

The astigmatic mirrors of the multipass cell cause the beam to travel in a path such that the beam spots on the mirrors trace out a Lissajous pattern or the beam spots trace out a pattern that is sinusoidal in X and Y but has different frequencies in two directions. For a reentrant path, the X, Y co-ordinates of the spot pattern on the mirrors are given by

$x_i = X_0 \text{ Sin}(i\Theta_x)$ and $y_i = Y_0 \text{ Sin}(i\Theta_y)$

$\Theta_x = \pi M_x/N$ and $\Theta_y = \pi M_y/N$

X_0 and Y_0 define the size of the spot pattern on the mirror. N is the number of passes on the mirror. N is the number of passes through the cell, and N is even so the beam enters and exits the cell through the same mirror. The parameter varies from 1 to N and indicates the order of appearance of each spot on the mirrors. M_x and M_y are integers that determine the shape of the beam spot pattern these parameters are related to the mirror radii of curvature and the separation between mirrors

Fg.2.2 Schematic Drawing of multipass cell

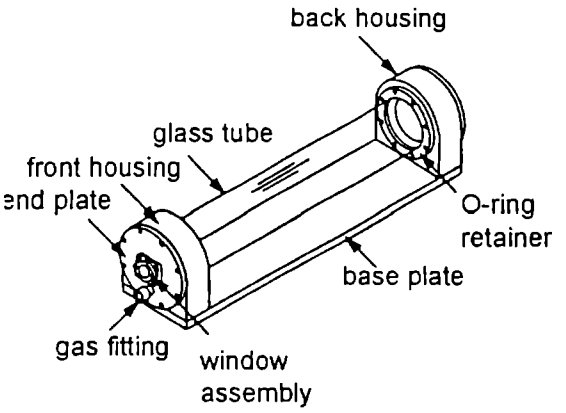

2.2.3 Detector

The detector used in this set up is Nirvana Model 2017 new Focus Inc. The photo receiver consists of two photodiodes designated as signal and reference. There are three outputs Linear, Log and signal monitor. This detector enables traditional balanced detection. In the balance mode the linear output provides a voltage proportional to the difference between the photocurrents of the signal and reference diodes. It also provides auto balance detection with zero DC voltage and noise suppressed AC signal proportional to received signal optical power. In this state the detection automatically balances the photocurrent from signal and reference diodes. The signal monitor output enables constant monitoring of the signal. The log output at auto-balanced state provides a convenient measurement of absorption present in the signal path. The log output voltage is given as

$$\text{Logoutput} \approx -\ln\left[\frac{P_{Ref}}{P_{Sig}} - 1\right]$$ The log output is bandwidth limited up to the selected gain compensation cut-off frequency Common mode noise within this bandwidth is cancelled in the log output. The split ratio of the detector is fixed to 2:1. by using the log output the chopper and lock-in-amplifier can be avoided.

The analog output from the photo detector is connected to one of the channels of the CB68 LP connector block and it is connected to the ADC-DAQ PCI 6023E which is connected to the PC. The PC interfacing is done using lab view 6.0. The software is programmed to obtain the spectrum as wavelength against absorption as the absorption in the cell is proportional to the output voltage.

2.2.4 Calibration

The calibration of the spectrophotometer is done following the method if internal standards. The line used for calibration is obtained from Hitran Database 1996. The present setup provides a resolution of 0.01nm. The schematic representation of experimental set up constructed is shown in fig.2.3.

Fig 2.3. Schematic representation of Experimental setup

a-Tunable diode Laser, b-Photo-detector, c-Computer, d-multipass cell, e sample holder, f-vacuum system

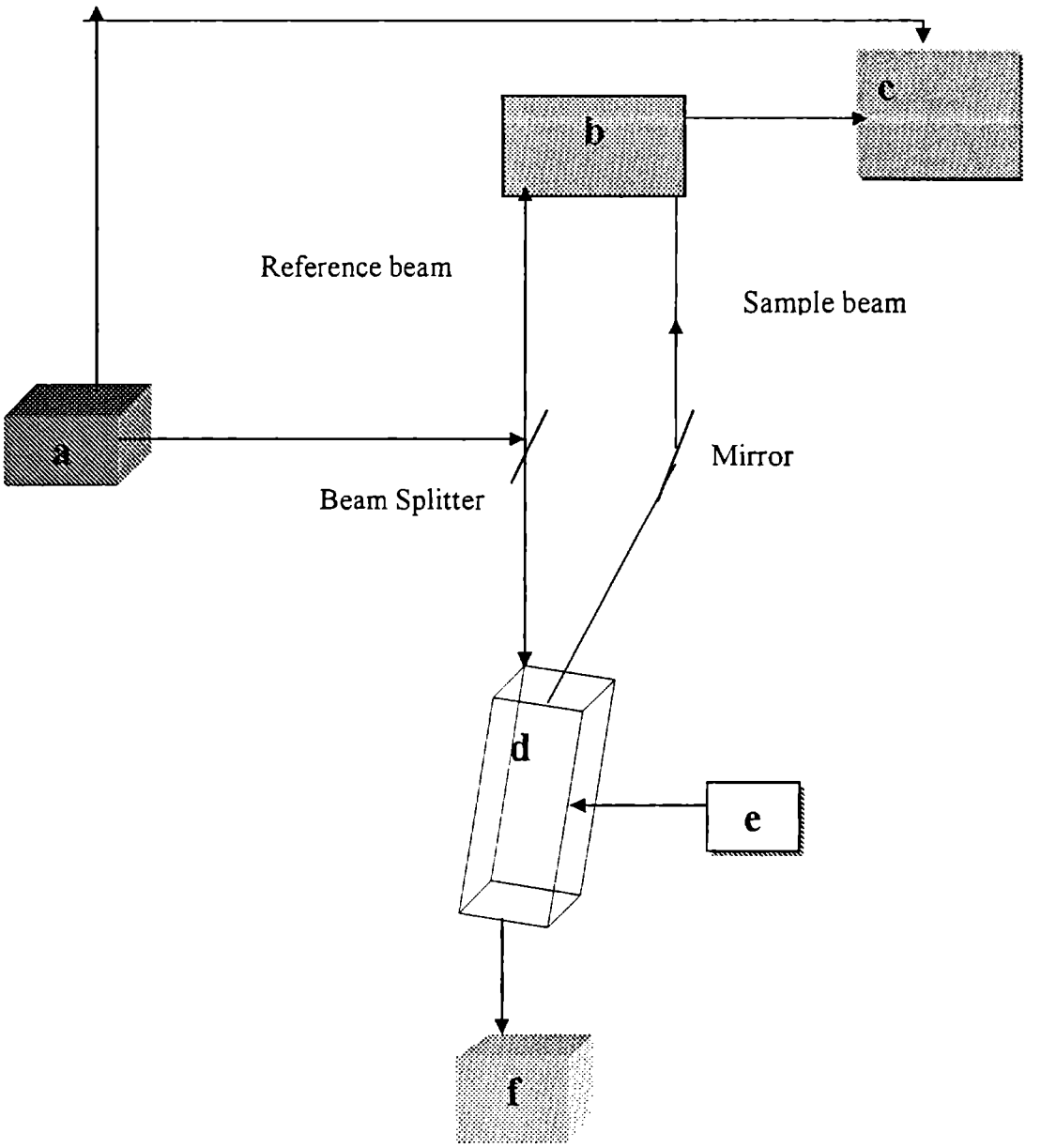

Experimental setup

2.3 High Resolution Spectrum of -OH group in methanol in the transition region Δv=3

2.3.1 Introduction

The interpretation of the vibrational overtone spectrum of methanol is done meticulously by Hänninen et.al [4]. Out of the 12 vibrational degrees of freedom one is a low-wave number large amplitude motion, which results in rich hot band structure in all systems [4]. Vibrational Hamiltonian model based on internal co-ordinates have recently been applied to methanol [5]. In this model methanol is assumed to be frozen in a staggered configuration with energy as a minimum value. The overtone spectrum of OH and CH stretching vibrational frequencies, in gas phase methanol, in the region Δv 3-6 have been recorded using photoacoustic technique by Howard et.al [6].

The torsional motion give rise to complicated fine structure in vibration – rotation bands of high frequency modes. Using the high-resolution spectrophotometer setup we were able to reproduce the rotational vibrational spectrum of methanol in the region Δv=3 The vibrational frequencies reported by Howard et.al agrees fairly well with our experimental results.

2.3.2 Theory

The model put forward by Hänninen et.al deals only with the k=0 torsional states. K is the rotational quantum number associated with the principal axis *a*. this corresponds to the smallest moment of inertia.

The torsional Hamiltonian considering the overall decoupled rotational and torsional motion would be [7].

$$H_{tor}/h_{co} = \frac{F}{\hbar^2} j^2 + \frac{1}{2} V_3 (1 - \cos 3\alpha) + \frac{1}{2} V_6 (1 - \cos 6\alpha) \qquad (1)$$

where C_o is the speed of light in vacuum, F is the constant for torsional motion, j is the torsional angular momentum operator, V_3 and V_3 are the Fourier coefficients of the torsional potential and $\alpha$is the torsional angle, which is defined to be zero, when the CH bond is trans to the OH bond [7].

Assuming $F = F'-V_RF''$

The matrix elements of the torsional Hamiltonian are

$$\langle V_R m|H_{tor}/h_{co}|V_R, m'\rangle =$$

$$\left(Fm^2+\frac{1}{2}V_3+\frac{1}{2}V_6\right)\delta_{m,m} -\frac{1}{4}V_3\delta_{m,}\delta_{m'\pm3}-\frac{1}{4}V_6\delta_{m,m'\pm6}. \qquad (2)$$

for the high frequency motions the kinetic energy Hamiltonian coefficients and diagonal harmonic force constants of the high frequency motions are assumed to be depended on the torsional angle. In the case of a single one-dimensional oscillator, the Hamiltonian is

$$H=\frac{1}{2}\left(gp^2+fq^2\right) \qquad (3)$$

where q is the general vibrational co-ordinate , and $p = -i\hbar\partial/\partial q$ is its conjugate momentum operator. The g-element and harmonic force constant are expanded as Fourier series,

$$\left.\begin{aligned} g &= g^{(0)\hat{}}+g^{(l)}\cos l(\alpha+\phi)+ \\ f &= f^{(0)}+f^{(l)}\cos l(\alpha+\phi)+ \end{aligned}\right\rangle \qquad (4)$$

in this case the Wilson's matrix is assumed to be independent of q. the index l indicates that the Hamiltonian operator is periodic with respect to the torsional angle $2\pi/l$. the quantity ϕ is the phase angle. The first two Hamiltonian take the forms

$$\left.\begin{aligned} H^{(0)} &= \frac{1}{2}\left(g^{(0)}p^2+f^{(0)}q^2\right) \\ H^{(l)} &= \frac{1}{2}\left(g^{(l)}\cos l(\alpha+\phi)\,p^2+f^{(l)}\cos l(\alpha+\phi)\,q^2\right) \end{aligned}\right\rangle \qquad (5)$$

the Hamiltonian given can be expressed in convenient form using shift operators which are defined as

$$a^{+} = \frac{1}{\sqrt{2}}\left(\alpha^{\frac{1}{2}} q - i\alpha^{\frac{-1\hbar}{2}} p \right)$$

$$a = \frac{1}{\sqrt{2}}\left(\alpha^{\frac{1}{2}} q + i\alpha^{\frac{-1\hbar-1}{2}} p \right) \qquad (6)$$

where

$$\alpha = 1/\hbar \sqrt{\frac{f^{(0)}}{g^{(0)}}} = \frac{2\pi C_o w}{\hbar g^{(0)}}$$

and now is the harmonic wave number of the harmonic oscillator. The shift operators operate on the harmonic oscillator Eigen functions in the usual way as

$$a^{+}|v\rangle = \sqrt{v+1}|v+1\rangle$$

$$a\,|v\rangle = \sqrt{v}|v-1\rangle \qquad (7)$$

the Hamiltonian operator $H^{(l)}$ can be written as

$$H^{(l)}\ l\ h\ Co = \frac{w}{4}\left(\frac{g^{(l)}}{g^{(0)}} + \frac{f^{(l)}}{f^{(0)}} \right) \cos\ l(\alpha + \phi)(aa^{+} + a^{+}a)$$
$$= \mu^{(l)} \cos\ l(\alpha + \phi)(aa^{+} + a^{+}a) \qquad (8)$$

Operators of the type a a and $a^{+}\ a^{+}$ are neglected because they connect states which differ a lot by energy [6]

2.3.3 OH Stretch

The OH stretch vibrational Hamiltonian is

$$H_{OH} = \frac{1}{2}\left(g_{RR} p_R + f_{RR} q_R^{2} \right) + H_{anh} \qquad (9)$$

The g_{RR} coefficient is constant but the f_{RR} force constant can be expanded as a Taylor series as

$$f_{RR} = f^{(0)}{}_{RR} + f^{(3)}{}_{RR} \cos 3\alpha \tag{10}$$

The torsional Hamiltonian is

$$H^{(3)}{}_{OH} \text{lhC}_o = \mu_{RR} \cos 3\alpha \left(aa^{+} + a^{-}a\right) \tag{11}$$

where

$$\mu_{RR} = \frac{w_R f^{(3)}{}_{RR}}{4 f^{(0)}{}_{RR}} \tag{12}$$

and the Hamiltonian matrix elements are

$$\left\langle v_R, m' \middle| \left(H_{OH}{}^{0} + H^{3}{}_{OH}\right) / hc_o \middle| v_R, m \right\rangle$$

$$= \left[w_R v_R + x_{RR} v_R (v_R + 1)\right] \delta m', m + \frac{2v_R + 1}{2} \mu_{RR} \delta_{m', m \pm 3} \tag{13}$$

The coupling between different high frequency modes is such that

$$V = \left(\sum_{j=1}^{3} V_{rj}\right) + V_R + \frac{1}{2}\left[\left(\sum_{j=1}^{3} V\theta j\right) + V_\phi\right] \tag{14}$$

The Hamiltonian matrix is in the block diagonal form where states with different V values are uncoupled. The coupling between the different torsional states is such that the dimensions of the different block matrices would be infinite. Hänninen et.al in their model included the torsional states with n = 0,±1, ±2,. ±8 to obtain converged Eigen values for the lowest torsional states.

The OH stretching states are $|000,000, V_R, 0\rangle$ these states are coupled to the CH and OH stretching combination states of the type $|100,000, V_R - 1, 0\rangle$ by a harmonic term. The combination states are coupled by Fermi-resonance to the OH stretching and CH_2 combination states. Thus the dimension of the OH stretching vibrational Hamiltonian blocks is 187×187, when the torsion is included.

2.4 Experimental considerations

The recording of absorption spectra using the TDL set up is accomplished by scanning the laser wavelength range and detecting the signal. However there are several conditions to be satisfied in the experimental arrangement. The first condition is laser should be operated in a single mode. This can be achieved by operating the laser at low power and mounting the laser on a vibration free table.

The multipass cell has to be evacuated fully to avoid signal distortions due to atmospheric water vapor. The multipass cell is connected to the vacuum pump using a flexible alloy tube 1.25 m in length. The vacuum pump may also induce vibrations on the multipass cell. To avoid this the tube connecting them is fixed to vibration arresting clamps. The sample to be fed into the cell is taken in a round bottom flask is connected to one of the nozzles of the multipass cell using a flow controller and a bend tube.

2.5 Experimental and Results

The light from the laser source is allowed to split into two using a neutral density filter, which is adjusted to allow 40% transmittance. The reflected beam from the filter is considered as the reference beam and is focused to the reference diode of the detector segment. The transmitted beam is focused into the cell where the sample is fed at a pressure of 0.02 m bar. The multipass cell is tilted to get maximum number of passes. This is done by adjusting the number of spots obtained in the cell. The reference to signal ratio is adjusted to 2:1. The scan speed is set to 0.02nm.. The ray coming out of the cell is focused to the signal photodiode. The diode circuit is adjusted to get the log output. The log output is connected to the A/D converter. The output from the A/D converter is interfaced with PC using lab view 6.0.

Methanol (>99%) obtained from MERCK, Mumbai was used for recording the spectrum without further purification. The spectrum of obtained using the high-resolution spectrophotometer setup is shown in fig.2.4. The experimental parameters are given in table 2.1. The conspicuous peaks obtained agree fairly well

with the values reported by Howard et.al. for the $\Delta v=3$ region. The spectrum obtained by Howard et.al using photoacoustic technique shows P, Q, R branch heads at frequencies 10515 cm^{-1}, 10531 cm^{-1}, 10546 cm^{-1} respectively The experimental results using high-resolution setup and the reported values are given in table 2.2.

Table. 2. 1

Experimental Parameters	
Laser Power	= 2.8 mW
Scan Speed	= 0.02 nm
Temperature	= 26°C
Pressure	= 0.02 m bar
Path Length	= 36 M

Table.2.2

Comparison of Experimental Results

V	Description	Experimental (cm^{-1})	Reported (cm^{-1})
	P	10508.2653	10515
		10511.7684	
OH ($3\nu_1$)		10515.3201	
	Q	10528.1347	10531
		10531.9937	
		10536.0442	
	R	10545.0484	10546
		10548.5516	
		10551.6716	

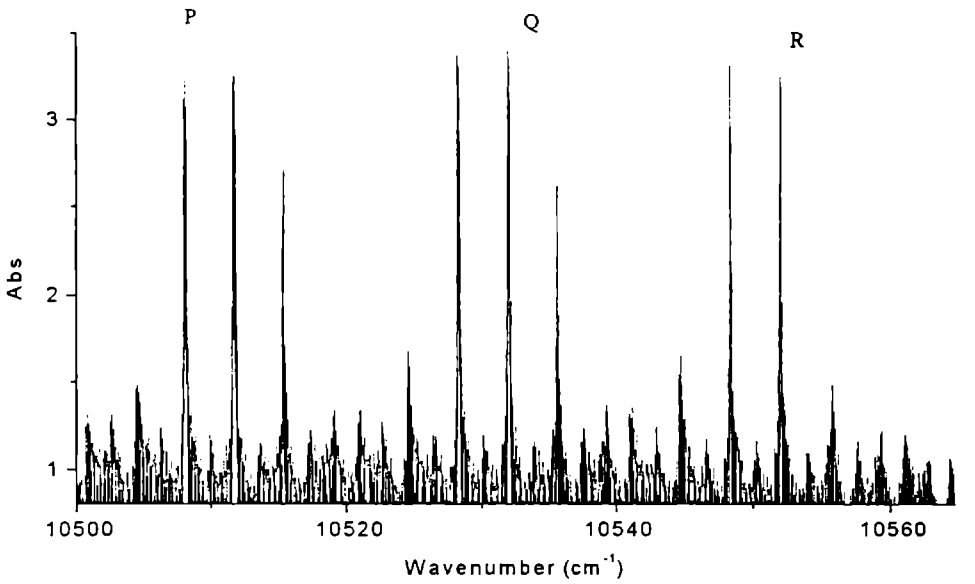

Fig.2.4

P, Q and R branches of -OH group in methanol in the transition region $\Delta v=3$

References

1. V.S Ltokhov, Laser Analytical Spectrochemistry, Adam Higler, Boston, 1985
2. Engler W Garfinkel M, Solid State Electron, 8, 585, 1965
3. N Subhash, M.K Satheesh Kumar, T.M.A Rasheed K.P Moosad, and K.Sathyanandan, J.of Optics, 16 51, 1987
4. V Hänninen, M. Horn and L.Halonan, *J.Chem.Phys*, 111, 3018, 1999
5. L.Halonan, *J.Chem.Phys*, 106, 7931, 1997
6. Howard L Fang, Donna M Meistera nd Robert L Swofford, J Phys.Chem 88, 404, 1984

7 X.Wang, and D.S Perry, *J.Chem.Phys*, 109, 10795, 1998

Chapter 3

Vibrational Overtone spectroscopy

3.1 NIR Spectroscopy

Near-infrared spectroscopy can be a workhorse technique for materials analysis in industries such as agriculture, pharmaceuticals, chemicals and polymers. A near-infrared spectrum represents overtone bands that are harmonics of absorption frequencies and combination bands in the mid-infrared. Near-infrared absorption includes a combination-band region immediately adjacent to the mid-infrared and the overtone regions.

All four near-infrared regions contain "echoes" of the fundamental mid-infrared absorptions. For example, vibrations in the mid-infrared due to the C-H stretches will produce four distinct bands in each of the overtone and combination regions. As the bands become more removed from the fundamental frequencies they become more widely separated from their neighbors, more broadened and are dramatically reduced in intensity. As near-infrared bands are less intense, more sample can be used to produce spectra and sample preparation problem are greatly reduced or eliminated. In addition, long path lengths and the ability to view through glass in the near-infrared allows to contain samples to be measured in common media such as culture tubes, cuvettes and reaction bottles. This is unlike mid-infrared where very small amounts of a sample produce a strong spectrum; thus sample preparation techniques must be employed to limit the amount of the sample that interacts with the beam.

Infrared bands correspond to the frequencies of vibrations between the bonds of the atoms making up the material. Because each material is a unique combination of atoms, no two compounds produce the exactly the same Infrared spectrum. Therefore, near-infrared spectroscopy can result in a positive identification (qualitative analysis) of each different material. In addition, the size of the peaks in the spectrum is a direct

indication of the amount of material present. With modern software algorithms, near-infrared is an excellent tool for quantitative analysis too.

NIR spectroscopy offers a practical alternative to time consuming, solvent intensive wet-testing methods and liquid chromatography techniques. NIR is ideal for quick and reliable raw material identification while also being a powerful analytical tool capable of accurate multi-component quantitative analysis. NIR is also ideal for process monitoring due to various sampling techniques and fiber optic sampling.

Advantages of NIR include:

- No sample preparation

  Can view through glass and packaging materials
- Nondestructive measurements

  Fast, sample throughout accurate, reliable analysis
- Reduced costs
- Time saving (can analyze 10 times more samples in a day)

  Remote sampling with low cost fiber optics

3.2 Local Mode Model

This model was introduced by Henry and Siebrand in their attempt to model radiationless electronic transitions in polyatomic molecules.[1-4] They found that the Frank Condon factors for $T_1 \rightarrow S_0$ and $S_1 \rightarrow S_0$ transitions are governed by the anharmonicity of the CH stretching modes. They also found semi-quantitative agreement between the anharmonicity parameter in the Frank-Condon factors and the known anharmonicity of the CH molecule.

The local mode concepts and normal mode concepts are complementary In normal modes the molecules are considered as 3N-6(5) uncoupled harmonic oscillators, which vibrates in infinitesimal amplitudes. This model is found to be successful in explaining the fundamental and lower overtone spectra of polyatomic molecules. Continuous pumping of energy into the vibrational modes of a molecule leads to

dissociation, which is of non-harmonic in nature. Here the molecule violates the normal mode concepts by following a low energy pathway leading to dissociation.

Consider the CH stretching vibrations of benzene. There are six identical CH bonds and hence six CH stretching vibrations [5]. These belong to various symmetry species. If we supply sufficient energy it will eventually dissociate losing six hydrogen atoms in the process

$C_6H_6 \rightarrow C_6 + 6H$

the dissociation in above equation requires almost six times the CH bond dissociation energy. But the process actually happen is

$C_6H_6 \rightarrow C_6H_5 + H$

The difficulty here is that no normal vibration of benzene leads to CH stretching being localized in only one bond. These considerations together with a very early observation of up to eight quanta of CH stretching in benzene led to the concept of local mode of vibration.

For diatomic molecules the relation between anharmonicity constant X and dissociation energy D is clear from the relation

$$X = -w^2/4D \qquad (1)$$

Where X is the anharmonic constant. When a diatomic molecule concept is followed there exists much ambiguity in the relation between normal mode anharmonicity constants X_{kk}, bond dissociation energies D_i and normal mode dissociation energy D_k. since in normal modes the vibrational energy is evenly distributed among a number of equivalent chemical bonds. The dissociation energy D_k will be the sum of all bond energies Di

$$D_k = \Sigma_i D_i \qquad (2)$$

This implies a large value of D_k and hence a small value for diagonal normal mode anharmonicity constants. Physically dissociation means rapture of a single chemical bond. The vibration associated with this rapture is not a normal mode but it is a local mode and $D_i << D_k$. thus the corresponding anharmonicity constants X_{ii} will be much larger than X_{kk}. Thus it can be inferred that for higher vibrational levels, the

vibrational energy becomes increasingly more diagonal in a local mode representation than in a normal mode representation. It implies that the molecule will oscillate in a pattern closer to a local mode rather than a normal mode.

Ellis in 1928 has given the empirical evidence [6-8] for the one dimensional anharmonic oscillator in the overtone spectrum of benzene. The energy levels of a one dimensional anharmonic oscillator given by the perturbation theory as [9]

$$\Delta E_{v,0} = -\frac{1}{2}\left(X_1 + \frac{1}{2}X_2\right) + \left(v + \frac{1}{2}\right)X_1 + \left(v + \frac{1}{2}\right)^2 \qquad (3)$$

Ellis fitted the observed overtone bands to the equation

$$\Delta E_{v,0} = Av + Bv^2 \qquad (4)$$

where A and B are constants and v is the overtone level.

The empirical constants A and B in eqn.(4) are related with eqn. (3) as X_1= A-B and X_2= B the anharmonicity. X_1 and X_2 are related to conventional spectroscopic parameters through $X_1 = w_e$ and $X_2 = w_eX_e$

Henry and coworkers used these local mode ideas to obtain normal mode anharmonicity constants and has described the overtone spectra of molecules NH_3 C_6H_6, CH_2Cl_2 and many others. in terms of the normal mode anharmonicity components. They concluded that higher vibrational levels of X-H (X= C,N,O.....) containing molecules cannot be describe in terms of a set of symmetry allowed normal mode components but instead by a relatively small number of most anharmonic motions namely localized excitation of band modes [10-11]. Swofford et.al, in their study of the fifth overtone spectra of benzene, give a quantum mechanical description of the single bond based one dimensional appearance of CH overtone spectra [12]. Overtone spectra of wide variety of molecules have been interpreted using local modes [10] in addition to pure overtones; it is found that there exists additional weak features in many overtone spectra. These are combination bands arising from excitation of more than one local mode (local-local combination or excitation of local-normal combinations. This implies the presence of non-zero couplings between local modes and between local and normal modes. However the magnitudes of these couplings are found to be much smaller than

diagonal local mode anharmonicity values. Thus the local mode description can be used as a good zero order picture to start within the calculations of vibrational spectra. Henry and co-workers coined the following empirical rules [10] related to overtone spectra.

(i) Local mode overtones involving high frequency oscillators are most intense but fall off rapidly in intensity with increasing vibrational quantum number.

(ii) Local-local and local-normal combinations occur generally with much less intensity than pure local mode overtones

(iii) Combination bands fall off more quickly in intensity than do the pure overtones with increase in quantum number.

3.3 Refinements in local mode model

Refinements in local mode model though inclusion of the terms neglected in the zero order local mode model have been suggested by many workers. Sage and Jortner [13-16] used Morse oscillator function to model the CH bond potential and included the Wilson G matrix cross terms involving CH bending and stretching vibrations in the Hamiltonian

The local mode picture uses the local mode model as the starting point and considers the interaction between the equivalent local modes and can thus be used to interpret the entire spectra at least down to first overtone level.

The general form of the coupled local mode Hamiltonian used for an XH_n system is [17-23]

$$H = w\sum v_i + wx\sum (v_i + v_i^2) + \frac{w}{2}\sum_{i=1}^{n}\sum_{j=1}^{n}\gamma(a_i^+ - a_i)(a_j^+ - a_j) + \frac{w}{2}\sum_{i=1}^{n}\sum_{j=1}^{n}\varphi(a_i^+ + a_i)(a_j^- + a_j) \qquad (5)$$

Here the first two terms represent the unperturbed local mode energy and the last two terms represent the harmonic coupling between the local modes. w and wx are the mechanical frequency (X_1) and anharmonicity ($-X_2$) of the XH bonds, V_i and V_j are the quantum numbers for the i^{th} and j^{th} X-H bond respectively. The parameter γ characterizes the kinetic energy coupling between the different XH oscillators and ϕ the corresponding potential energy coupling. These coupling parameters are related to Wilson G and F matrix elements respectively.

$$\gamma = -\frac{1}{2}\frac{G_{ij}}{G_{ii}} \qquad (6)$$

$$\varphi = \frac{1}{2}\frac{F_{ij}}{F_{ii}} \qquad (7)$$

The operators a^+ and a are related to the normalized momentum coordinate variables through

$$p = (a^+ - a) \qquad (8)$$

$$q = (a^+ + a) \qquad (9)$$

and the usual raising and lowering properties in the harmonic oscillator limit [24]

$$\langle v+1|a^+|v\rangle = (v+1)^{1/2} \qquad (10a)$$

$$\langle v-1|a|v\rangle = v^{1/2} \qquad (10b)$$

These properties are shown to be valid to a good approximation even for Morse oscillators [25]. This is called ladder approximation. Since manifolds corresponding to different values of total quantum number ($\sum v_i$) are well separated in energy, inter manifold coupling are neglected.

3.4 Anharmonicity

If motion of molecular groups responsible for absorption on infra-red radiation is strictly harmonic there will be no absorption of radiation at overtone and combination frequencies of fundamental vibrations. However, these molecular motions are more harmonic than other resonant vibrations in nature. The deviation from simple harmonic motion of molecular group increases with the amplitude of oscillations become very large as the amplitude approaches that required for dissociation of group. It is the function of masses and force constant 'k' of the atoms involved. Hydrogen, being the lightest atom oscillates with large amplitude when undergoing stretching mode. Therefore, its motion deviates appreciably from harmonic. It is said to undergo anharmonic oscillations. The restoring force acting upon the vibrating atom is no longer is a single function of displacement from the equilibrium of the atom, but complex function of many dimensions. The degree of anharmonicity of molecular motion can be determined by measuring the difference between the observed frequencies of overtone vibrations and the simple multiple of the fundamental vibrations.

$$v_v = v_o(1-v_x)$$

where v_v is the observed frequency of v^{th} harmonic v_o is the frequency of the fundamental vibration and 'x' is positive constant indicate anharmonicity. This simple formula is very useful for prediction or identification of overtone and combination bands.

Overtone and combination bands are observed in the infrared spectra not only because of a mechanical anharmonicity of motion, but also because of an electrical anharmonicity in the variation of displacement with motion. Absorption of infrared radiation occurs only when the displacement changes during the course of resonant vibrations with asymmetry that corresponding to a transition of the molecule [10].

3.5 Experimental techniques

Numerous investigations of overtone spectra of the X-H stretching vibrations have been carried out by various workers. Recently new techniques to measure the highly excited overtones of molecular vibrations in liquid phase have been developed. Thermal blooming spectroscopy and Photo Acoustic spectroscopy are widely used techniques to record higher overtone absorption peaks. Conventional spectrometers can be used to record the spectra of molecules in the liquid phase and in gaseous phase. But the path length in the spectrometer is minimum and one cannot go for higher overtones using a conventional spectrometer.

Thermal lens was first observed and described by Gordon and co-workers in 1964 [26-27] the application of duel beam photo thermal technique was first employed by Long et.al [28]. Point by point division of the lock in signal by the corresponding relative power of the pumping laser gives the absorption of the sample in arbitrary units

Photo Acoustic Technique is now the most widely used technique to obtain the higher overtone spectra of molecules. The vibrational overtone excitation laser beam passes through a photo acoustic cell equipped with a microphone and glass Brewster windows.

3.6 Birge-Sponer Plots

A Birge-Sponer plot represents the value of an overtone band center, $\tilde{\nu}_i$, divided by the corresponding number of vibrational quanta, v_i as a function of this quantum number [32]. The resulting curve is a line described by equation

$$\tilde{\nu}_i = A_i v_i^2 + B_i v_i \Rightarrow \frac{\tilde{\nu}_i}{v_i} = A_i v_i + B_i \qquad (11)$$

The intercept B_i is proportional to the harmonic frequency of the vibrational mode involved, and its slop, A_i is the vibrational anharmonicity. This is a quite simple model and is very useful in vibrational band assignment. In the case of a family of combination bands of the form $nv_i + v_j$, two different modes are involved i and j. subtracting the

fundamental frequency of the second mode, $\tilde{\nu}_j$, from the combination band transition frequency recovers the Birge-Sponer dependence of the first mode,

$$\frac{\tilde{\nu}_{ij} - \tilde{\nu}_j}{\nu_i} = A\nu_i + B \qquad (12)$$

3.7 Applications of Overtone Spectroscopy

The most important application of spectroscopy finds its place in the characterization of CH bonds in organic compounds. This serves as sensitive probe into the structural information in polyatomic molecules. From the IR spectroscopic studies it is difficult to understand the influence of environment on a particular CH oscillator. The overtone spectra give the anharmonicity values of local mode oscillators which determine the shape of the oscillator potential, but the IR studies yields only the frequencies of isolated CH bonds.

The local mode parameters X_1 and X_2 are characteristics of the particular CH oscillator and thus gives rise to distinct absorption peaks corresponding to the distinct non-equivalent CH oscillators in the molecule. The non-equivalence of CH oscillators occurs because of many reasons. It is well known that the aryl and alkyl CH bonds are non-equivalent due to the difference on states of carbon hybridization. In an alkane there exist no-equivalent CH bonds as primary, secondary and tertiary. Non-equivalence of CH bonds can also arise from conformational origin, inter and intramolecular environmental origin etc.

Much work has been carried out on the effect of substituent atoms or groups on CH oscillators of molecules, which are reflected by shifts in the overtone transition energy and local mode parameters [29-31]

3.8 CH bond length

Mizugai and Katayama [32] Wong and Moor [33] and Gouch and Henry [34] have noted a correlation between CH overtone frequencies and CH bond lengths. The overtone frequencies are a particularly sensitive probe of CH bond length changes. At

$\Delta\ v_{CH}$=6 a bond length change of 0.001A^0 corresponds to a frequency shift of 69 cm^{-1} [33]. A shift of 10 cm^{-1} in wave number corresponds to a bond length change of 0.001A^0 The change in aryl CH bond length can be calculated using the relation

$$r_{CH}^{LM}(A^0) = 1.084 - \left(\frac{\Delta\nu}{11\Delta\nu_{CH}}\right)0.001$$

where 1.084 is the bond length of aryl CH in benzene Δv is the frequency shift from benzene for the given overtone transition.

The following chapter analyses the effect of substitution in certain organic molecules using the local mode model described above.

References

1. W.Siebrand, *J.Chem Phys.* 46 440 1967.
2. W.Siebrand, *J.Chem Phys* 47, 2411, 1967.
3. W.Siebrand and D.F Williams *J.Chem Phys* 49, 1860 1968.
4. B. R Henry and W.Siebrand , *J.Chem Phys* 49, 5369, 1968.
5. J.M Hollas " High Resolution Spectroscopy" II ed. John Weily & Sons,1998, p. 250
6. J.W Ellis, T*rans.Faraday. Soc.*25, 888,1929.
7 J.W Ellis *Phys. Rev.* 32, 906, 1928.
8. J.W Ellis *Phys.Rev.* 33,27,1929.
9. E.B Wilson, Jr, J.C Decius and P.C Cross, " Molecular Vibrations" Mc Graw Hill New York, 1945
10. B.R Henry *Acc.Chem.Res.* 10,27,1977.
11. B.R Henry *J. Phys Chem.* 80, 2160, 1976.
12.R.L Swofford, M.E Long, and A.C Albrecht, *J. Chem.Phys.* 65, 179,1976.
13. M.L Sage, and J.Jortner, "Advances in Chemocal Physics" 47, 293, 1981
14. M.L Sage, *Chem. Phys.*, 35, 375, 1978.
15. M.L Sage, and J.Jortner, *Chem.Phys.Lett.* 62, 451, 1979.

16. M.L Sage *J.Phys.Chem.* 83, 1455, 1979

17 O. S Mortensen, B.R Henry M.A Mohammadi, J.Chem. Phys. 75, 4800, 1981

18. M.K Ahmed and B.R Henry J. Phys.Chem 90,1081 (1986)

19. T.M.A Rasheed, V.P.N Nampoori and K.Sathyanandan *Chem.Phys.*108 349, 1986

20 B R Henry, A.W, Tarr, O.S Mortensen, W.F Murphyand D.A.C Compton, *J.Chem. Phys* 79, 2583, 1983.

21. A.W Tarr and B.R Henry *J.Chem. Phys* 84, 1355, 1986

22 L Halonen and M.S Child, *J. Chem. Phys* 79,4355,1983

23 L Halonen and M.S Child, *J. Chem. Phys* 79,559, 1983

24. Leonard I. Schiff, "Quantum Mechanics" 3rd edition McGraw-Hill 1968 p.182

25.O.S Mortensen, B.R Henry, and M.A Mohammadi, *J.Chem.Phys.* 75, 4800 1981.

26. J.P Gordon, R.C.C Leite, R.S Moor S.P.S Porto and J.R Whinnery *Bull.Am.Phys.Soci.* (2),9,501, 1964

27. J.P Gordon, R.C.C Leite, R.S Moor S.P.S Porto and J.R Whinnery, *J.Appl.Phys.* 36, 3, 1965.

28. M.E Long, R.L Swoffed and A.C Alberecht, *Science*, 191, 183,1976.

29. Y Mizugai and M .Katayama, *J Am.Chem Soc.* 102, 6424 1980.

30. R Nakagaki and I Hanazaki, *Spectrochim. Acta.* 404 57, 1984

31. K.M Gough and B.R Henry, *J Chem.Phys.* 87, 3433, 1983.

32 Y Mizugai and M .Katayama, *J. Am.Chem.Soc.*102, 6424, 1980

33 J.S Wong and C.B Moor J Chem Phys. 77, 603, 1982.

34 K.M Gough and B.R Henry, *J.Phys Chem.* 88, 1298, 1984

CHAPTER 4

NIR overtone analysis of halo and nitro substituted methylbenzens

4.1 Introduction

Methylation of benzene leads to several important changes. It reduces the point group symmetry to C_2v when the methyl rotor is nearly free [1]. The fundamental vibration of toluene is an old problem, which still stimulates interest. [2-4]. Toluene is well known for its 6-fold barrier to internal rotation (torsion). Thus in the ground state methyl group will rotate almost freely [5]. As vibrational energy is increased the methyl torsion becomes more hindered but still relatively free. The nearly free internal rotation affects the vibration rotation band envelope [1]. The methyl rotor accelerates the intermolecular vibration redistribution [6]. The torsion of the methyl group will have an effect on the CH bond lengths in the molecule and this will be pronounced on the peak positions in the CH stretching overtone spectra. It will also affect the dipole moment function of the aryl bond and changes very little with rotation of the methyl group.

The *ab initio* optimizations of toluene at the planar and perpendicular conformers show that the methyl CH bond lengths change more than the aryl CH bond lengths with methyl torsion. The calculated variation of the methyl CH bond lengths is about 3mA° at both the HF/6-31G(d) and HF/6-311+G (d,p) level calculations [5]. The change in the methyl bond length varies approximately as a $\sin^2\theta$ function [7]. As a result the frequency and anharmonicity of the CH oscillator are expected to vary with θ.

4.2 Theory of vibrational states of methylated benzene

The total vibrational Hamiltonian for a system of five-coupled harmonic oscillator is

$$H = \sum_{i=1}^{5}\left(\frac{p^2 i}{2\mu} + v(r_i)\right) + H' \quad \text{.....(1)}$$

$$H = \sum_{i=1}^{4}(\xi_i p_i p_{i+1} + \eta_i r_i r_{i+1}) \quad \text{.....(1}a\text{)}$$

using nearest neighbor ring XH bond interactions, as in fig. 1, none of the oscillators has a common nucleus. $V(r_i)$ is the anharmonic potential function for a diatomic oscillators all of which are defined by identical parameters. Here the unperturbed basis is chosen as the product of harmonic oscillator basis kets. If $|n\rangle i$ indicates the Eigen ket of the i^{th} oscillator with n quanta of excitation, then the ground and excited states of the set of five ring CH oscillators are

$$|0\rangle = \prod_{i=1}^{5}|0\rangle_i$$

$$|v_i\rangle = |v\rangle i \prod_{j\neq 1}|0\rangle_j,$$

$$|v_i v_j\rangle = |v\rangle_i |v\rangle_j \prod_{k\neq j, k\neq i}|0\rangle_k \quad \text{.....(2)}$$

In the above notation each ket is product of five bond oscillator kets. The ket $|0\rangle$ contains no quantum of excitation. For the other ones only the number of quanta of different oscillators is indicated. Thus the excited state $|v_i\rangle$ indicates the states where only the i^{th} oscillator is excited to v, $|1_i 1_j\rangle$ is a state where both the i^{th} and j^{th} oscillators are excited to v=1 state. The matrix elements of the Hamiltonian in the above basis are

$$\langle v_i\, v_j|H|v_i\, v_j\rangle = \omega(v_i + v_j) - x[v_i(v_i+1) + v_j(v_j+1)] + \frac{5}{2}\left(\omega - \frac{1}{2}x\right) \quad \text{.....(3)}$$

$$\langle v_i + 1\, v_{i+1} - 1|H|v_i\, v_{i+1}\rangle = \frac{1}{2}k_i[(v_i+1)v_{i+1}]^{1/2} \quad \text{.....(4a)}$$

$$\langle v_i - 1\, v_{i+1} + 1|H|v_i\, v_{i+1}\rangle = \frac{1}{2}k_i[v_i(v_{i+1}+1)]^{1/2} \quad \text{.....(4b)}$$

where

$$k_i = \omega[\xi_i \mu + \eta_i / f] \quad \text{.....(4c)}$$

ξ_i and η_I are kinetic and potential energy interaction terms, respectively; μ is the reduced mass and f is the harmonic force constant; $4\pi^2c^2\omega^2 = f/\mu$ and x is the anharmonicity constant defined by the parameters of the potential function, this is treated as a fitting parameter.

In the first excited state (v=1) the Hamiltonian equation (1) has a 5×5 tri-diagonal representation. We can obtain a block digitalization into 3×3 A_1 and 2×2 B_2 matrices by using symmetrized basis kets,

$$|S1_i\rangle = \sum_k a_{ik}|1_k\rangle \quad \text{.....(5)}$$

where

$$\begin{bmatrix} 1/\sqrt{2} & 0 & 0 & 0 & 1/2 \\ 0 & 1/\sqrt{2} & 0 & 1/\sqrt{2} & 0 \\ 0 & 0 & 1 & 0 & 0 \\ 0 & 1/\sqrt{2} & 0 & -1/\sqrt{2} & 0 \\ 1/\sqrt{2} & 0 & 0 & 0 & -1/\sqrt{2} \end{bmatrix}$$

for the second excited state, v=2, promotion oscillator σ is used for each oscillator, [8]

$$\sigma_i|v\rangle_i = |v+1\rangle_i \quad \text{.....(6)}$$

In terms of the product states,

$$\sigma_i|1_i\rangle = |2_i\rangle, \sigma|1_j\rangle = |1_i1_j\rangle, etc \quad \text{.....(6a)}$$

$$\Delta_i = \sum_k a_{ik}\sigma_k \quad \text{.....(7)}$$

The application of the five Δ_I operators on the set of five kets $|S1_k\rangle$ leads to fifteen linearly independent kets $|S2_k\rangle$ comprising $9A_1+6B_2$ modes.

Of the five ring CH bonds in toluene, two (1,5) are at the ortho, two (2,4) at the meta and the remaining one (3) is at para position with respect to the methyl group as shown in the figure 1. Assuming interaction between the ortho-meta pairs 1-2 and 4-5 to be the same (K_1) and that between the para and meta position to be K_2, we get the fundamental frequencies

$$\omega_{1,3}(A_1) = \omega - 2x \pm \frac{1}{2}\left(K_1^2 + 2K_2^2\right)^{1/2}$$

$$\omega_2(A_1) = \omega - 2x$$

$$\omega_{4,5}(B_2) = \omega - 2x \pm \frac{1}{2}k_1 \quad \text{.....(8)}$$

for the second excited state, the energy levels and the overtone manifold can be obtained by solving numerically the $9\times9A_1$ and $6\times6B_2$ matrices set up with the basis kets.

4.3 NIR analysis of ortho and meta Chlorotoluene

4.3.1 Introduction

Nakagaki and Hanazaki have analyzed the effects of methylation and chlorination on the aryl CH local mode frequencies at various sites by studying the overtone spectra of mono, di, tri, tetra and penta methylbenzenes [9]. The model suggested by them predicts A terms of any benzene derivative containing chlorine atoms and methyl group assuming additivity of substituent effect. They have demonstrated the validity of their model by comparing the observed and predicted results in *p*- chlorotoluene. The best fit values of the shift in local mode frequency of aryl CH oscillators at different sites for chlorination and methylation obtained by assuming the additivity of the shift in local mode frequency are reproduced table 4.4.1.

The aryl CH overtone spectrum of liquid phase *o*- chlorotoluene and *m*-chlorotoluene. *o*-chlorotoluene shows single peaks at all quantum levels, *m*-chlorotoluene shows more than two peaks at two quantum levels. It is shown below that the peak positions agree with the weighted mean value of local mode frequencies of the non-equivalent CH oscillators, for *o*-chlorotoluene and for *m*-chlorotoluene, obtained from Nakagaki and Hanazaki model.

4.3.2 Experimental.

High purity *o*- chlorotoluene and *m*- chlorotoluene(>99%) obtained from E-Merck, Germany is used for present investigation. The overtone absorption spectrum in the region 2000nm-700nm is recorded from pure liquid (pathlength-1cm and reference-air) at room temperature (26±2°C) Figs 4.4.3-4.4.6 show the overtone spectrum of *o*-chlorotoluene and fig. 4.4 7-4.4.10 show the overtone spectrum of *m*-chlorotoluene in the second through fourth overtone levels.

4.3.3 Results and discussions:

The dominant bands observed in the near infrared spectra are due to aryl CH overtone. The spectra also show the overtones of methyl CH oscillators. The average peak positions and the aryl CH local mode parameters A and B obtained from the Birge-Sponer plot of $\Delta E_{v\leftarrow 0}/V$ verses V are given in Table 4.4.2 for *o*-chlorotoluene and *m*-chlorotoluene.

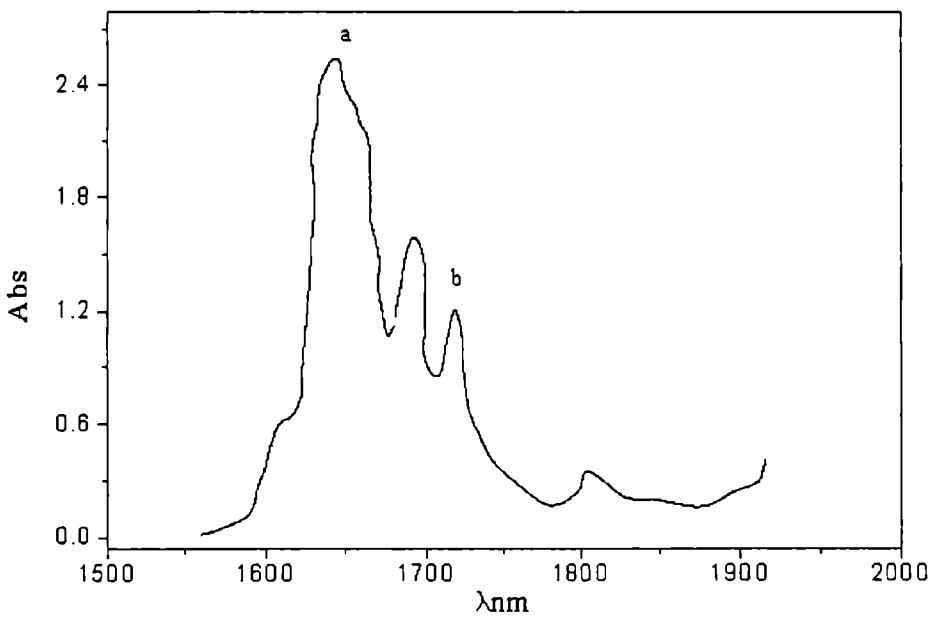

Fig.4.3.1 CH overtone spectrum of o-chlorotoluene
in the region Δv=2 a -aryl band b-methyl band

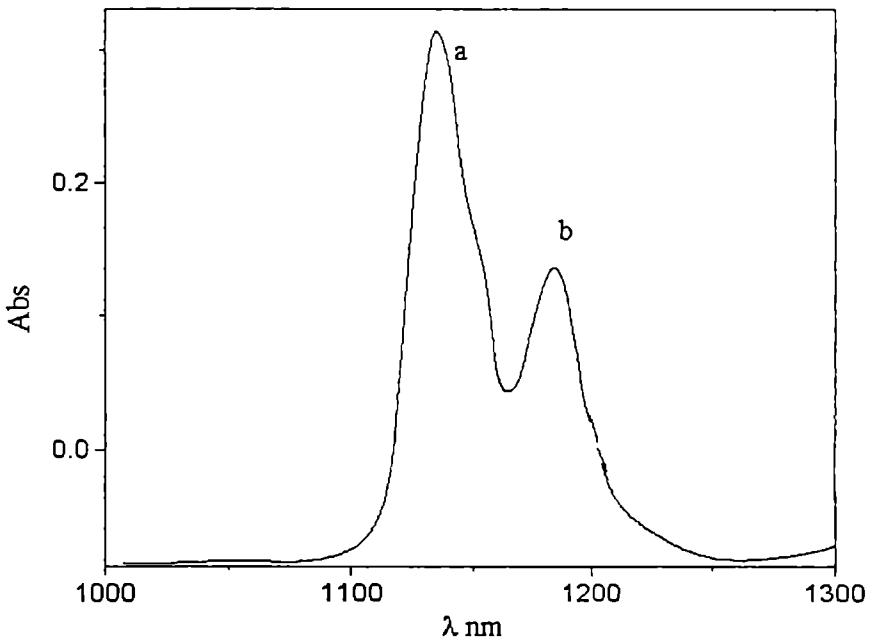

Fig. 4. 3. 2 CH overtone spectrum of o-chlorotoluene
in the region Δv=3 a-aryl band, b-methyl band

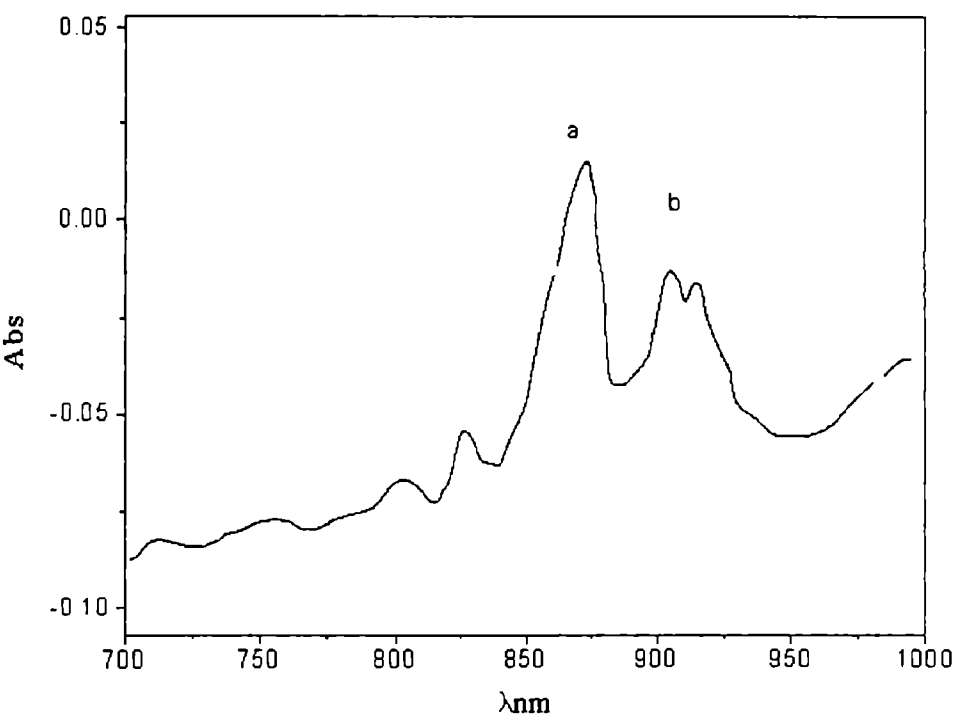

Fig.4.3.3 CH overtone spectrum of o-chlorotoluene
in the region Δv=4 a-aryl band , b-methyl band

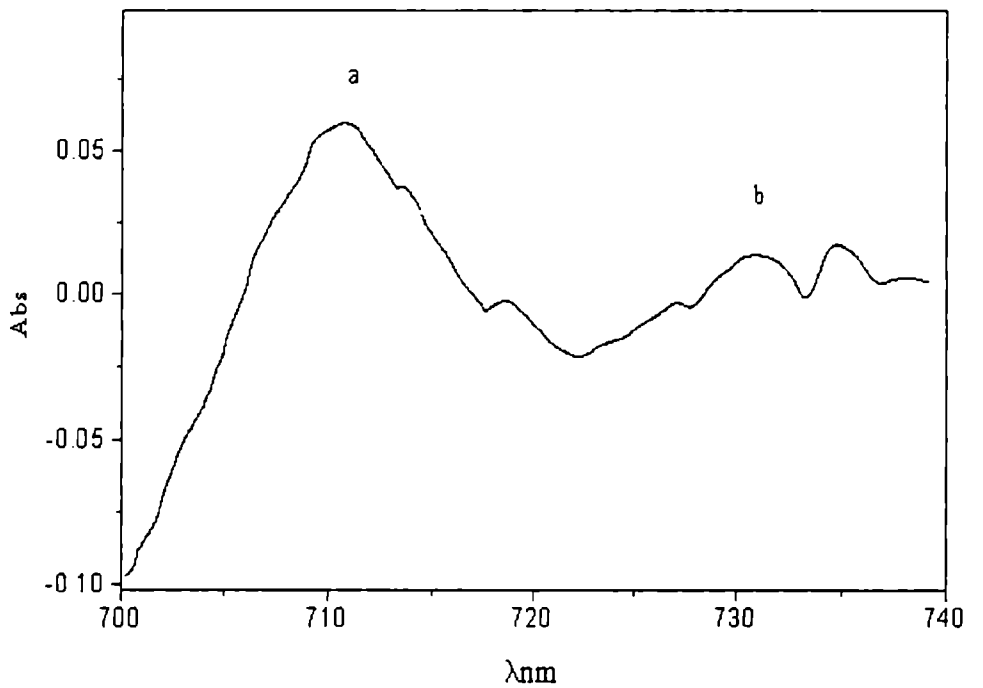

Fig.4.3.4 CH overtone spectrum of o-chlorotoluene
in the region Δv=5 a-aryl band

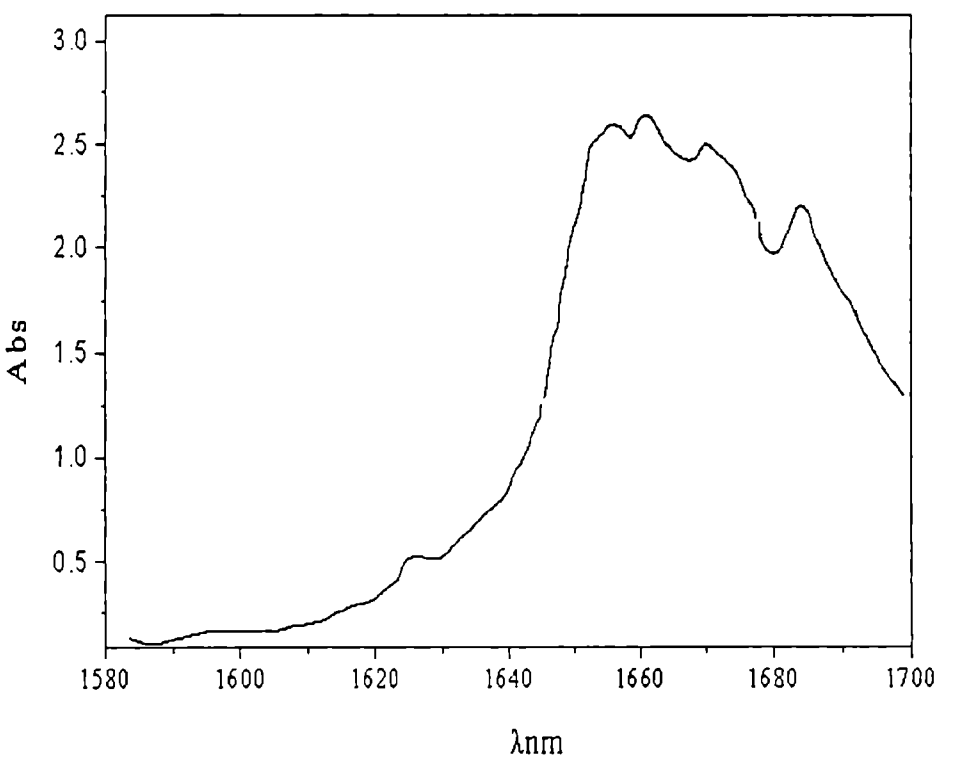

Fig.4.3.6 CH overtone spectrum of m-chlorotoluene
in the region Δv=2 region

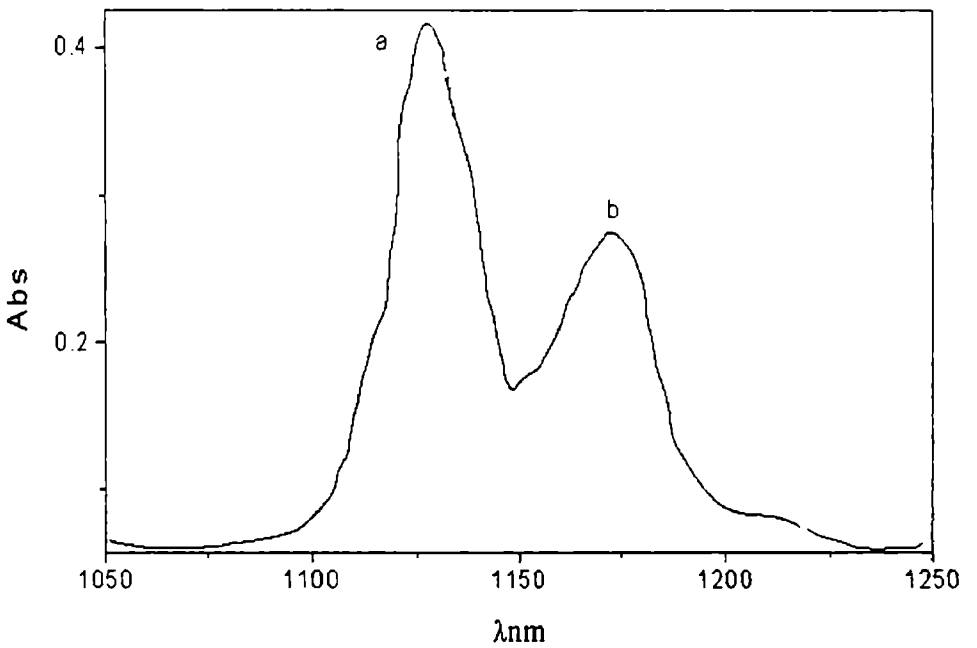

Figh.4.3.7 CH overtone specrum of m-chlorotoluene in the region Δv =3

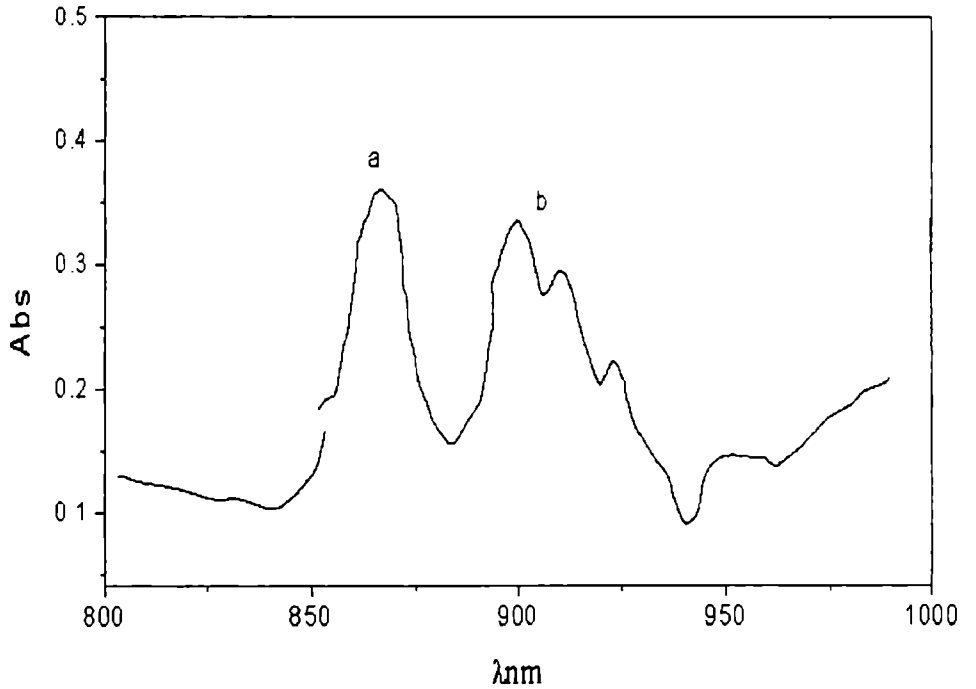

Fig.4.3.8 aryl and alkyl CH overtone spectrum in m-chlorotoluene in the region Δv=4

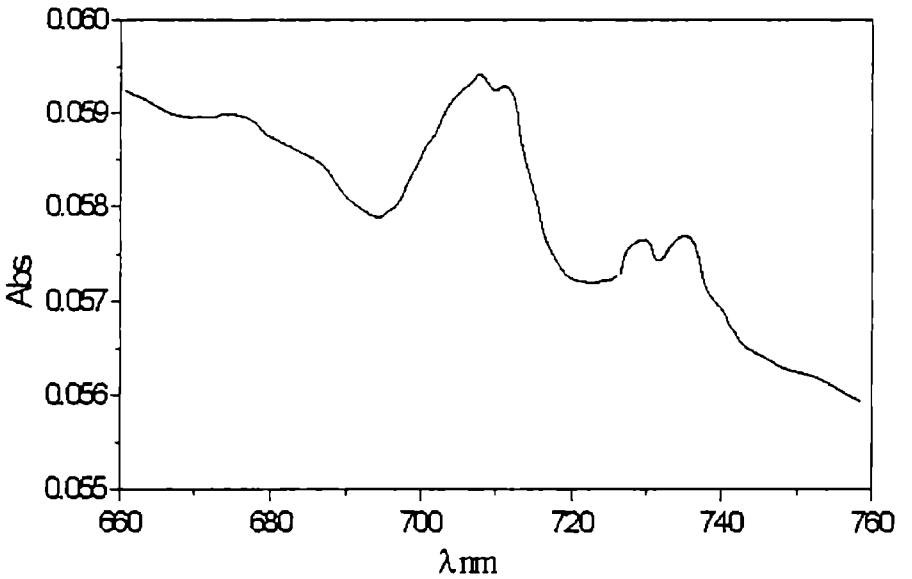

Fig.4.3.9 CH overtone spectrum of m-chlorotoluene in the region $\Delta v=5$

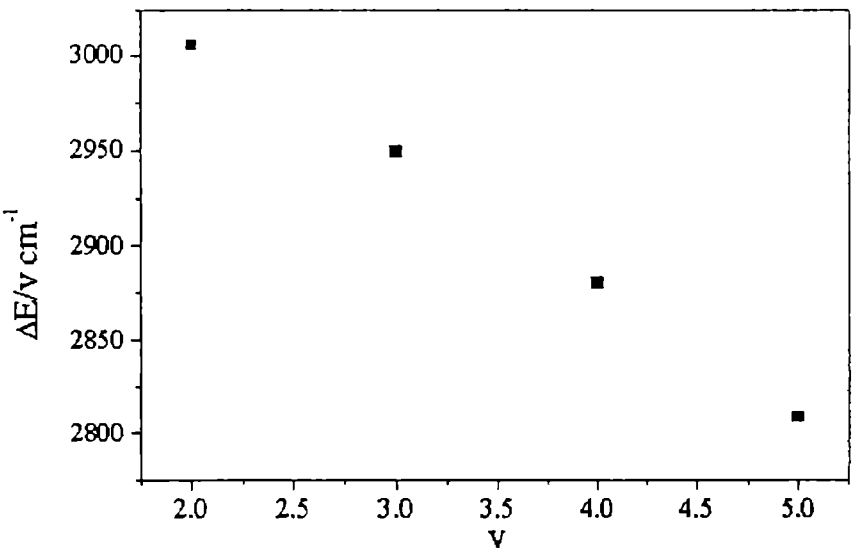

Fig.4.3.9 B-S plot for the aryl CH overtone spectrum of o-chlorotoluene

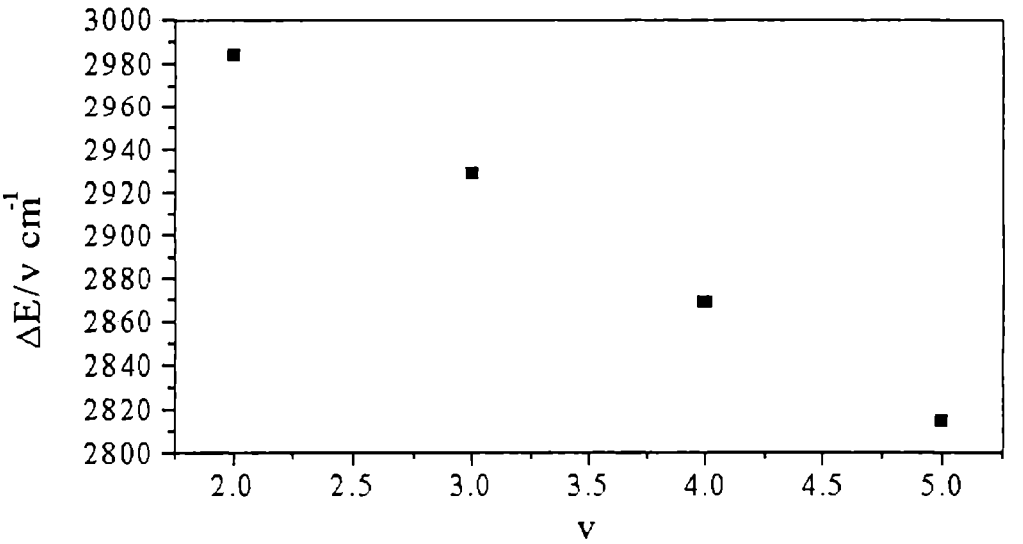

Fig.4.3.10 B-S plot for the aryl CH overtones in m-chlorotoluene

A comparison with the overtone peak positions and local mode parameters in benzene shows that the aryl CH overtone transition energies in *o*-chlorotoluene and *m*-chlorotoluene are blue shifted with respect to those in benzene due to an increased A value (Δ = 2.2 cm^{-1} for *o*-chlorotoluene and 2.7 cm^{-1} for *m*-chlorotoluene)

We shall now attempt to apply the model of Nakagaki and Hanazaki to the aryl CH overtones in *o*-chlorotoluene and *m*-chlorotoluene. Unlike the case of *p*-chlorotoluene where there are only two types of non equivalent CH bonds in the ring, all the four aryl CH bonds in *o*-chlorotoluene and *m*-chlorotoluene are non equivalent.

Denoting the shift in A value with respect to benzene due to methylation and chlorination as Δ^M and Δ^C respectively, we have six such parameters for the CH bonds at ortho, meta and para positions with respect to the substituents. Following the numberings given below and using suffices *o*, *m* and *p* for ortho, meta and para positions, the different oscillators are subjected to shifts as follows.

Since the observed liquid phase spectra show only the unresolved structure of CH overtone transitions, we have to consider the relevant average value of shift over the different sites. i.e.

$$\Delta_{av.} = [\Delta^M_o+\Delta^C_o+2\Delta^M_m+2\Delta^C_m+\Delta^M_p+\Delta^C_p] / 4 \qquad \text{for } o\text{-chlorotoluene}$$

and $$\Delta_{av.} = [2\Delta^M_o+2\Delta^C_o+\Delta^M_p+\Delta^M_m+\Delta^C_m+\Delta^C_p] / 4 \qquad \text{for } m\text{-chlorotoluene}$$

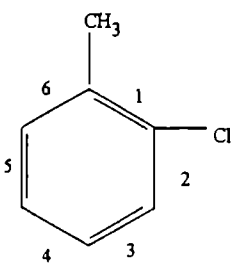

o-Chlorotoluene

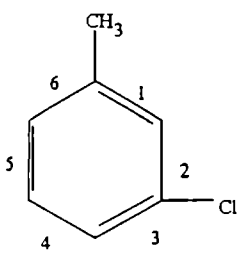

m-Chlorotoluene

Using the best-fit values of shifts reported by Nakagaki and Hanazaki, we get

$\Delta_{av.}$ = 2.8 cm^{-1} for *o*-chlorotoluene. This value is comparable with experimentally measured shift of 2.2cm^{-1} For *m*-chlorotoluene, the calculated and observed shifts are 0.8 and 2.5 cm^{-1} respectively Thus a correction is applied to the equation used to calculate the average shift. Instead of adding the shift due to the CH2 oscillator, which is exactly in between the halogen and the methyl group, it is subtracted form the total shift due to the other CH oscillators as given below

$$\Delta_{av} = \frac{[(\Delta_O^M + \Delta_o^C) - (\Delta_p^M + \Delta_o^C + \Delta_M^M + \Delta_M^C + \Delta_O^M + \Delta_p^C)]}{4}$$

applying this equation we observe that the average shift calculated agrees fairly well with the experimental result. In his case the calculated shift is 2.4 cm^{-1} and the observed shift is 2.7 cm^{-1} It is well established from overtone studies that an electron-withdrawing group increases the mechanical frequency of CH oscillators of the ring. A comparison of the mechanical frequencies of the three isomers of chlorotoluene is given in table 4.3.3. It is observed that the aryl mechanical frequency in p-chlorotoluene shows the highest value compared to the other two molecules. The two ortho CH oscillators with respect to chlorine atom (a, table4.3.3) in p-chlorotoluene show highest mechanical frequency than that of benzene while the other two oscillators (b, table4.3.3) shows a lower frequency than that of benzene [9]. This shows that withdrawal of electrons affects only the ortho CH oscillators of chlorine atom. This may because the other two CH oscillators are shielded by the methyl group. Hence, the withdrawal does not affect them significantly. The steric repulsion of the methyl group to the lone pair electrons in halogens [10] may account for the low mechanical frequency of aryl CH in o-chlorotoluene. Thus, it may conclude that the steric hindrance exerted by methyl group overpowers the resonance withdrawal effect of halogen for the two CH oscillators ortho to alkyl group.

Table 4.3.1. Best fit values of shift in aryl CH local mode frequency (cm^{-1}) due to methylation and chlorination[9]

Shift in A	methylation	chlorination
Δ_o	-16.86	+13.58
Δ_m	-2.46	+7.24
Δ_p	-0.69	+5.50

Table 4.3. 2. Observed transition energies (cm^{-1}) of aryl CH overtones in *o*-chlorotoluene and *m*- chlorotoluene and the local mode parameters (cm^{-1}) obtained from Birge-Sponer plot. The corresponding quantities for benzene are also given for a comparison.

V	o- chlorotoluene cm^{-1}	m- chlorotoluene cm^{-1}	p-chlorotoluene [9] cm^{-1}	Benzene [9] cm^{-1}
2	5959.5	5966.9		5955.8
3	8789.0	8785.0	8727	8758.8
4	11508.0	11474.4	11414	11445.2
5	14044.0	14072.5	13965	14015.0
6			16420	
A	3096.7 ± 1.5	3097.02 ± 2.5	3107.6 ± 6	3094.5
B	-56.6 ± .5	-56.6 ± .7	-56.7 ± 1.2	-58.3
γ^*	-0.997	-0.999		

Table 4.3.3 Comparison of mechanical frequencies in o, m, p, chlorotoluene (all values in cm^{-1})

o-chlorotoluene	3153.1	
m-chlorotoluene	3153.6	
p-chlorotoluene[9]	3162.3 (a)	3142.7 (b)
toluene[9]	3151.2	
benzene[12]	3148	

4.4 Overtone spectroscopic analysis of meta and para fluorotoluene in the NIR region

4.4.1 Introduction

There are two main differences between vibrational spectra of partially F-substituted benzenes and those of benzene.

(i) the partial substitution of hydrogen atoms produces a reduction of the molecular symmetry and a corresponding increase of the number of active infra red vibrational modes [11].

(ii) F induced σ-electron with drawing effects leads to a decrease in the CH bond lengths and to a corresponding increase of the CH excitation frequencies. The second depends on the electro-negativity of the substituent.

4.4.2 Experimental

The NIR overtone spectrum of meta and para fluorotoluene is recorded using Hitachi 3410 spectrophotometer, for a path length of 1 cm at room temperature (26°C). the sample of purification >99% obtained from MERK Germany is used without further purification. The spectra obtained for the different vibrational overtone transitions in the Δv=2, 3 and 4 regions are given in figures 4.4.1-4.4.7 Distinguished peaks were obtained for the aryl CH and methyl CH oscillator. The peaks where assigned with respect to the parent molecule. The observed peak values are applied in the Birge-Sponer relation and the local mode parameters were obtained. Only peaks satisfying Birge-Sponer relation is considered as the pure overtone peaks.(fig 4.4.8-4.4.11)

4.4.3 Results and Discussion

The local mode parameters for the aryl CH and alkyl CH bonds in methyl benzene were calculated by Nakagaki and Hanazaki [9] and also by P.N Ghosh et al [1] and that for fluorobenzene was done by D.Bassi et.al. [11] The mechanical frequency, anharmonicity constants and observed frequencies for the aryl CH and alkyl CH oscillators are given in table 4.4.1 and table 4.4..2 respectively Analysis done by Nakagaki and Hanazaki clearly indicates that the addition of a CH_3 molecule increases the aryl CH bond length an hence the mechanical frequency of the local oscillator decreases considerably from that of benzene [12] as the number of methyl group increases the mechanical frequency decreases to a value of 34 cm^{-1} Halogen substitution shifts the overtone maxima to higher energy while methyl group had the opposite effect. The opposing effect of the methyl and fluoro substituent give rise to two distinct aryl and alkyl CH overtone progressions. The higher frequency progression is assigned to be associated with aryl oscillators adjacent to the fluorine and the lower progression is assigned to the oscillators ortho to the methyl group as described elsewhere [13,14].

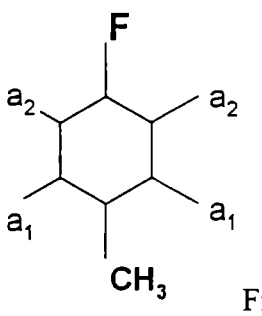

Fig. a p-fluorotoluene

a_1 and a_2 indicates the lower and higher frequency CH oscillators in p-fluorotoluene. (Fig.a)

The methyl Stretching frequencies are sensitive to the type and location of the substituent on the aromatic ring. The frequency shift increase with the number of substituents. [15]. Sowa and Henry have analysed the methyl stretching frequencies in mono halotoluenes.

Though it is expected that the addition of fluorine atom to the ring decrease the aryl CH bond length and hence a higher mechanical frequency, the analysis done by Bassi et.al indicate that the mechanical frequency decreases from that of benzene. In our observation the addition the addition of both fluorine and methyl molecule to the ring cause a decrease in the aryl CH bond length. The substantial hike in the mechanical frequency of the aryl CH oscillator underscores this observation. The mechanical frequency shows an increase of the order of 18 cm^{-1} and 28 cm^{-1} respectively for m and p fluorotoluene. The analysis of alkyl group mechanical frequencies shows that the values have increased much from that of toluene [1]. This indicates more donation of electron to the ring in the fluorinated toluene and hence the alkyl CH bond length decreases. The mechanical frequency shows an increase of the order of 20 cm^{-1} and 35 cm^{-1} respectively for m and p fluorotoluene.

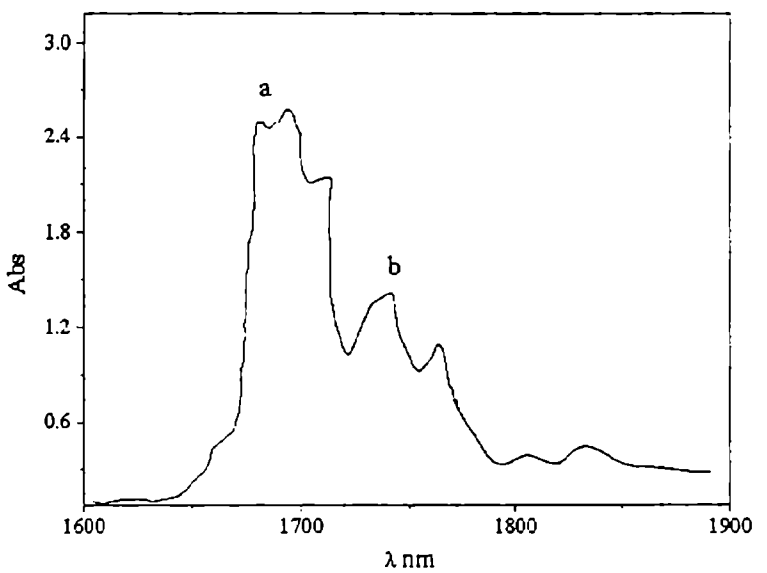

Fig.4.4.1 CH overtone spectrum of m-fluorotoluene
in the region Δv=2 a-aryl, b-alkyl peak

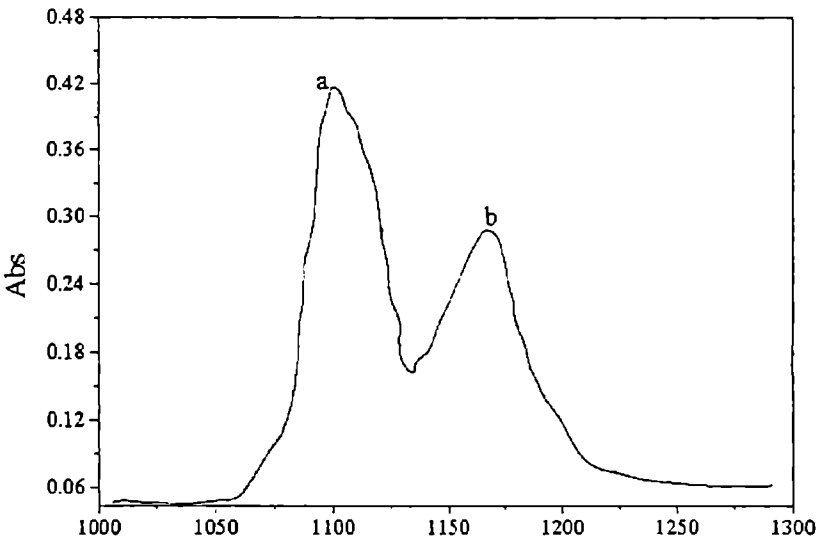

Fig.4.4.2 CH overtone spectrum of
m-fluorotoluene in the region Δv=3. a-aryl b-alkyl peak

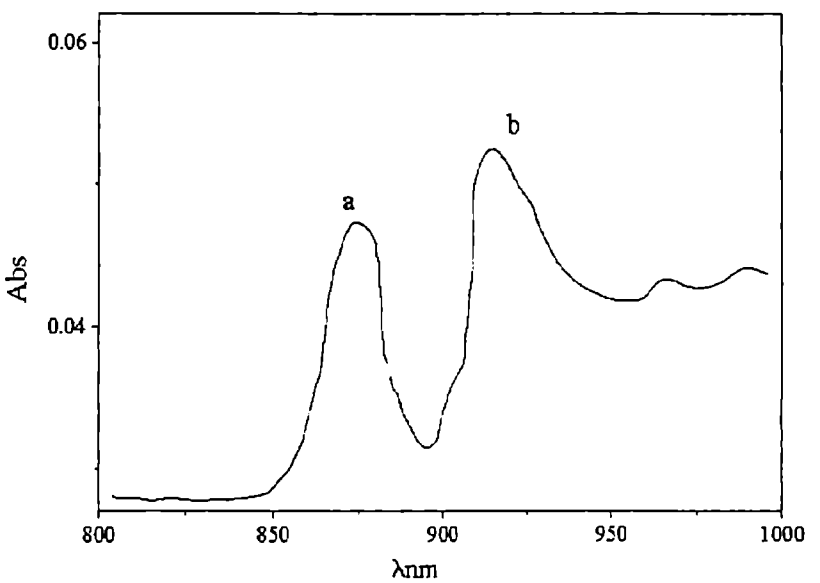

Fig.4.4.3 CH overtone spectrum of m-fluorotoluene
in the region Δv=4 a-aryl, b-alkyl peak

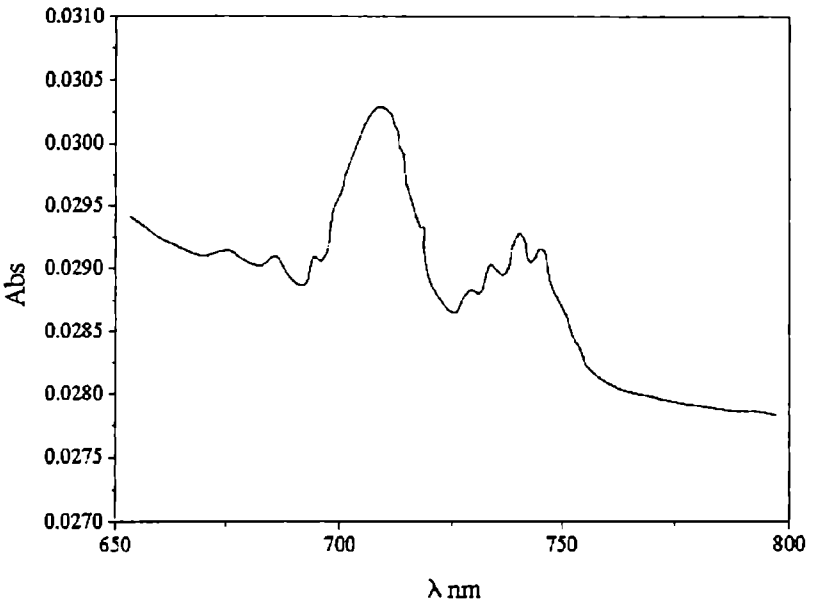

Fig.4.4.4 CH overtone spectrum of m-fluorotoluene in the region Δv=5

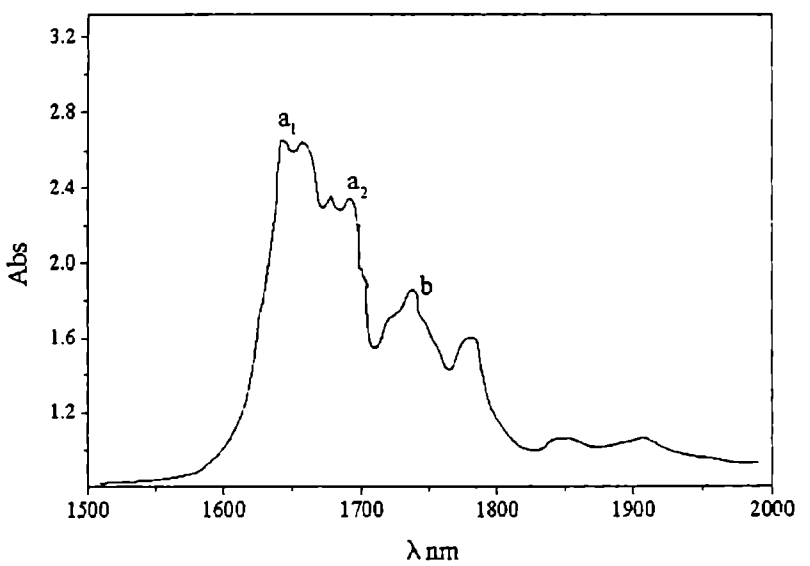

Fig. 4.4.5 CH overtone spectrum of p-fluorotoluene in the region Δv=2 a- aryl peaks (a_1 a_2 corresponds to lower and high energy peaks)and b-alkyl peaks

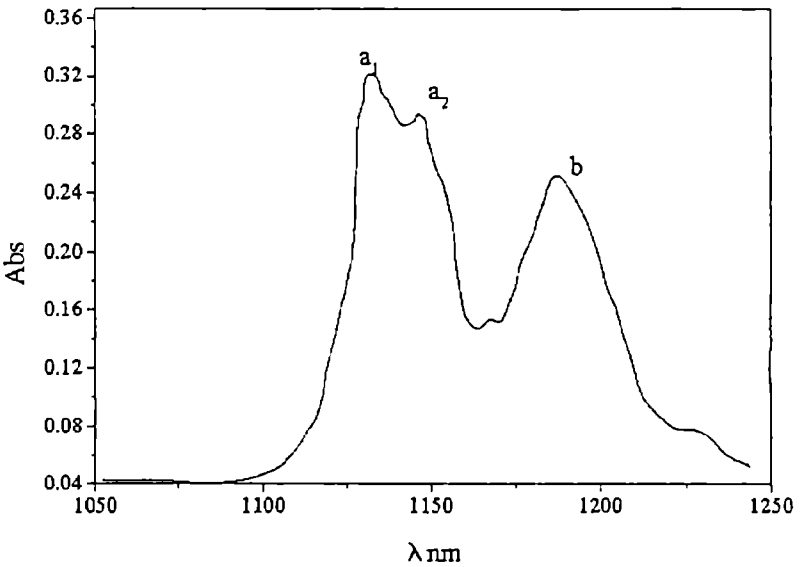

Fig. 4.4.6 CH overtone spectrum of p-fluorotoluene in the region Δv=3 a- aryl peaks (a_1 a_2 corresponds to lower and high energy peaks)and b-alkyl peaks

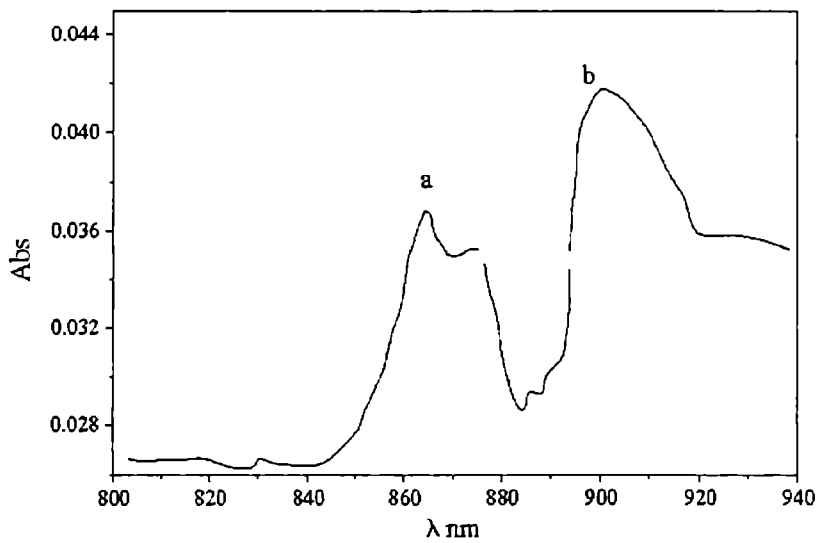

Fig. 4.4.7 CH overtone spectrum of p-fluootoluene in the region Δv=4 a -aryl band and b alkyl band.
a_1 and a_2 are the high and low frequency components

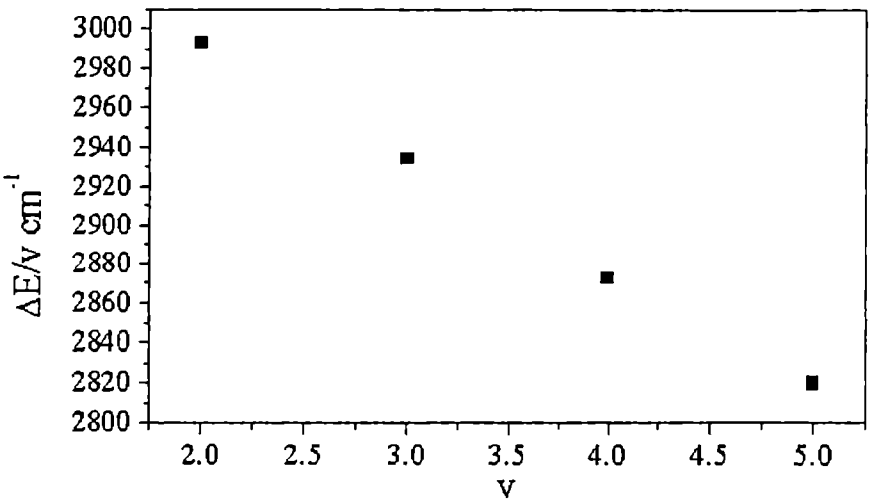

Fig.4.4.8 B-S plot for the aryl CH overtones in m-fluorotoluene

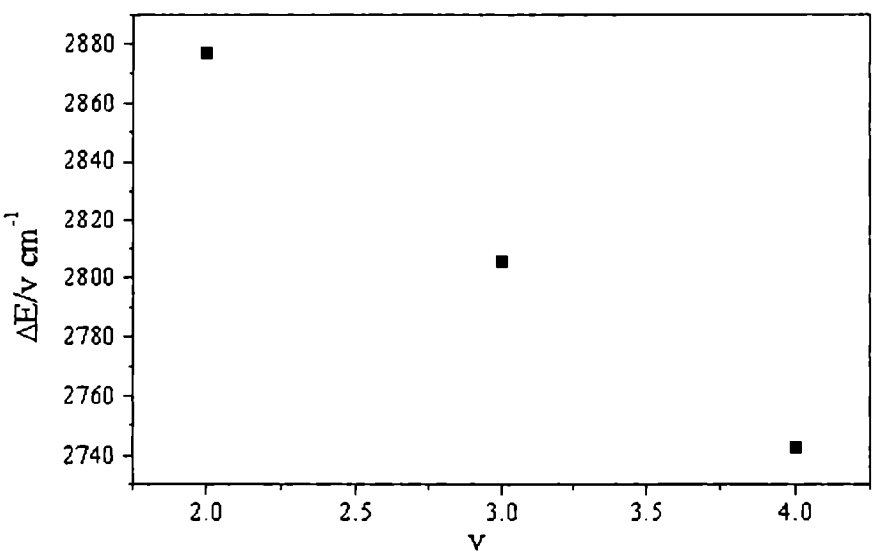

Fig.4.4.9 B-S plot for the alkyl CH overtones in m-fluorotoluene

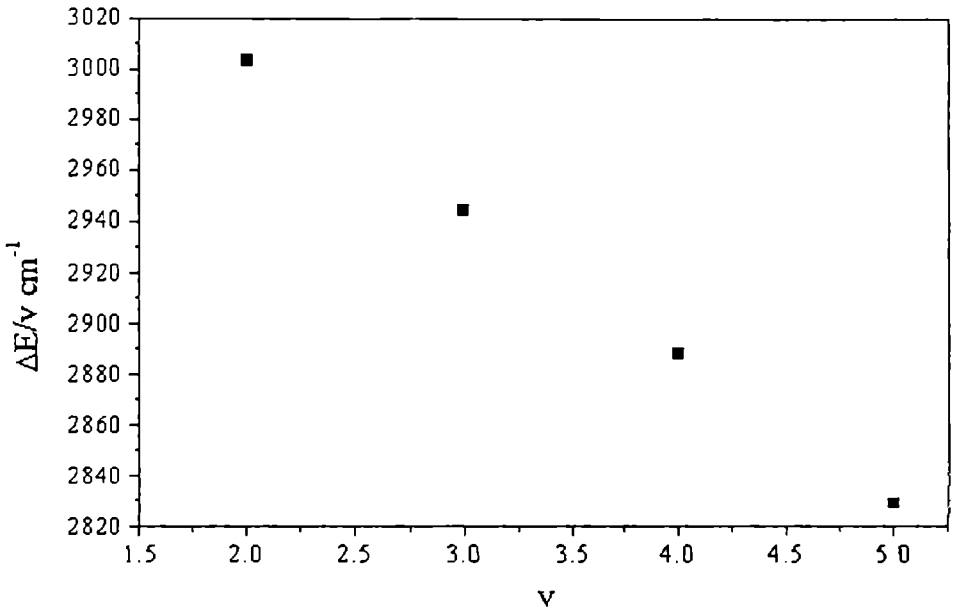

Fig.4.4.10 B-S plot for the aryl CH overtone spectrum of p-flurotoluene

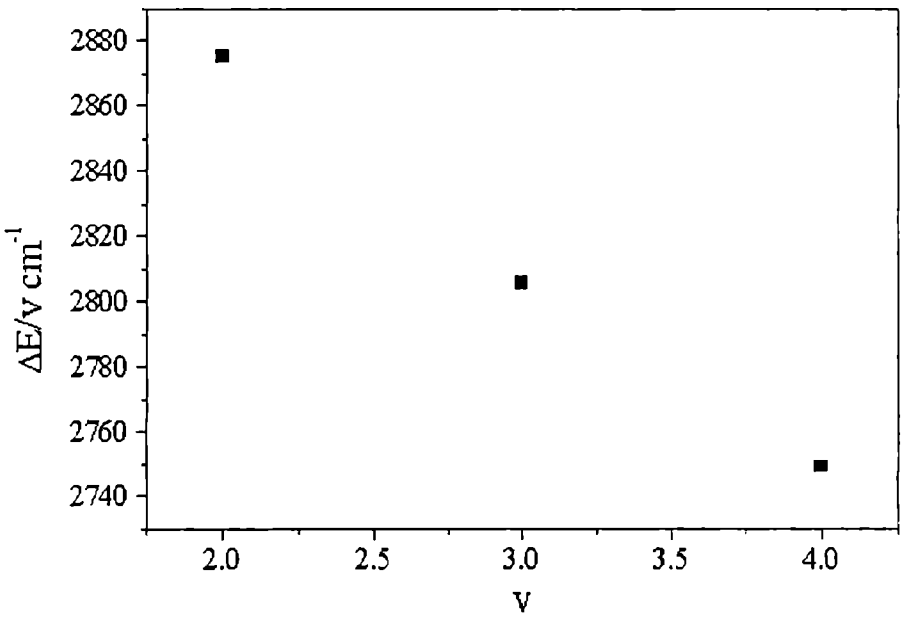

Fig. 4.4.11 B-S plot for the alkyl CH overtone spectrum of p-flurotoluene

Table 4.4.1

Vibrational overtone frequencies, mechanical frequencies and anharmonicity constants of Aryl CH oscillator in *m* and *p* fluorotoluenes (all values in cm^{-1}) a_2-shows the transition frequencies and mechanical frequencies for the aryl CH ortho to fluorine atom and a_1-denotes that ortho to methyl group

Molecule	v=2	v=3	v=4	v=5	ω	ωx	γ
m-fluorotoluene	5986	8803	11492	14098	3167 ± 3.2	-58 ± 2.4	-0.9996
p- fluorotoluene	6006 (a_2)	8832 (a_2)	11550 (a_2)	14144 (a_2)	3176 ± 4.1	-58 ± 1.2	-0.9999
	5975 (a_1)	8756 (a_1)	11432 (a_1)	10492 (a_1)	3180 ± 7.3	64.7 ± 2.3	-0.99933
Methylbenzene					3151	-59	
Fluorobenzene					3142 ± 2	-59 ± 0.6	
Benzene[12]					3148		

Table 4.4.2

Vibrational overtone frequencies, mechanical frequencies and anharmonicity constants of Alkyl CH oscillator in *m* and *p* fluorotoluenes (all values in cm^{-1})

Molecule	v=2	v=3	v=4	ω	ωx	γ
m-fluorotoluene	5754	8417	10969	3077 ± 2.2	-67 ± 2.8	-0.9994
p- fluorotoluene	5751	8416	10996	3063 ± 1.8	-58 ± 1.2	-0.9989
Toluene [1]				3042	-60	

4.5 NIR analysis of ortho, meta and para nitrotoluene

4.5.1 Introduction

2-, 3- and 4-Nitrotoluenes are produced commercially, as a mixture, by nitration of toluene. 2- and 4-Nitrotoluenes are used mainly to produce intermediates in the production of colourants. All of these isomers are also used in much smaller quantities in the production of agricultural, pharmaceutical and rubber chemicals. Human exposure to nitrotoluenes can occur during their production and use, although few data are available.

Nitrotoluenes have been detected in effluents from the manufacture or use of nitrotoluenes and in surface and groundwater. These substances are toxic to aquatic organisms. The substance may cause long-term effects in the aquatic environment

The localized nature of CH stretching overtones indicates that changes relative to a parent molecule reflect the nature of substituent effects [16]. Local mode analysis has been used to understand non-bonded steric interaction in alkanes [17-19]

It has been already recognized that the substituents produce preferential orientation in aromatic substitution and considerable effort was made to analyse the mode of operation of this directed aromatic substitution and correlate it with the molecular properties of substituents [20].

In several methyl substituted butanes it is observed that the intra-molecular steric crowding of the methyl groups provides a barrier to large amplitude vibrational motions. Consequently, the local mode anharmonicity decreases regularly as steric hindrance increases due to increased methyl substitution [21,22]

It is well known that the substituent effect influences the product distribution due to steric effects. In nitrotoluene, the para- product increases as the size of alkyl group increases and block ortho-position. With a $-CH_3$ group, the production yield for ortho-nitrotoluene is 58% while that of para-nitrotoluene is only 37%. But with $C(CH_3)_3$ the yield for ortho-nitrotoluene decreases to 16% and that for para-nitrotoluene increases to 73%. This indicates the steric hindrance offered by the

alkyl group to its ortho nitro group.

The effect of ortho substituent is studied in detail by comparing the rotation of nitro group in o-nitrotoluene and in nitrobenzene [23]. The barrier to rotation for $-NO_2$ group in o-nitrobenzene is approximately 25 K Cal/mol. When a methyl group is added ortho to the $-NO_2$ group the barrier to rotation drops to 13 K Cal/mol. [23]. It is apparent that the substitution at different position affects the potential barrier significantly.

4.5.2 Experimental.

High purity o-nitrotoluene, m-nitrotoluene and p-nitrotoluene (>99%) obtained from CDH Mumbai are used for present investigation. p-nitrotoluene obtained in solid form is dissolved in spectrograde CCl_4. The overtone absorption spectrum in the range 2000nm-700nm is recorded from pure liquids (pathlength-1cm and reference-air) at room temperature (26±2°C) The overtone spectra of ortho, meta and para nitrotoluenes in the regions v=2-5 are given in fig. 4.5.1-4.5.9.

4.5.3 Results and Discussion

The absorption frequencies for each overtone are given in Table 4.5.1. The mechanical frequency (X_1) and anharmonicity constants (X_{CH}) for aryl CH oscillator are given in 4.6.2. In the analysis of the observed frequencies, we have considered only the pure overtone peaks, satisfying the Birge-Sponer relation [24]. Like the halo substituents the nitro group will also shift the overtone maxima to high energy. The opposing effect of the methyl group and nitro substituent give rises to two distinct aryl overtone progressions in p-nitrotoluene (fig.a) similar to p-fluorotoluene. The higher frequency progression is assigned for the oscillators adjacent to nitro group and lower frequency progressions to the oscillators near to methyl group.

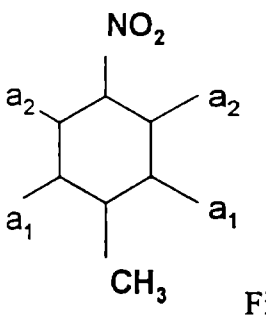

Fig. a p-nitrotoluene

a_1 correspond to lower frequency CH oscillators and a_2 correspond to higher frequency CH oscillators

The Hammet σ constants, [20] both inductive part (σ_I) and resonance part (σ_R) for the nitro group ($-NO_2$) is $\sigma_I = +0.63$ and $\sigma_R = +0.16$ and for methyl group is $\sigma_I = -0.05$ and $\sigma_R = -0.11$. This indicates that the nitro group has significant electron-withdrawing ability from the ring and the methyl group has electron-donating ability to the ring. It is well established from the overtone spectroscopic studies of many substituted benzenes that the local mode mechanical frequency of aryl CH is increases due to electron withdrawing substitution and decreases due to electron donating substitution. The $-NO_2$ group, a strong electron withdrawing group with a positive σ_R and σ_I values, deactivate the aromatic ring by decreasing the electron density on the ring through both resonance and inductive withdrawing mechanisms. Consequently, the π electron density reduces and this creates a net positive charge on the CH carbon atoms, which in turn pulls the electron cloud of the hydrogen atoms towards them. Thus, aryl CH bond lengths decreases and force constant increases. This results in an increase in the mechanical frequency of the aryl CH oscillator from that of benzene. The local mode mechanical frequencies obtained for aryl CH in the three molecules are found greater than that of benzene [12].

The increase in mechanical frequency of the aryl CH in ortho, meta and para nitrotoluenes are found in the order $o < m < p$.

The aryl CH oscillator in o-nitrotoluene shows lowest mechanical frequency compared to other substitutions. This may be attributed to the steric effect of methyl group to its ortho substituent. In o-nitrotoluene the methyl group which is ortho to the $-NO_2$ group causes greater localization of π-electrons on the $-NO_2$ group. This may act as a shield against the withdrawal of electrons to a certain extent. In fact the mechanical frequency is comparable to that of toluene [9]. Thus, in our observation Steric repulsion outweighs the resonance effect of the $-NO_2$ group, which is electron withdrawing.

Solvation effect studies done by Susan E. Barrow *etal.* Clearly indicates a greater localization of partial negative charge near ortho group. This effect is in tune with the steric influence of the substituent to which $-NO_2$ group is ortho [22].

It is showed that in 2,4, dinitrotoluene and 2,4,6 trinitrotoluene, the $-NO_2$ group which is ortho to methyl group is not reduced while the one at para position is reduced much. This result is attributed to the screening effect of methyl group to its ortho substituent.

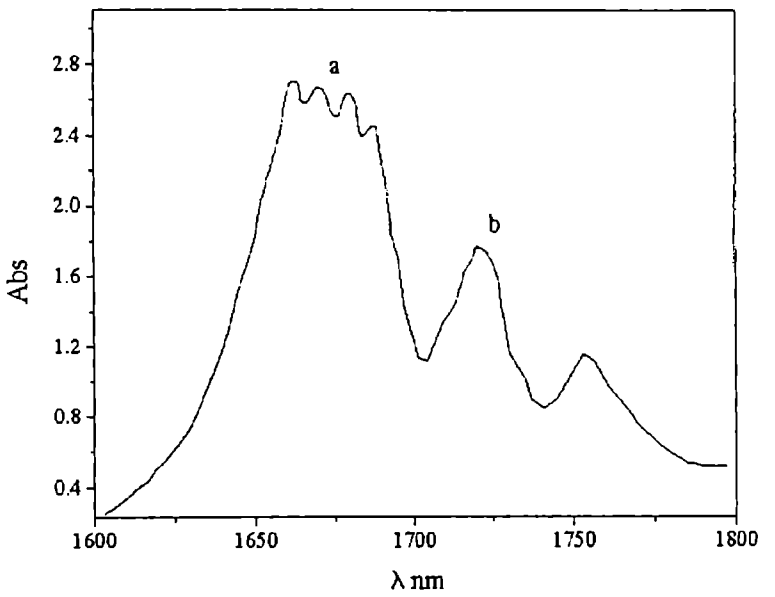

Fig.4.5.1 CH overtone spectrum of o-nitrotoluene in the region $\Delta v=2$ a-aryl band , b-methyl band

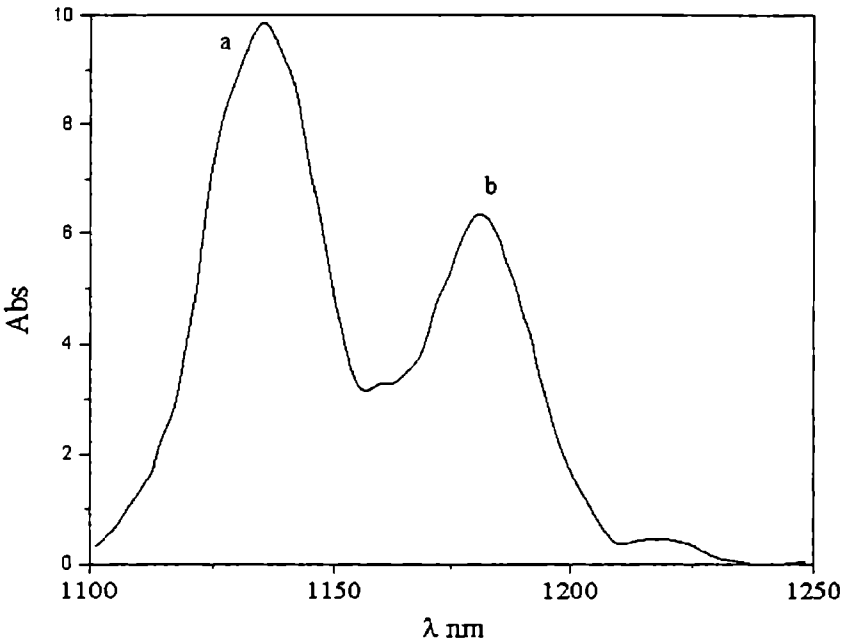

Fig.4.5.2 CH overtone spectrum of o-nitrotoluene in the region Δv=3 a-aryl band , b-methyl band

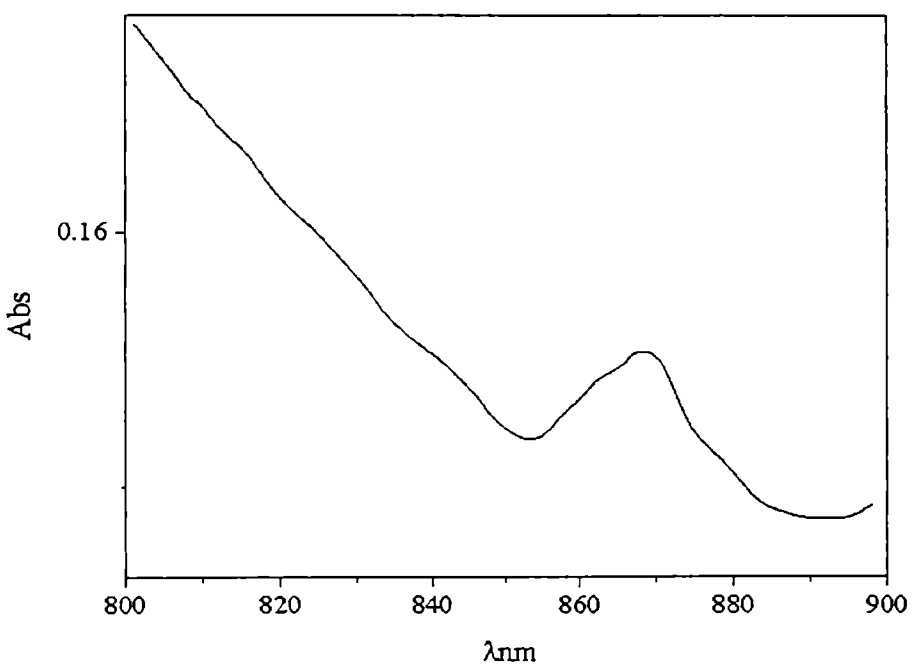

Fig.4.5.3 CH overtone spectrum of o-nitrotoluene in the region Δv=4

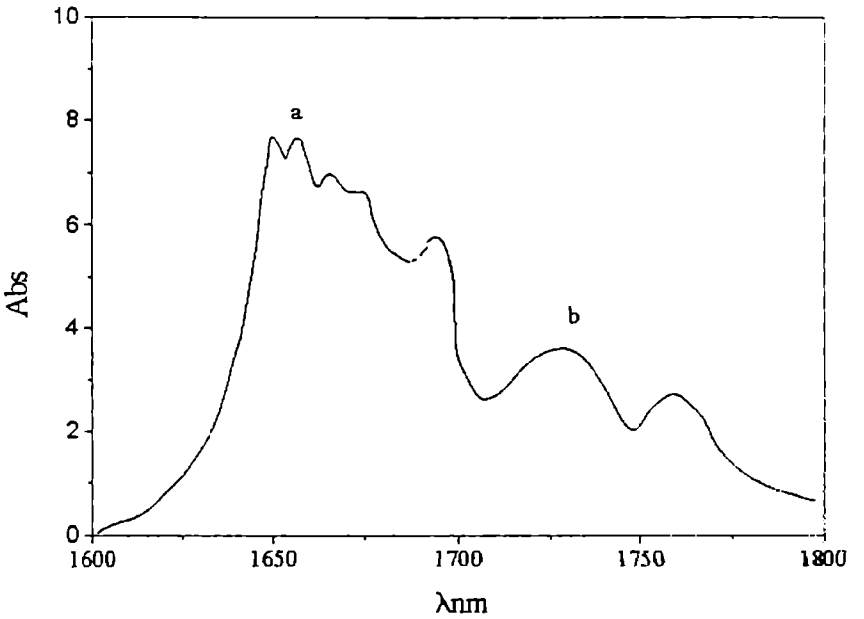

Fig.4.5.4 CH overtone spectrum of m-nitrotoluene in the region Δv=2 a-aryl band , b-methyl band

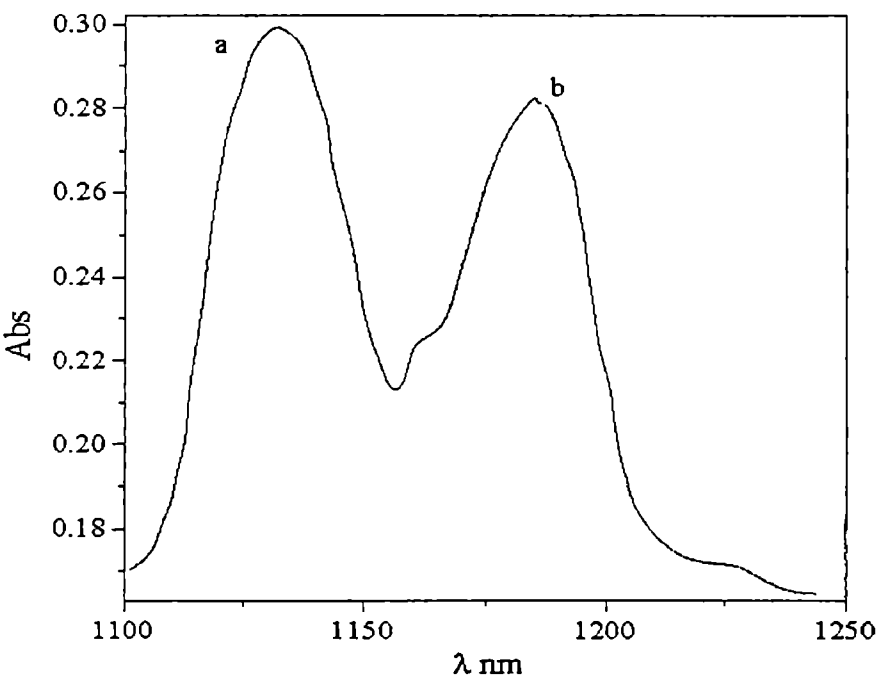

Fig.4. 5.5 CH overtone spectrum of m-nitrotoluene in the region Δv=3 a-aryl band , b-methyl band

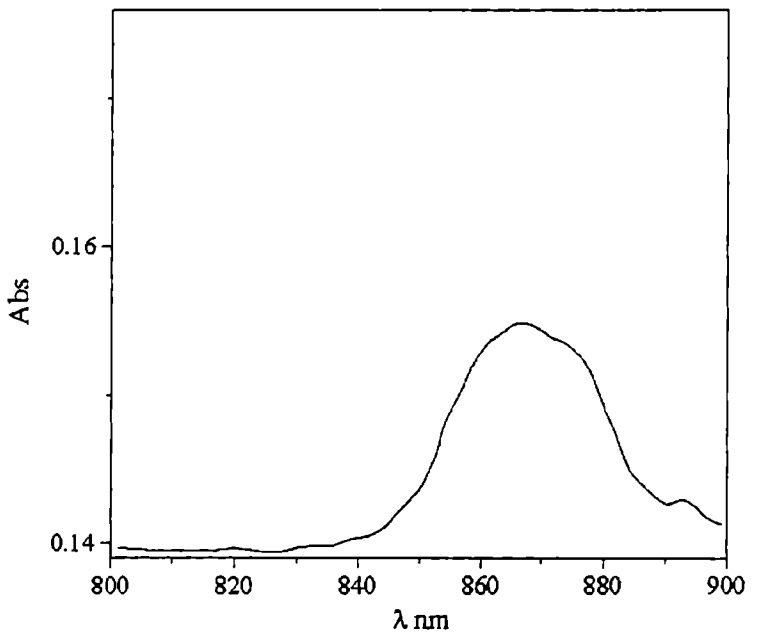

Fig.4.5.6 CH overtone spectrum of m-nitrotoluene
in the region Δv=4

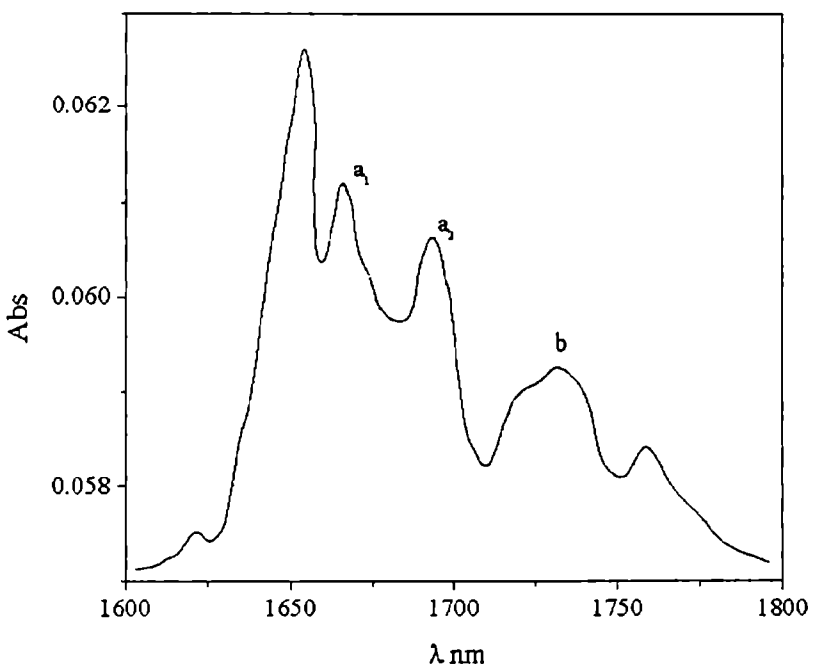

Fig.4.5.7 CH overtone spectrum of p-nitrotoluene
in the region Δv=2 a_1 and a_2 are aryl band and b-methyl band

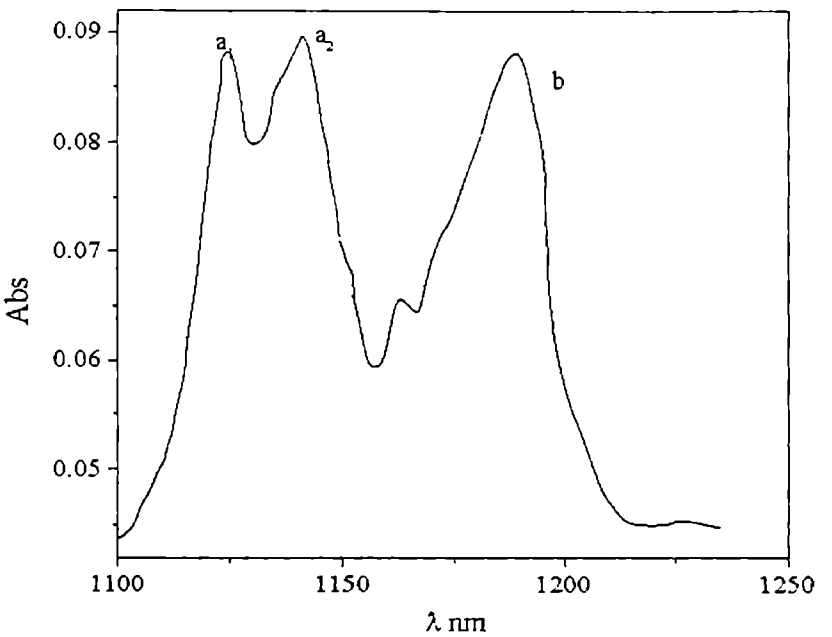

Fig.4.5.8 CH overtone spectrum of p-nitrotoluene in the region $\Delta v=3$ a_1 &a_2-aryl band , b-methyl band

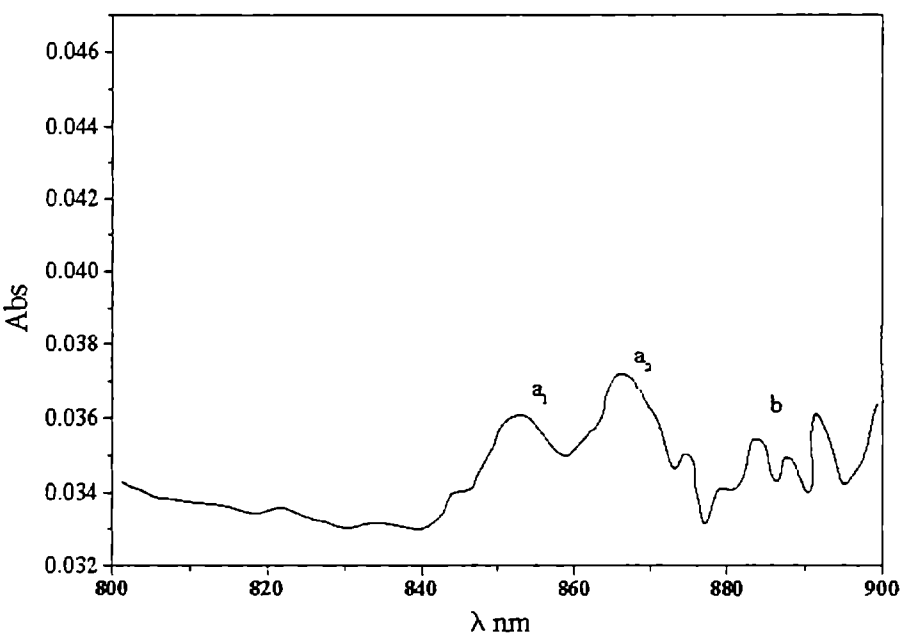

Fig.4.5.9 CH overtone spectrum of p-nitrotoluene in the region $\Delta v=4$ a_1 and a_a-aryl band , b-methyl band

local mode theory is given in table 4.5.3. The bondlength of the aryl CH was calculated for various level of theory by Igor et.al [25] and Yuri Vetal.[26]. For (B3-LYP)/6-31G* C level shows the CH bond length in o-nitrotoluene is 1.083 A°.[25,26]. Using local mode model It is observed that the bond length in p-nitrotoluene decreases by 0.002 A^{0} from that of benzene.[16].

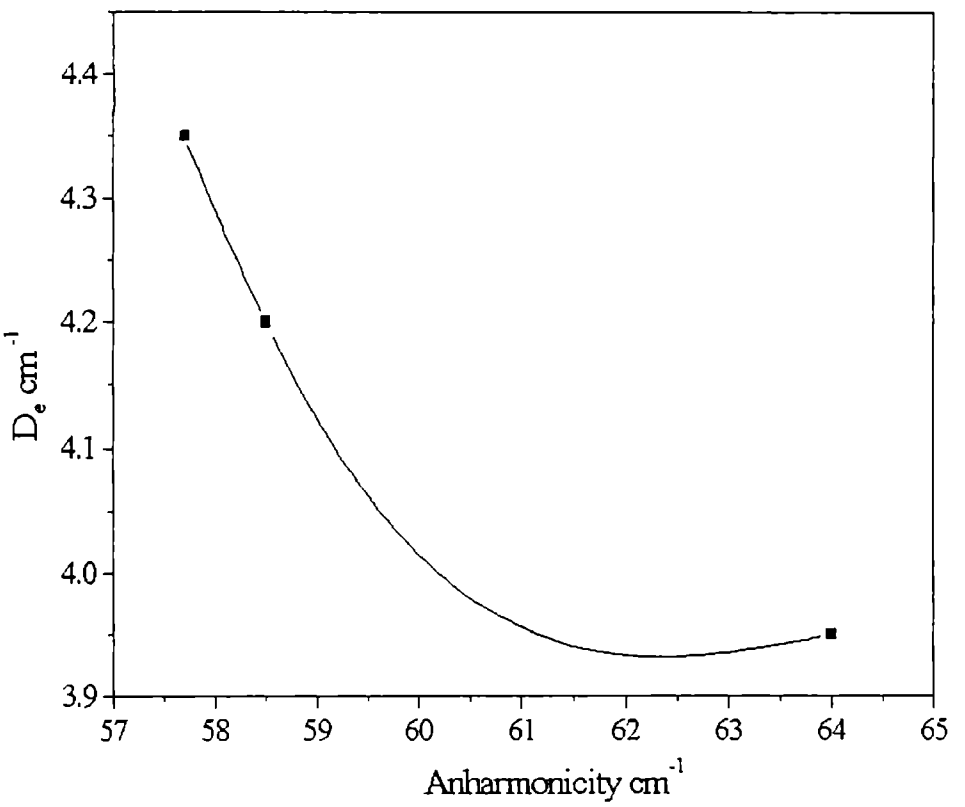

Fig.4.5.10 Dissociation energy V_sAnharmonicity graph for the three isomers of nitrotoluene

Table.4.5.1

Overtone transitions	o-nitrotoluene	m-nitrotoluene	p-nitrotoluene	
v =2	5994.4 (a)	5999.8 (a)	5997.4 (a_1) 6024 (a_2)	|2 0>
	5794.4 (b)	5761 (b)	5753.7 (b)	
v =3	8815.8 (a)	8821.2 (a)	8772.9 (a_1) 8849 (a_2)	|3 0>
	8460.2 (b)	8432.4 (b)	8426.7 (b)	
v =3	11527.6 (a)	11538 (a)	11461.3 (a_1) 11500 (a_2)	|40>
	11014.4 (b)	11004.7 (b)	10921.8 (b)	
v =4		14118.5 (a)	14023.3 (a)	|5 0>
	13408.4 (b)	13495.2 (b)		

Observed frequencies satisfying Birge-Sponer relation, for the CH stretching overtone spectra of nitrotoluene (all values in cm^{-1}) a- aryl CH peaks [a_1 and a_2 are absorptions corresponding to low frequency and high frequency CH] , b- alkyl CH peaks

Table 4.5.2

Molecule	$X_1 (w_{CH}+X_{CH}) cm^{-1}$	X_{CH} cm^{-1}	γ
o-nitrotoluene	3170 ± 1.7	-57.7±0.5	-0.99995
m-nitrotoluene	3175 ± 2.3	-58.5±0.6	-0.99988
p-nitrotoluene	3187 ± 0.9 (a_1)	-64±0.6 (a_1)	-0.99857
	3198 ± 1.1 (a_2)	-62.2 ±0.2 (a_2)	-1
Benzene [12]	3148		

Mechanical frequency (X_1) and anharmonicity constants (X_{CH}) of the aryl CH stretching modes in nitrotoluenes. γ is the least square coefficient.

Table 4.5.3

Dissociation energies and bond lengths for Aryl CH bond calculated for each molecule

	(all values are in cm^{-1})	(all values are in A^0)
o-nitrotoluene	4.35×10^4	1.083
m-nitrotoluene	4.2×10^4	1.083
p-nitrotoluene	3.95×10^4	1.082

Table 4.5.4

Molecule	$X_1 (w_{CH}+X_{CH}) cm^{-1}$	X_2 cm^{-1}	γ
o-nitrotoluene	3108.7± 2.1	-71.2±0.3	-0.9996
m-nitrotoluene	3072.8 ±6.3	-64.6±1.6	-0.999
p-nitrotoluene	3097.9±5.9	-73±3.6	-0.999

Mechanical frequency (X_1) and anharmonicity constants (X_{CH}) of the alkyl CH stretching modes in nitrotoluene.

References

1. P.N Ghosh, P.K Panja, C.M.Pal *Chem.Phys Lett.* 148, 337, 1988.
2. J. K Wilmshurst and R.B Bernstein,*Can .J .Chem* 35, 1195 ,1971.
3. C. La.Lau, R.G Synder, *Spectrochimica Acta* 27A, 2073. 1971.
4. J. A Graeger *Spectrochimica Acta* 41A, 607,1985,
5. H. J Kjaergaard, D.M Turnbull, B.R Henry, *J.Phys,Chem*, 101, 2589, 1997.
6. C.S Parmenter, B.M Stone *J.Chem.Phys,*84, 4710, 1986.
7. L. Anastasakas, TA Wild man *J.Chem. phys* 99, 99, 1993.
8. L Halonen and M.S.Child, *J.Chem.Phys.* 79, 559,1983.
9. R Nagakaki. And I. Hanazaki. *Spectrochim. Acta* A 40, 57,1981.
10. Walker, A. Robert, Richard, C .Erik and Weisshaar, James C. *J.Phys.Chem.* 100: 18, 7333, 1996.
11. D. Bassi, C. Corb, L. Lubich, S. Oss, M. Scotoni, *J.Chem Phys*, 107,1106, 1997
12. C.K.N Patel, A.C Tam, R.J Kerl.. *J.Chem.Phys.*, 71,1470, 1979.
13. B.R Henry, K.M Gouch and M.G Sowa, *Int. Rev. Phys.Chem* 5, 133, 1986
14. K.M Ahmed and B.R Henry *J.Phys Chem.* 90, 1737 1986.
15. M.G Sowa, B.R Henry *J. Chem.Phys* 95, 3040, 1991.
16. M.K Gouch, B.R Henry . *J. Phys. Chem.* Vol.87, No.18. 1983.
17 Henry R B, J.D Miller. *Chem.Phys Lett.*, 60, 81, 1981
18. M.A Mohammadi, B.R Henry *Proc. Natl. Acd.Sci USA*, ,78, 686, 1981.
19. B.R Henry, M.A Mohammadi , J.A Thomson *J. Chem. Phys*, , 75, 3165, 1981,
20. N L Fergusen,. "The Modern Structural theory of Organic Chemistry" Prentice Hall of India Pvt. Ltd.. New Delhi, vol.2. 1969B R Henry, J.A Thomson,.. *Chem.Phys Lett.*, 69, 275, 1980.

21. B R Henry, R.J.D Miller, *Chem.Phys Lett.*, 60, 81, 1978,

22. E.S Barrows, et.al. *Environ.Sci. Technol.*, 30, 3028,1996.

23. M.L Sage; J Jortner. *Adv. Chem. Phys.*, 47,293, 1981.

24. F.S Igor, V V Lev, K. Attila and I. Hargittai *J. Mol.Structure.* 445, 259,1998

25. Yuri V II'ichev and W.Jakob *J.Phys.Chem*, A104, 7856, 2000

CHAPTER 5

NIR overtone analysis of hydroxymethylbenzenes and hydroxynaphthalene

5.1 NIR overtone analysis of hydroxymethylbenzenes

5.1.1 Introduction

Hydroxymethylbenzenes are also called Cresols or hyrdoxytoluenes or methylphenols. They are isomeric substituted phenols with a methyl substituent at one of the o-, m-, or p- positions relative to the OH-group. Physically, they are white crystalline solids or yellowish liquids with a strong phenol-like odor. The compounds are highly flammable, moderately soluble in water and soluble in ethanol, ether, acetone, or alkali hydroxides. Chemically, these alkylphenols undergo electrophilic substitution reactions at the vacant o- or p-positions or undergo condensation reactions with aldehydes, ketones, or dienes.

Cresols have a wide variety of uses as solvents, disinfectants, or intermediates in the preparation of numerous products. They are commonly used in p-cresol is used in the production of lubricating oils, motor fuels, and rubber polymers, while m-cresol is also used in the manufacture of explosives. They are also used in Musk ambrette, Thermosetting cross linked resin, Insecticide intermediates, Intermediates for germicides like PCMC and in the manufacture of vitamin E.

For decades substituted phenols have been the subject of spectroscopic investigations [1]. The existence of *cis(syn)* and *trans(anti)* orientations of the hydroxy group with respect to the substituent has been suggested as early in 1936. Allinger et al obtained two stable *anti* conformers with different orientations of the methyl hydrogens with espect to the hydroxy group and one *syn* conformer [2.] Kudchadker et. Al [3] found that the *syn* conformer in which the two methyl hydrogens are close to hydroxy group to be the most stable structure. Microwave studies of o-cresol by Welzel et.al [1] indicates that the substituent's influence on the barrier seems to be predominantly of a steric nature. They conclude that in *anti*-o-cresol the hydrogen of the OH group is much closer to the methyl group which seems to be a reason for the higher barrier.

The -OH group is a typical ortho, para director increases the electron density at positions ortho and para to it by a resonance mechanism but does not markedly increase the electron density at the meta position by resonance mechanism [4] Since oxygen is highly electronegative, the hydroxyl group could decrease the electron density at all positions by an inductive mechanism. However, the presence of non-bonded 2p electron pairs on the oxygen allows donation of electrons to the aromatic ring (resonance effect). For oxygen resonance effects are more important than inductive effects and the net effect is an increase in electron density on the ring. The alkyl group also donates electrons to the ring.

5.1.2 Experimental.

High purity o- methylphenol, m- methylphenol and p-methylphenol (>99%) obtained from SRL Mumbai are used for present investigation. The overtone absorption spectrum in the range 2000nm-700nm is recorded from pure liquid for a path length of 1cm and air as reference at room temperature (26±2°C).

5.1.3 Results and discussion

The near infrared vibrational spectra of ortho meta and para substituted methyl phenols for the transitions v= 2-5 are shown in the fig. 5.1.1-5.1.13. The absorption frequencies corresponding to the transitions are given in table.5.1.1. All the three molecules show well distinguished peaks for aryl CH, alkyl CH and OH local oscillators. Except for OH oscillator in m-methylphenol. The overtone spectrum of ortho and para methylphenols show strong single peak for the OH oscillator for the overtone transition Δv =3. Strong absorption frequencies corresponding to in plane and out of plane stretching frequencies for the alkyl CH are observed in the transition region Δv =4. In this analysis we consider only the pure overtone peaks which satisfy Birge-Sponer relation

The hydroxy group in phenols lies in the ring plane, even the neighborhood tert-butyl group does not disturb this confirmation. With this

arrangement one of the free electron pairs on the oxygen atom is conjugated with π-electron system of the benzene ring [5].

The mechanical frequency (w_{CH}), and anharmonicity constants (X_{CH}) of aryl CH, alkyl CH and OH oscillators in methyl phenols are given in table 5.1.2 The mechanical frequency for ortho and para methyl phenols are found to be lower than that of meta isomer. ie. in the order O< M>P In methyl phenol the mechanical frequencies of the three isomers shows blue shift from that of benzene [6]. Since the -OH group is ortho para directing at these positions alkyl group may donate more electrons to the ring. Hence, the mechanical frequency is lower in these cases compared to meta position.

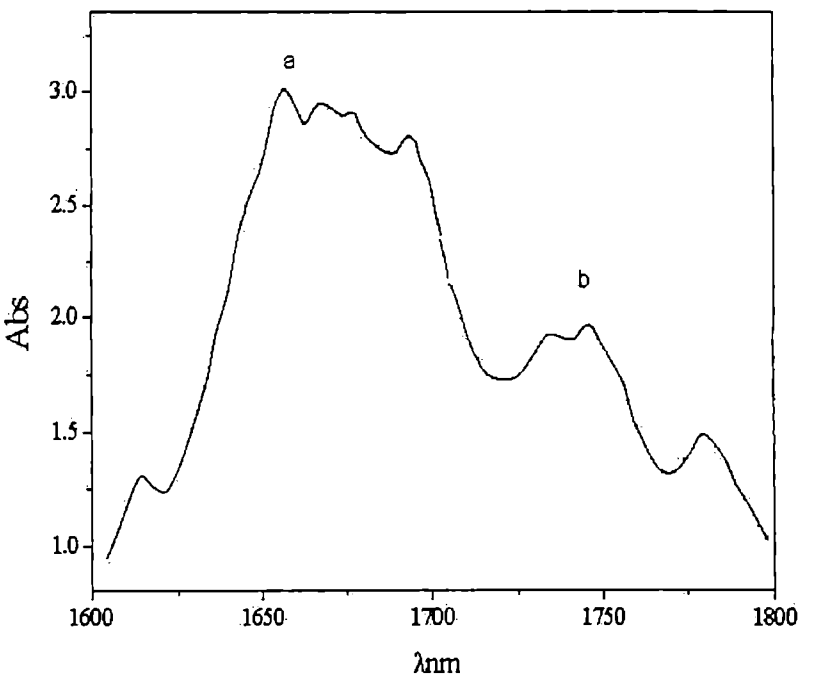

Fig.5.1.1 CH overtone spectrum of o-methylphenol in the region Δv=2 a-aryl b-methyl bands

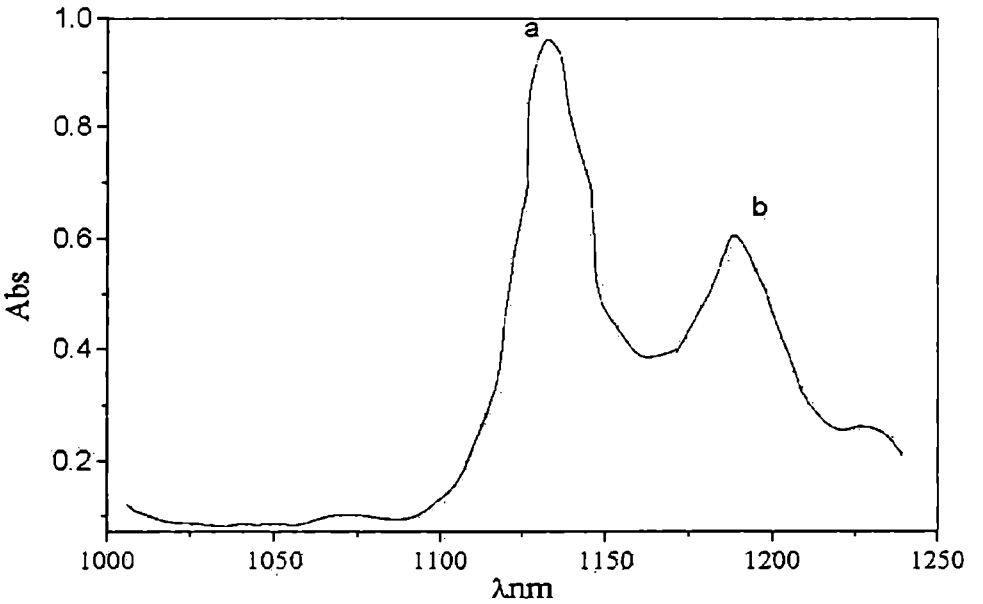

Fig.5.1.2 CH overtone spectrum of o-methylphenol for $\Delta v=3$
a-aryl and b-methyl bands

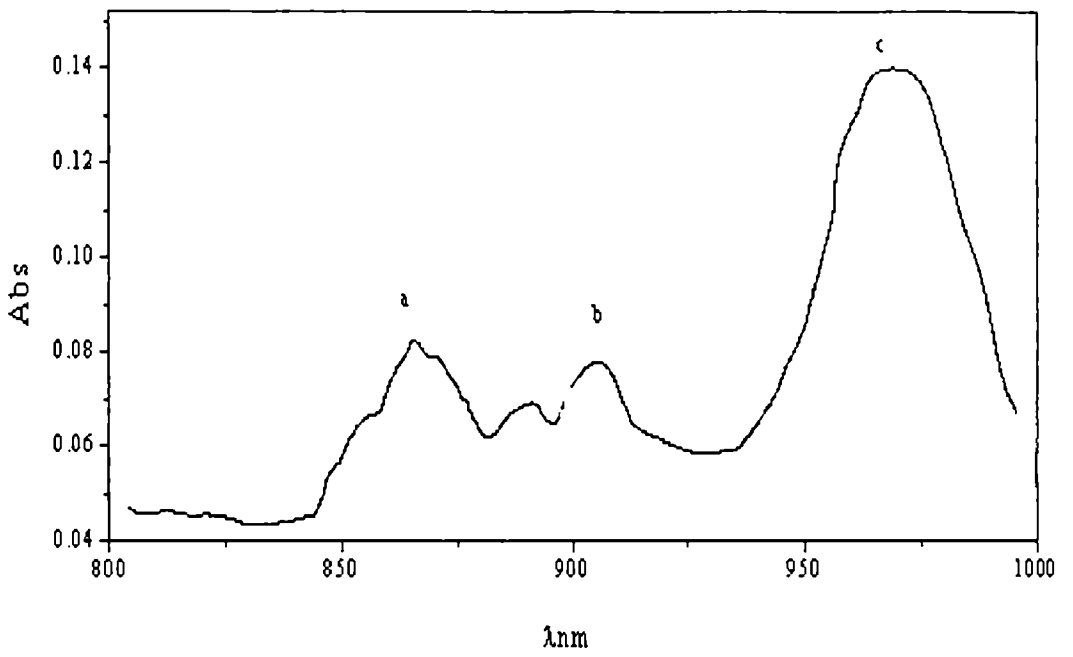

Fig.5.1.3 Overtone spectrum of aryl and alkyl CH (for Δv=4) and OH (for Δv=3)
a-aryl band, b-alkyl band, c-OH band

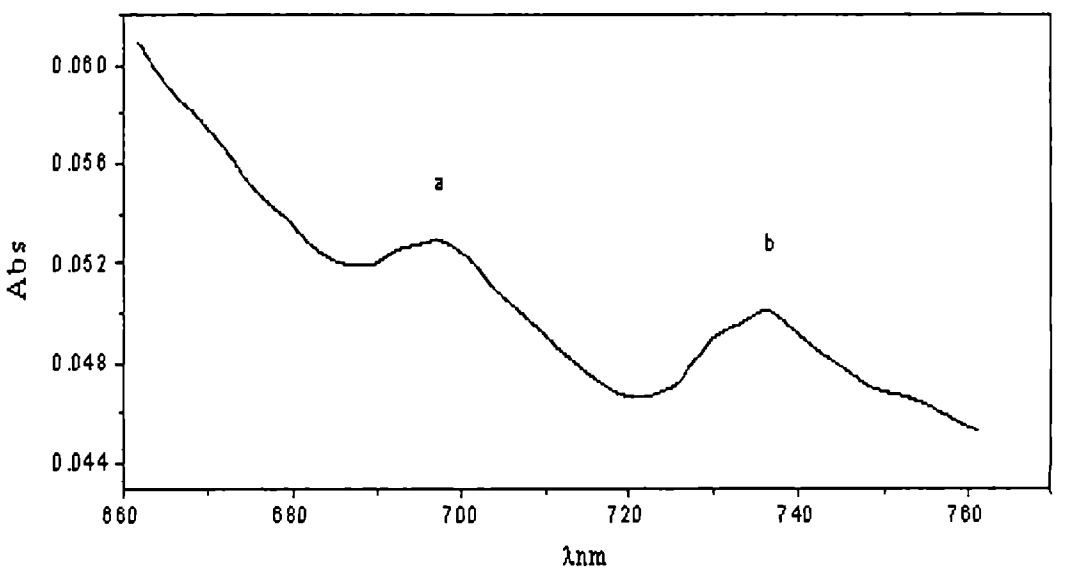

Fig 5.1.4 Aryl CH (for Δv=5) and OH (forΔv=4) Overtone spectrum of o-methylphenol
a-aryl band, b-OH band

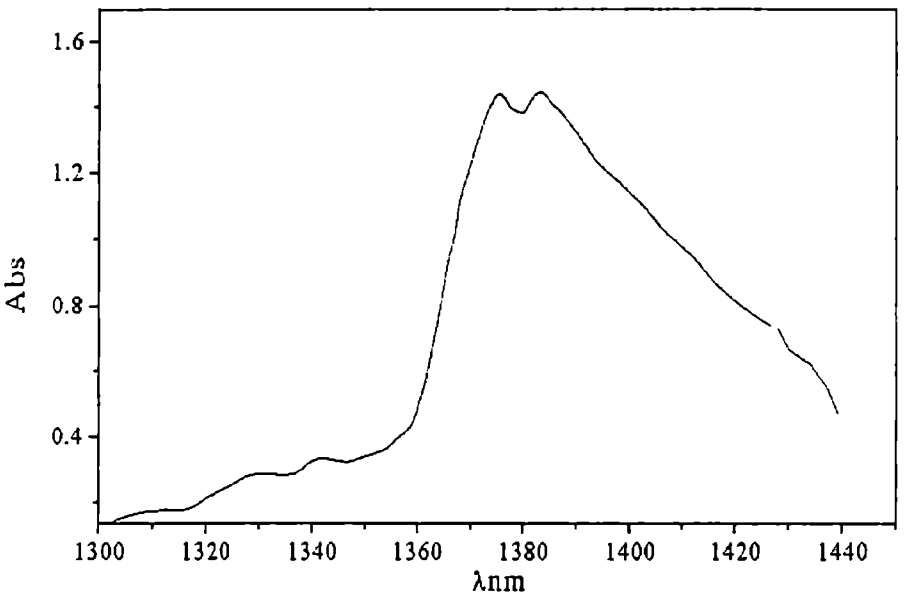

Fig.5.1.5 OH overtone spectrum of o-methylphenol in he region Δv=2

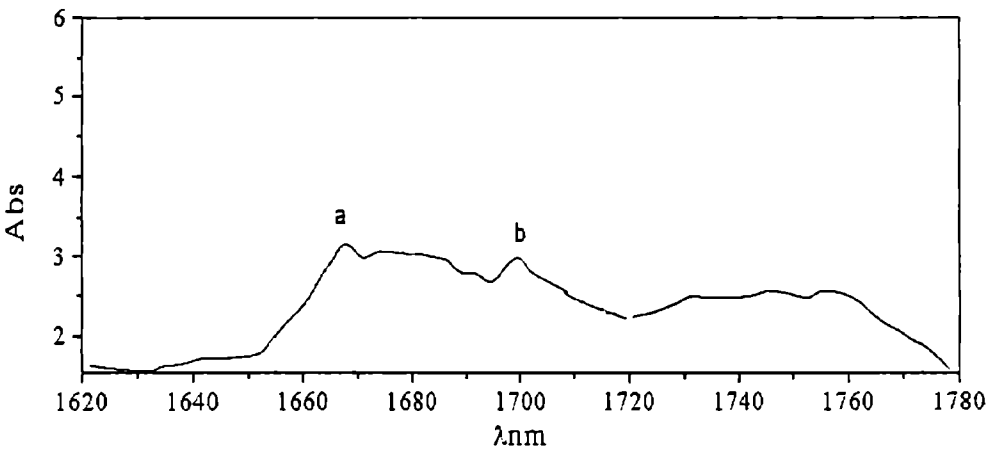

Fig.5.1.6 CH Overtone spectrum of m-methylphenol in the region Δv=2
a-aryl band and b-methyl band

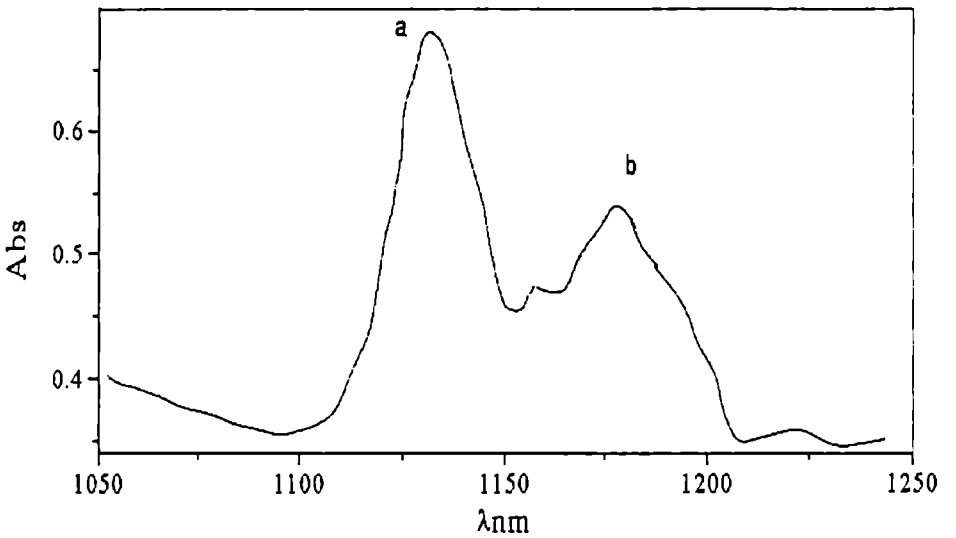

Fig.5.1.7 CH Overtone spectrum of m-methylphenol in the region Δv=3
a-aryl band and b-methyl band

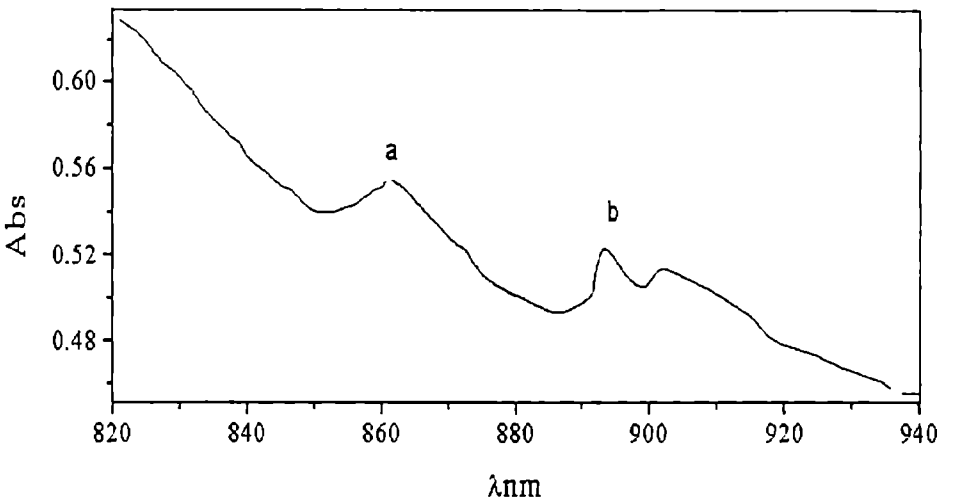

Fig.5.1.8 CH Overtone spectrum of m-methylphenol in the region Δv=4
a-aryl band and b-methyl band

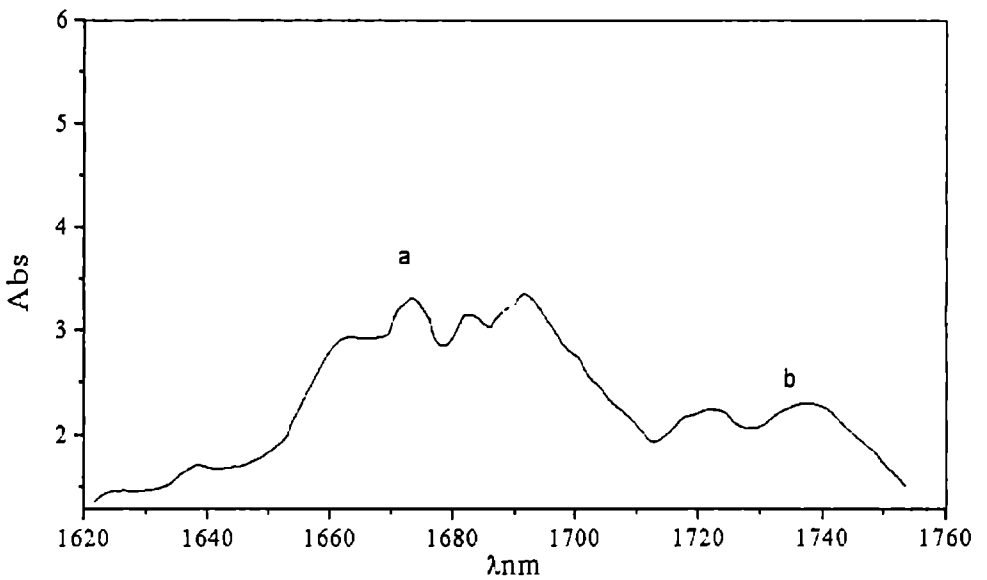

Fig.5.1.9 CH Overtone spectrum of p-methylphenol in the region Δv=2
a-aryl band and b-methyl band

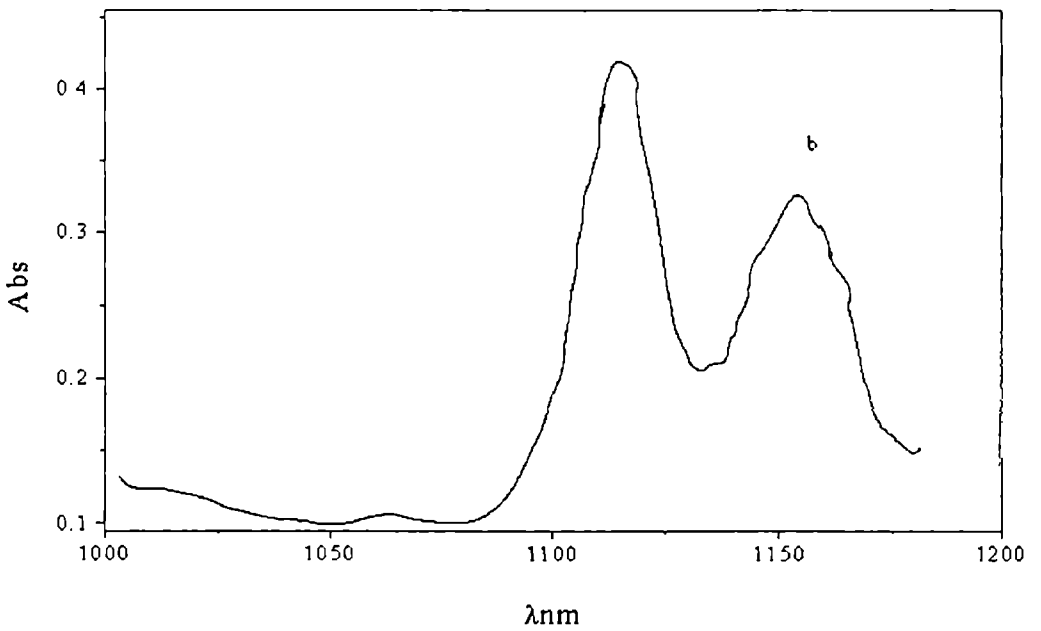

Fig 5.1.10 CH overtone spectrum of p-methylphenol in the region Δv=3 a-aryl band, b-meathyl band

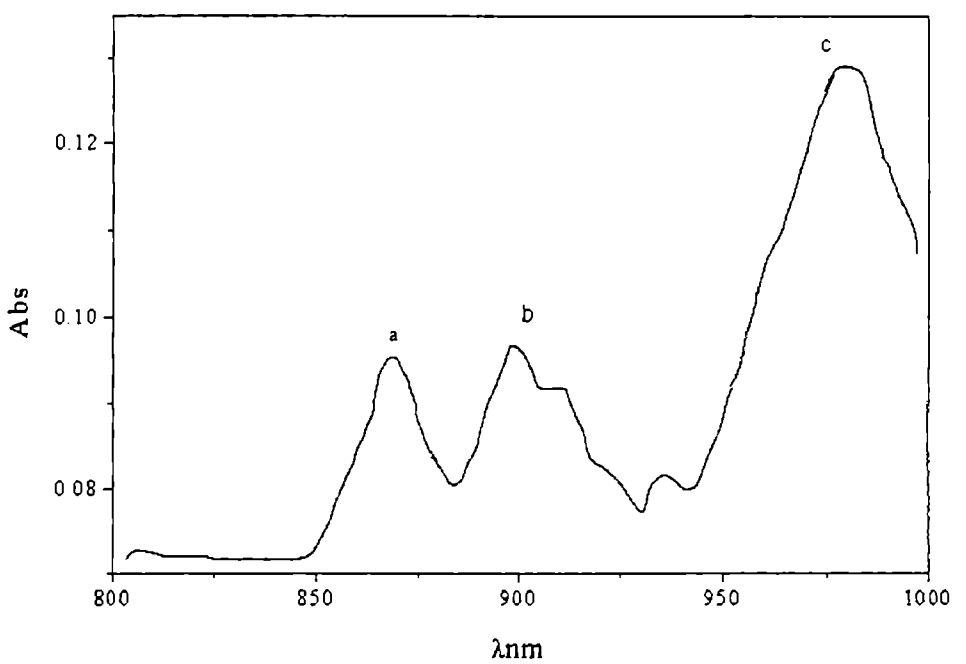

Fig 5.1.11 CH and OH overtone spectrum of p-methylphenol in the region Δv=4 for CH and Δv=3 for OH a-aryl band, b-meathyl band, c-OH band

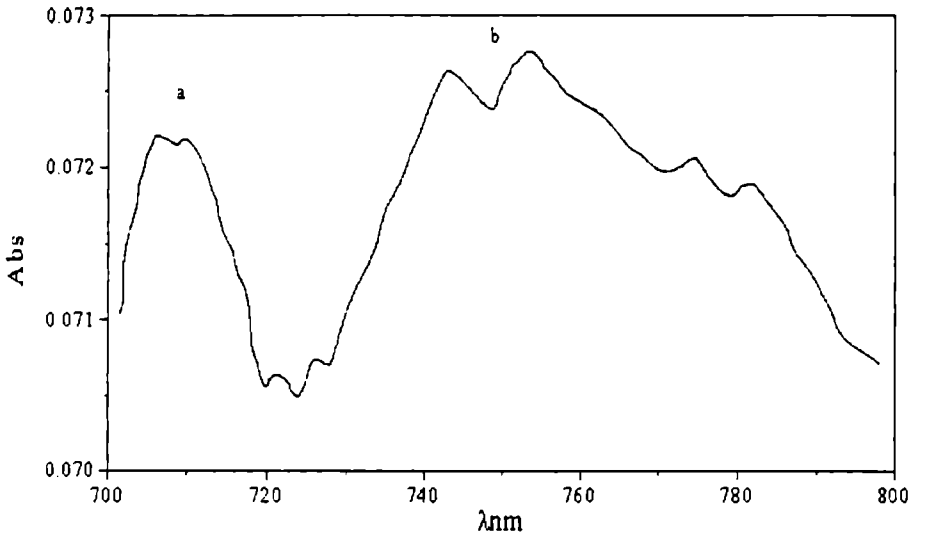

Fig 5.1.12 CH and OH overtone spectrum of p-methylphenol in the region Δv=5 and 4 respectively a-aryl band, b-OH band

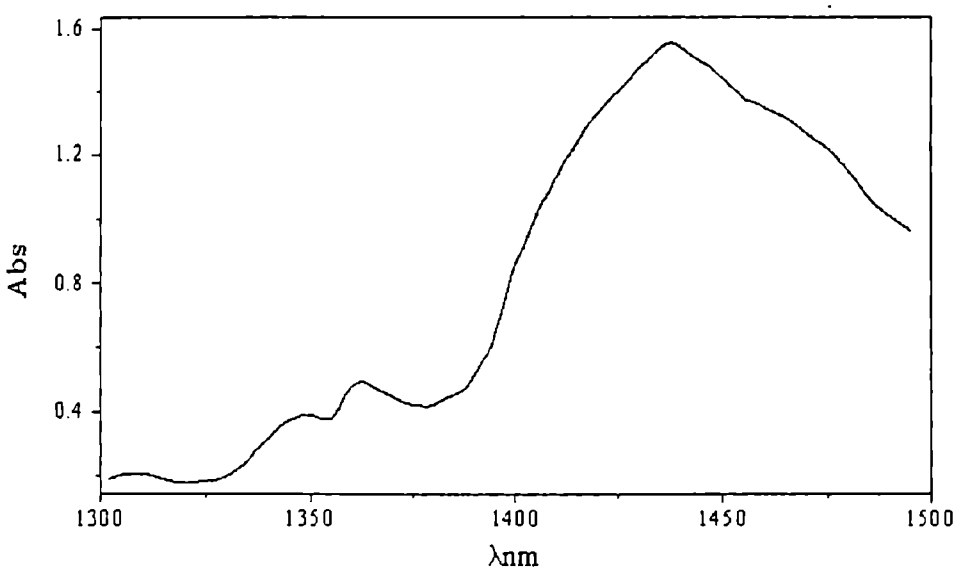

Fig.5.1.13 OH Overtone spectrum of p-methylphenol in the region Δv=2

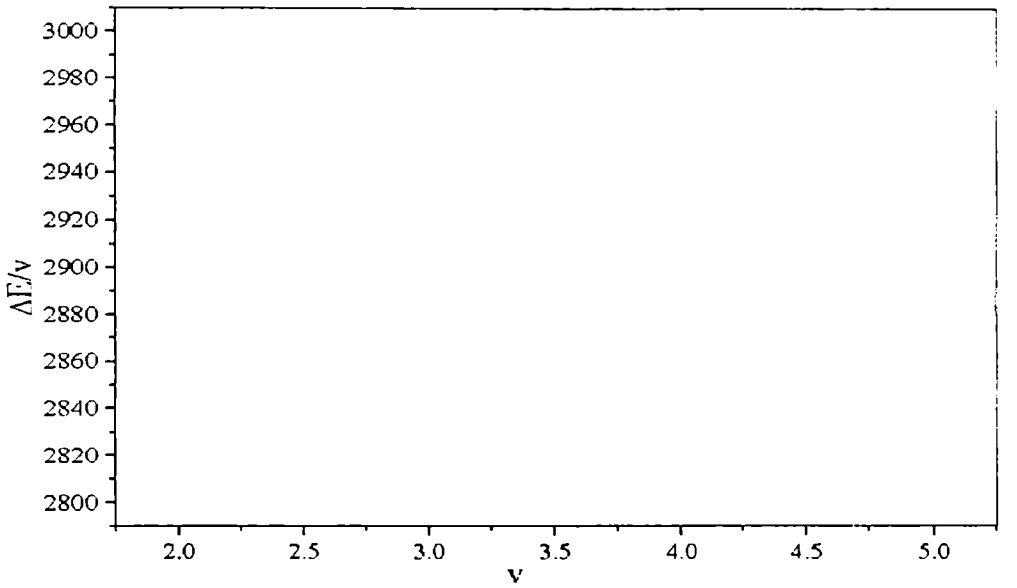

Fig.5.1.14 B-S plot for the Aryl CH overtones in o-cresol

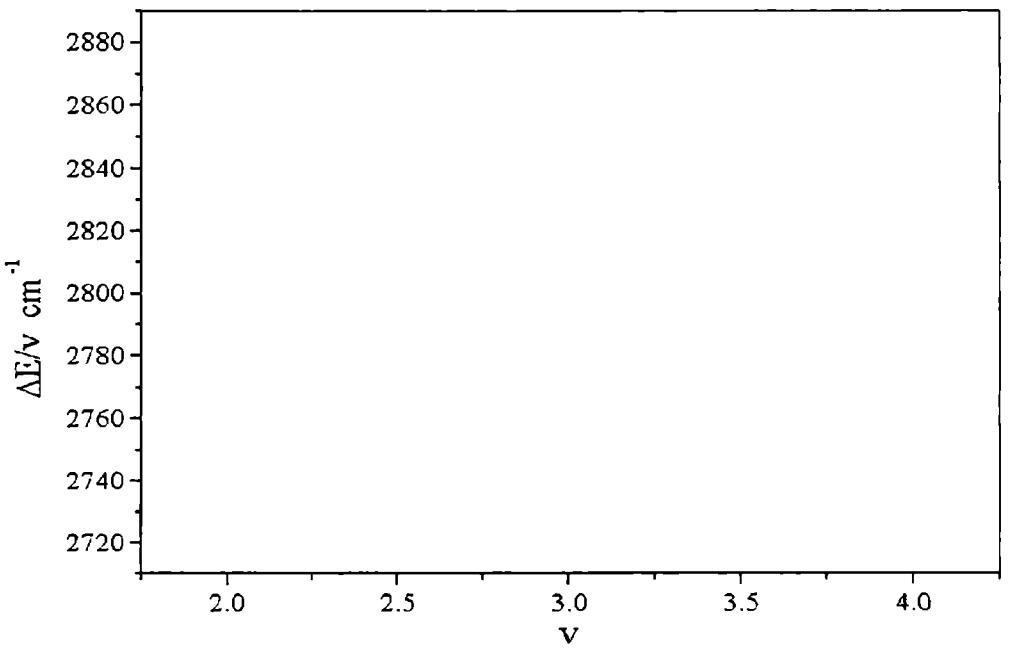

Fig. 5.1.15 B-S plot for the alkyl CH oscillator in o-cresol

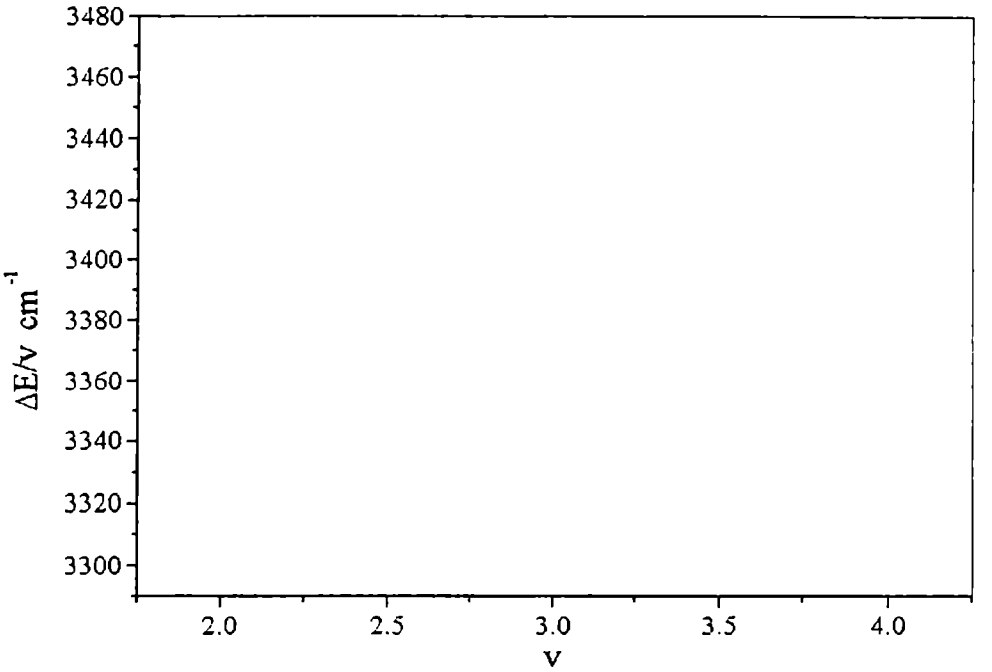

Fig. 5.1.16 B-S plot for the OH overtone peaks in o-cresol

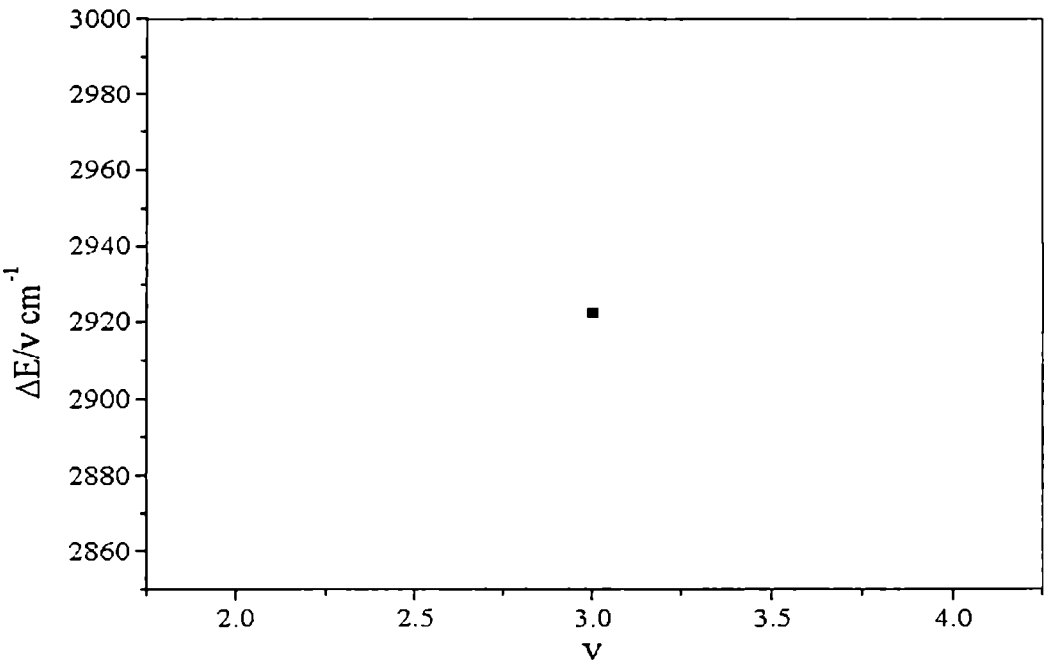

Fig.5.1.17 B-S plot for the aryl CH overtones in m-cresol

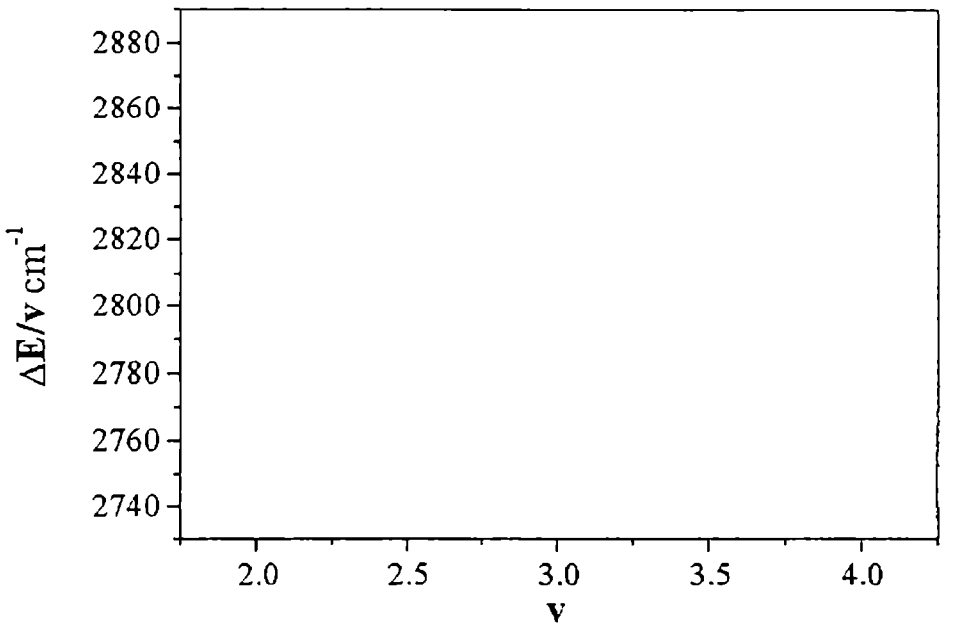

Fig. 5.1.18 B-S plot for the alkyl CH oscillator in m-cresol

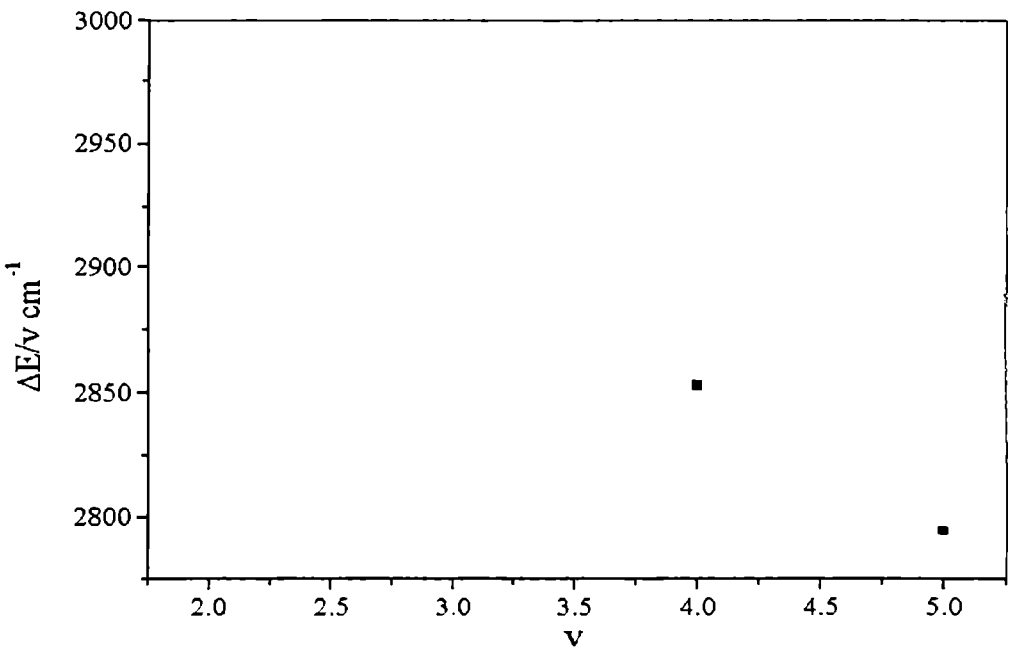

Fig.5.1.19 B-S plot for the aryl CH overtones in p-cresol

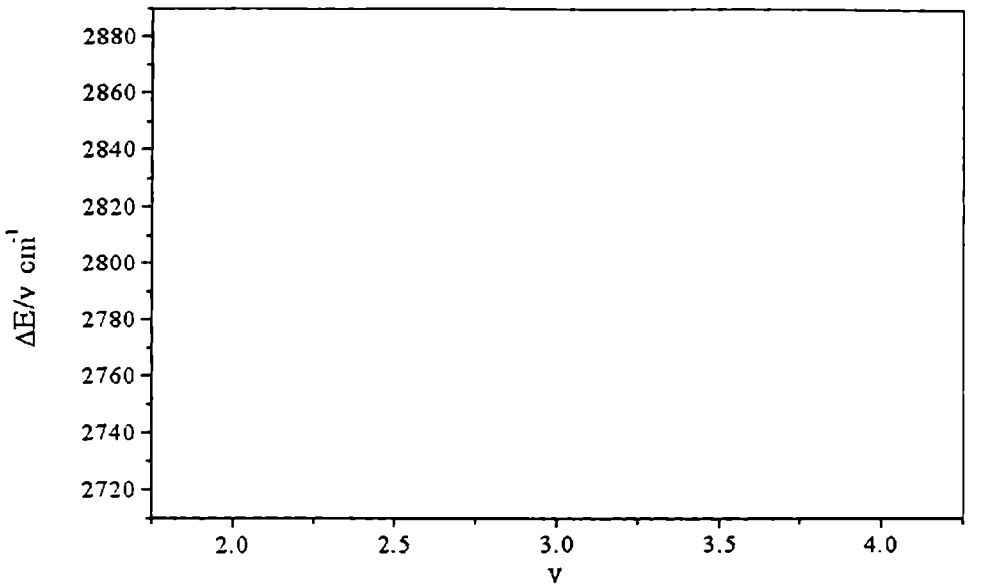

Fig.5.1.20 B-S plot for the alkyl CH overtones in p-cresol

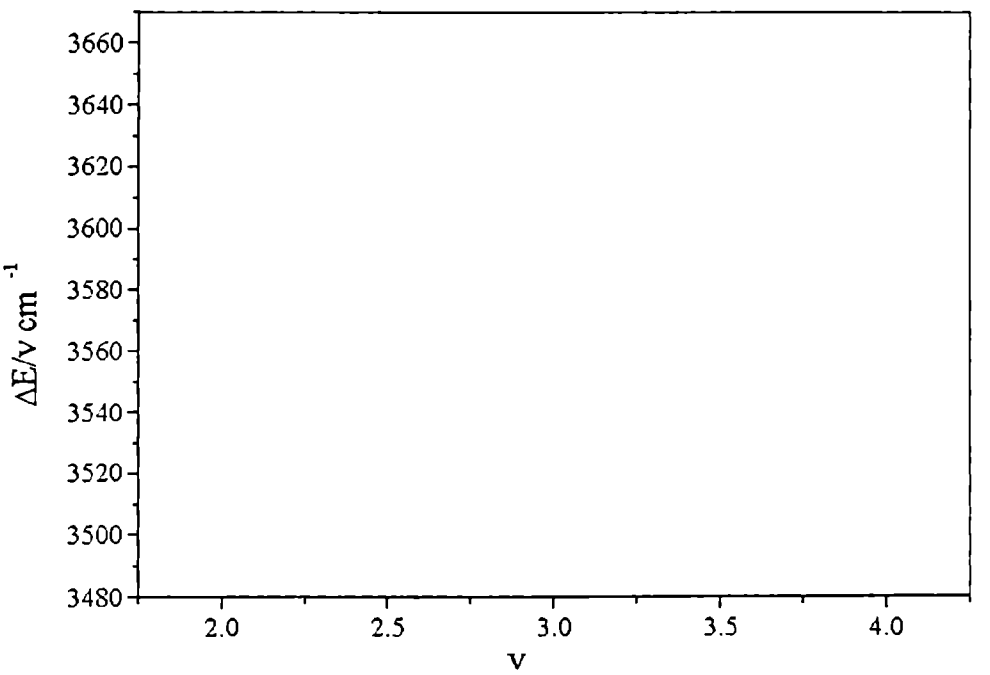

Fig.5.1.21 B-S plot for the OH overtones in p-cresol

The mechanical frequency of alkyl CH oscillators agrees to this argument. The higher mechanical frequency in this case, for ortho and para isomers indicates that higher degree of donation at these two positions compared to meta substituted methyl group.

It is well known that the electron withdrawing group increases the acidity while a donating group reduces the acidity in aromatic acids. Alkyl group by their electron donating properties weaken the acidity of phenol [7]. The acid strengths [8] and ionization constants [7] of phenol and methylphenols are given in tab. 5.1.3. From table it is clear that m-methyl phenol is more acidic than the other two isomers. The local mode analysis indicates that the mechanical frequency for CH oscillators in m-methylphenol is larger compared to that in ortho and para isomers. This result shows that the donation by alkyl group in m-methylphenol is lower compared to the other two substitutions. Thus our experimental results are comparable with the order of P_{ka} values of the three isomers.

The bond length of the aryl CH oscillators were calculated. for the three molecules were calculated and is given in table 5.1.4. The aryl CH bond length of meta isomer is found to be lower than that of benzene by 0.001A° The bond length of the other two isomers does not show any shift from benzene. B3 LYP 6-311++G* level calculation of p-cresol done by Zane. A et.al shows the CH bondlength is of the order of 1.085 A° [9]. This indicates a lower electron density in the ring CH in m-methylphenol and hence a higher P_{ka} value.

The mechanical frequency (w_{CH}) and anharmonicity constants (X_{CH}) of OH oscillator in ortho and para methyl phenols are given in table5

Table 5.1.1. Observed peaks and assignments (all values in cm^{-1}) a–alkyl, m-methyl

Overtone transitions	Local Oscillator	o-methylphenol	m-methylphenol	p-methylphenol
| 2 0>	a-CH	5980	5970	5953
	m-CH	5748	5750	5745
	OH	6929		6910
| 3 0>	a-CH	8780	8767	8743
	m-CH	8388	8405	8349
	OH	10163		10061
| 4 0>	a-CH	11490	11440	11411
	m-CH	10922	10968	10922
	OH	13224		13061
| 5 0>	a-CH	14049		13972

Table 5.1.2. Mechanical frequency ($w_{CH}+X_{CH}$) and anharmonicity constants (X_{CH}) of Aryl, alkyl and OH oscillators

Oscillators	parameters	o-methylphenol	m-methylphenol	p-methylphenol
Aryl CH	$w_{CH}+X_{CH}$	3167 ± 6.5	3171 ± 1.2	3158.3 ± 2.8
	X_{CH}	-59.5. ± 2.2	-62 ± 1	-60.8 ± 0.5
	γ^*	-0.9995	-1	-0.9999
Alkyl CH	$w_{CH}+X_{CH}$	3087 7±3.5	3072.8±4.3	3085.9±2
	X_{CH}	-71.8±2.1	-66.3±1	-71.2±3
	γ^*	-0.999	-0.9998	-0.9999
OH	$w_{CH}+X_{CH}$	3703.15±4.6		3738.2±3.8
	X_{CH}	-79.3±1.5		-95±3.8
	γ^*	-0.9998		-0.999
Benzene [12]		3148		

γ^*- co-relation coefficient (all values in cm^{-1})

Table 5.1.3. Acid strengths P_{ka} and ionization constants

Compound	P_{ka}	Ionization constants
Phenol	9.92	1
o-methylphenol	10.29	
m-methylphenol	10.09	0.98
p-methylphenol	10.26	0.67

Table 5.1.4

Bond lengths obtained for aryl CH bond using local mode theory

Molecule	Bond Length (A^0)
o-methylphenol	1.084
m-methylphenol	1.083
p-methylphenol	1.084

5.2 Aryl CH and OH overtone spectrum of α- naphthol

5.2.1 Introduction

The hydroxy derivatives of naphthalene are known as naphthol. α- naphthol is a colourless solid of melting point 94^0C. It is a weak acid and is sparingly soluble in water. In water it ionizes to yield a resonance stabilized naphthoxide ion. But it is a stronger acid than phenol. [10]. The increased acidity is due to the greater stability of naphthoxide ion as compared to phenoxide ion. In naphthoxide ion it is delocalized over the ring. This compound finds vast application in the manufacture of insecticides and dyes. This compound can act as a stimulant in plant growth and hence is more important in the field of Biotechnology.

The overtone spectrum of α- naphthol in the ground electronic state characterized by strong CH and OH stretching vibrational bands. The positions of the corresponding vibrational energy levels are modeled by simple local mode approach. Here we account only stretching vibrational states. One major outcome of this analysis is the confirmation of intramolecular interaction between the hydroxyl group and aromatic nucleus.

The CH oscillators in naphthalene and biphenyl are reported to have a higher mechanical frequency than that of benzene. CH oscillators in α- naphthol is expected to exhibit the same property. On the contrary, in α- naphthol, it is observed that the mechanical frequency decreases from that of benzene. This lower frequency may be due to the intra-molecular interaction of hydroxyl group and aromatic nucleus in α- naphthol.

The HCAO local mode model neglects coupling to all lower frequency modes and approximately the coupling between CH bonds harmonic terms [11]. In recent investigations, it has been shown that local mode characteristics are dependent not only on type of CH oscillator but also on its environment [12]. It is well established from the IR spectra that there exists an intra-molecular interaction between hydroxyl group and aromatic nucleus [5]. As a remarkable feature of α- naphthol. In this paper we report a study on the overtone spectrum of α- naphthol in

particular to CH and OH overtones in order to understand more about the interactions in this kind of aromatic ring compounds. The structure of α- naphthol is depicted in figure. (a)

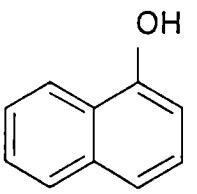

Figure (a)

The bond dissociation energies can be calculated using the Morse potential function.

5.2.2 Experimental

High purity α- naphthol (>99%) obtained from CDH Mumbai are used for present investigation. α- naphthol obtained in solid form is dissolved to saturation in spectrograde CCl_4. The overtone absorption spectrum in the range 2000nm-700nm is recorded from pure liquids (pathlength-1cm and reference-air) at room temperature (26±2°C) The aryl CH overtone spectra of α- naphthol in the regions Δv=2-5 and OH overtone spectra in the regions Δv =2-4 are given in fig.5.2.1-5.2.6

5.2.3 Results and discussion

The overtone bands at all levels show single peaks corresponding to overtone transition except for Δv =2 and Δv =5, for CH oscillators. In this analysis, we consider only the pure overtone peaks satisfying Birge-Sponer plot. The observed frequencies satisfying Birge-Sponer plot are given in Table.5.2.1.The mechanical frequency and anharmonicity constants for CH bond are calculated and are given in Table 5.2.2.

It is well established from overtone spectroscopic studies of many substituted benzene that the aryl mechanical frequency is increased due to electron withdrawing substitution and decreased due to electron donating substitution. [14]. The local mode parameters of biphenyl ring were determined by T.M.A Rasheed [15] and is observed that the frequency is larger by (≅ 13 cm^{-1}) than in benzene. This shift is

attributed to the resonance behavior of the biphenyl ring. In the case of fused benzene rings also a hike in the mechanical frequency is observed [11]. In hydrogenated naphthalene, Decalin, the mechanical frequency decreases to a substantial extent [11].

It is reported in naphthalene [10] that the aryl CH mechanical frequency shows a blue shift as compared to that of benzene [6]. In phenol also it is observed that the mechanical frequency increases from that of benzene Thus in α- naphthol it is expected to have a blue shift in mechanical frequency. On the contrary, it is observed that the mechanical frequency exhibits a red shift from that of benzene. This observation may be attributed to the intra-molecular interaction between hydroxyl group and the aromatic nucleus. This intra-molecular interaction may cause an increase in the π electron density and creates a net negative charge on the CH carbon atoms, which in turn repel the electron cloud of hydrogen. Eventually, CH bond length increases. This may lead to a lower force constant and hence a lower mechanical frequency for aryl CH bonds. The mechanical frequency, anharmonicity constant and dissociation energy for the OH bond are given in table. 5.2.1. The OH mechanical frequency shows a decrease (~10cm^{-1}) from that of phenol OH [16].

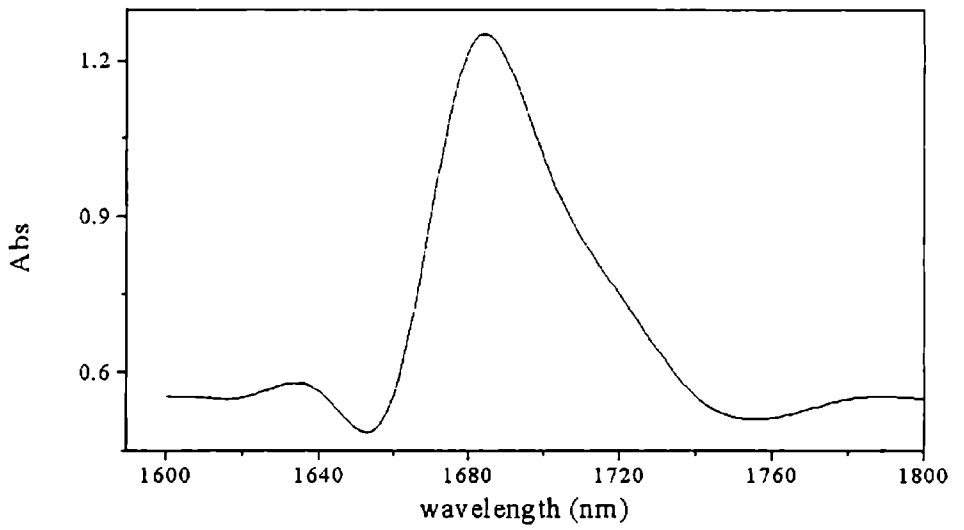

Fig. 5.2.1 CH overtone spectrum of α-naphthol in the region Δv=2

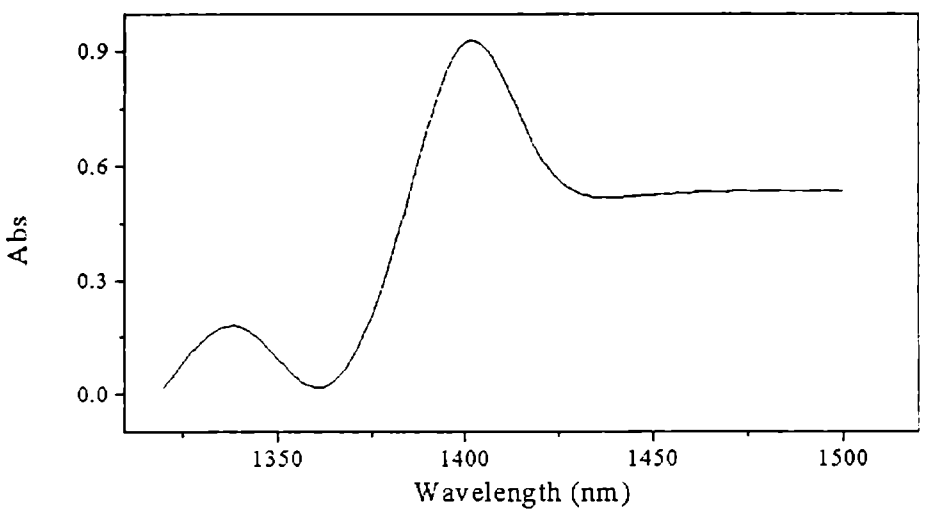

Fig. 5.2.2 OH overtone transition of α-naphthol in the region Δv=2

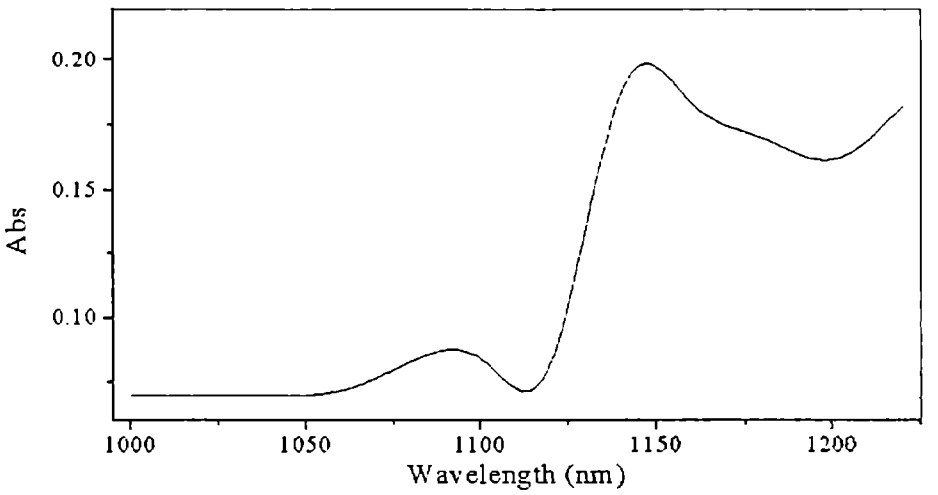

Fig.5.2.3 CH overtone spectrum of α-naphthol in the region Δv=3

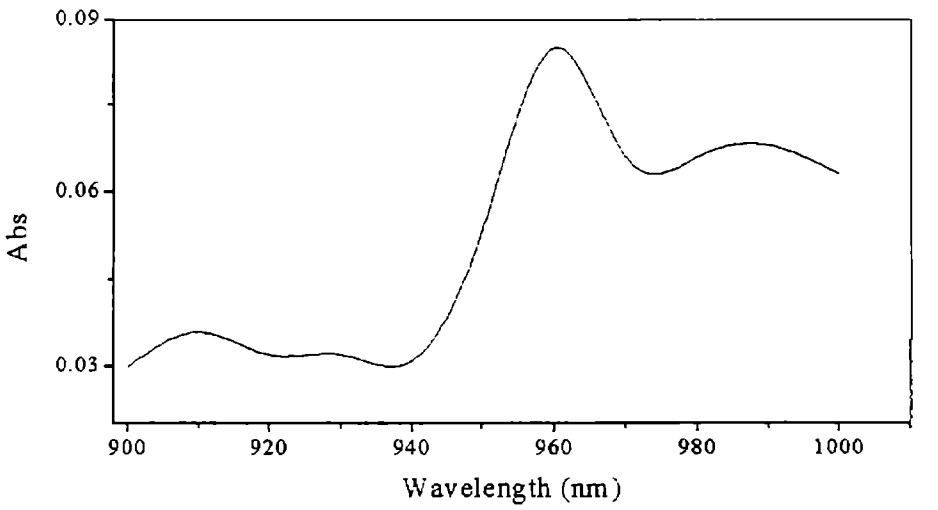

Fig.5.2.4 OH overtone spectrum of αnaphthol in the region Δ v=3

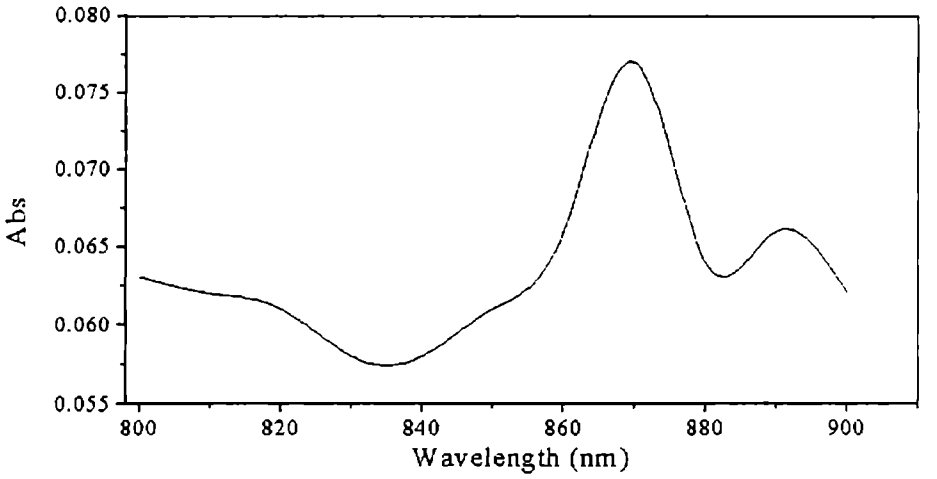

Fig.5.2.5 CH oertone spectrum of α-naphthol in the region Δv=4

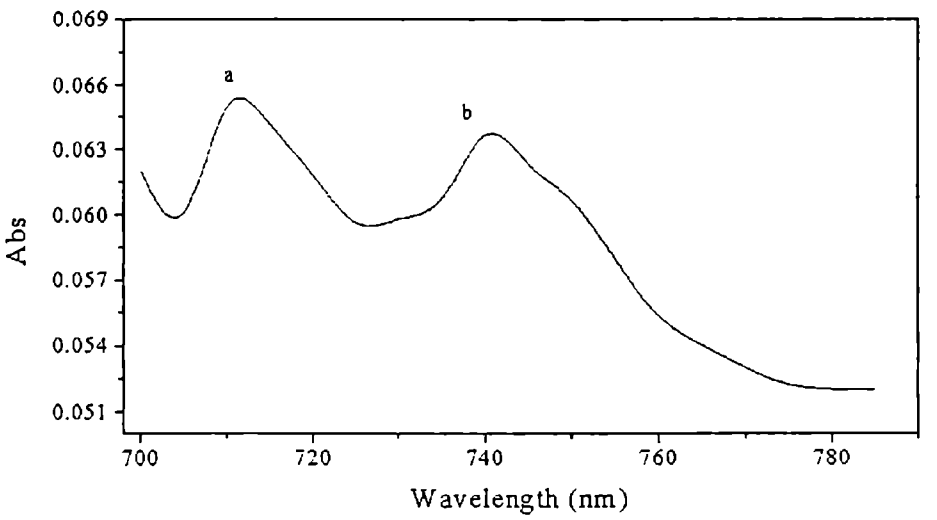

Fig. 5.2.6 CH (v=5) and OH (v=4) overtone spectrum of α-naphthol. a-aryl band and b-OH band

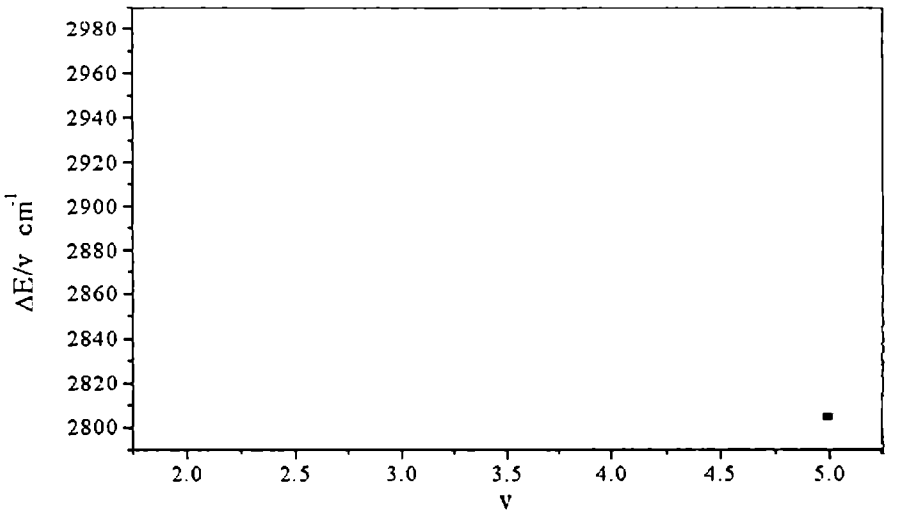

Fig.5.2.7 B-S plot for the aryl CH overtone spectrum of α-naphthol

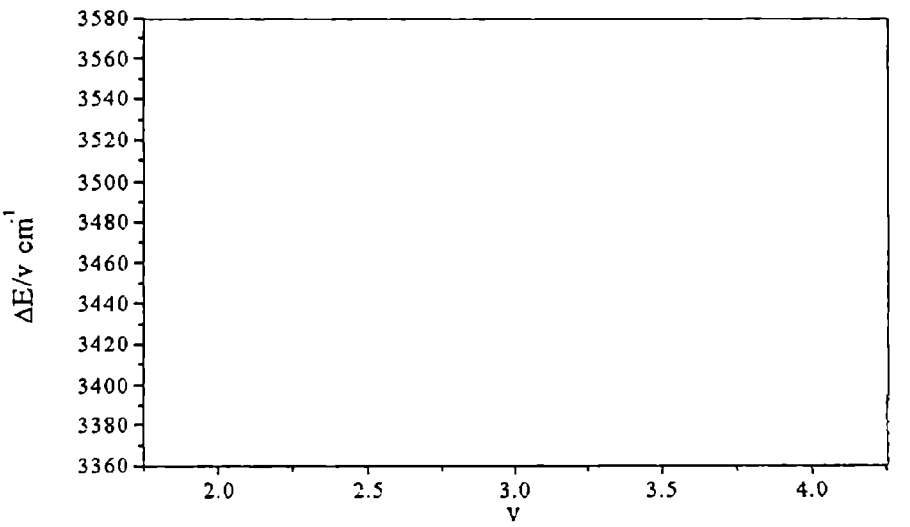

Fig.5.2.8 B-S plot for the OH overtone spectrum of α-naphthol

Table.5.2.1.

Overtone transition	1-naphthol	Naphthalene [11]	Assignment
$\Delta v=2$	5945 (CH) 7114 (OH)	5956	$\|2>\alpha$
$\Delta v=3$	8755 (CH) 10423 (OH)	8762	$\|3>\alpha$
$\Delta v=4$	11465 (CH) 13531 (OH)	11442	$\|4>\alpha$
$\Delta v=5$	14009 (CH)	14016	$\|5>\alpha$

Absorption frequencies of 1-naphthol satisfying Birge-Sponer relation for different overtone transitions of CH and OH oscillators (all values in cm^{-1})

Table.5.2.2 Mechanical frequencies (w_eX_e) and anharmonicity constants (X_e)

Molecule	w_eX_e	X_e	γ	D_e
α- naphthol (CH)	3140± 5.1	-55.5±1.3	-0.99935	44412.6
α- naphthol (OH)	3746± 6.5	-90.2±2.1	-0.99972	38892.8
Benzene [12]	3148			
Naphthalene [28]	3154 (CH_α)	-58.5		
	3171 (CH_β)	-58.9		
Phenol [29] (Aryl)	3165	-56		

(all values in cm^{-1}). γ is the least square coefficient D_e cm^{-1} is the dissociation constant for the molecules.

References

1. A.welzel, A Hellweg, I Merke, and W Stahi, *J. Mol.Spectr.* 215, 58,2002
2. N.A Puttnam *J.Chem.Soc.* 985, 5100,1960
3. S.A Kudehadker, R.M Hedges and B.J Zwolinski *J. Mol.Struct.* 43, 259 1978
4. C.S Parmenter, B.M Stone *J.Chem.Phys* ,84, 4710 ,1986
5. V.M Potapov, "Steriochemistry", Mir publishers, Moscow,1978
6. C.K.N Patel, A.C Tam, R.J Kerl.. *J.Chem.Phys.*, 71,1470, 1979
7 Henry Rakoff & Norman C Rose, "Organic Chemistry" , The Macmillan company New York 1967
8. Bently and Kirby "Elucidation of organic structures by physical and chemical methods" Part1 second edition 1972.

9.A.Zane, A.Daniel, L.Jaan, A.O Stacy and J.T.George (Jr) *Biochemistry* 40,2522, 2001

10.B.S Bahl, Arun Bahl Advanced Organic chemistry S.Chand Company ltd New Delhi 1995, p.1174.

11. Henrik.G. Kjaergaard and Bryan R. Henry, *J. Phys. Chem.*, 99 899, 1995
12. B R Henry, J.A Thomson,.. *Chem.Phys Lett.*, 69, 275, 1980.
13. M.L Sage and J Jortner. *Adv. Chem. Phys.* 47,293,198.
14. Y.Mizugai and M.Katayama. *J. Am. Chem. Soc.*, 102, 6424, 1980.
15. T.M.A Rasheed, *Spectrochimica Acta.*, 52A, 1493,1996
16. Unpublished results by co-workers

CHAPTER 6

Microwave and laser Raman spectroscopy of o-chlorotoluene

6.1 Introduction

The Microwave spectrum of o-chlorotoluene $C_6H_4CH_3Cl$ in its vibrational ground state has been studied earlier [1]. The spectra due to both isotopes species ^{35}Cl and ^{37}Cl were reported[1] Later the study was extended to include the excited torsional states of the molecules and from the intensity ratio of microwave line the torsional frequency is reported to be 163 ± 13 cm^{-1}[2]. No low lying vibrational levels were reported from infrared or Raman spectra in order to compare the results obtained by microwave spectra. Hence, the Raman spectra were recorded on a Ramalog Raman Spectrometer. A comparison of the low-lying vibrational data obtained by Raman spectra and microwave, which were not reported earlier, has been investigated here.

No pure vibrational data in the low vibrational modes of o-Chlorotoluene were available in the literature. However, a two-photon ionization and pulsed field ionization absorption spectra are reported by Richard *etal.*[3]. They have also used a HF/6-31G* level *ab* initio calculation to estimate the potential barrier hindering internal rotation of methyl group in the molecule. This study gives a one to one correspondence between microwave and vibrational spectrum of low lying vibrational states in o-chlorotoluene.

6.2 Experimental Details

The experimental details to obtain the microwave spectra are discussed in references [1,2]. The microwave spectrum was recorded at the University of Ulm,Germany. The rotational structures due to at least four vibrational states are clearly seen in the microwave spectra. A typical microwave spectrum is shown in Fig.1. The frequencies of these transitions in different vibrational levels are given in Table 6.1.

The frequencies are arranged in the descending order of the intensities. The v =1 state is believed to be the first torsional state of the molecule and a barrier height of 564 ± 34 cm^{-1} is reported by us from the microwave intensity ratio. The value reported by Richard *etal.* [3] is 481cm^{-1} In order to obtain the vibrational frequency directly as a comparison to the microwave data in Tab.1, the Raman spectrum was needed. The Raman spectrum is recorded on a Ramalog Raman spectrometer with argon ion laser as the source. The spectrum is shown in Fig.6.2.

6.3 Results and Discussion

Even though the torsional frequencies arising at v =1 state could be determined from the microwave intensities of the unsplit lines, a direct calculation of vibrational frequencies from the microwave intensity was difficult for v = 2, 3, 4 states. However the observed rotational lines for v = 1, 2, 3 and 4 states are believed to be the frequencies of modes given in Tab. 2, which are observed in the Raman spectrum. The torsional vibrational frequency can be estimated from the relation [4].

$$I_v = I_o\, e^{-hv/kT}$$

where I_v is the intensity of the first excited state and I_o is that of the ground state.

The ratio measured from unsplit lines $9_{18} \leftarrow 8_{17}$ and $12_{2,\,10} \leftarrow 11_{2,\,9}$ which were free from nuclear hyperfine interaction s plitting is 0.38 and the frequency corresponding to excited torsional state is calculated to be 163 cm^{-1} with an estimated error of 13 cm^{-1} [2]. The Raman spectrum obtained shows absorption at a frequency 168 cm^{-1}, which is in good agreement with the reported frequency corresponding to the first excited torsional state. The other excited frequencies obtained from the present study are given in Tab.2.

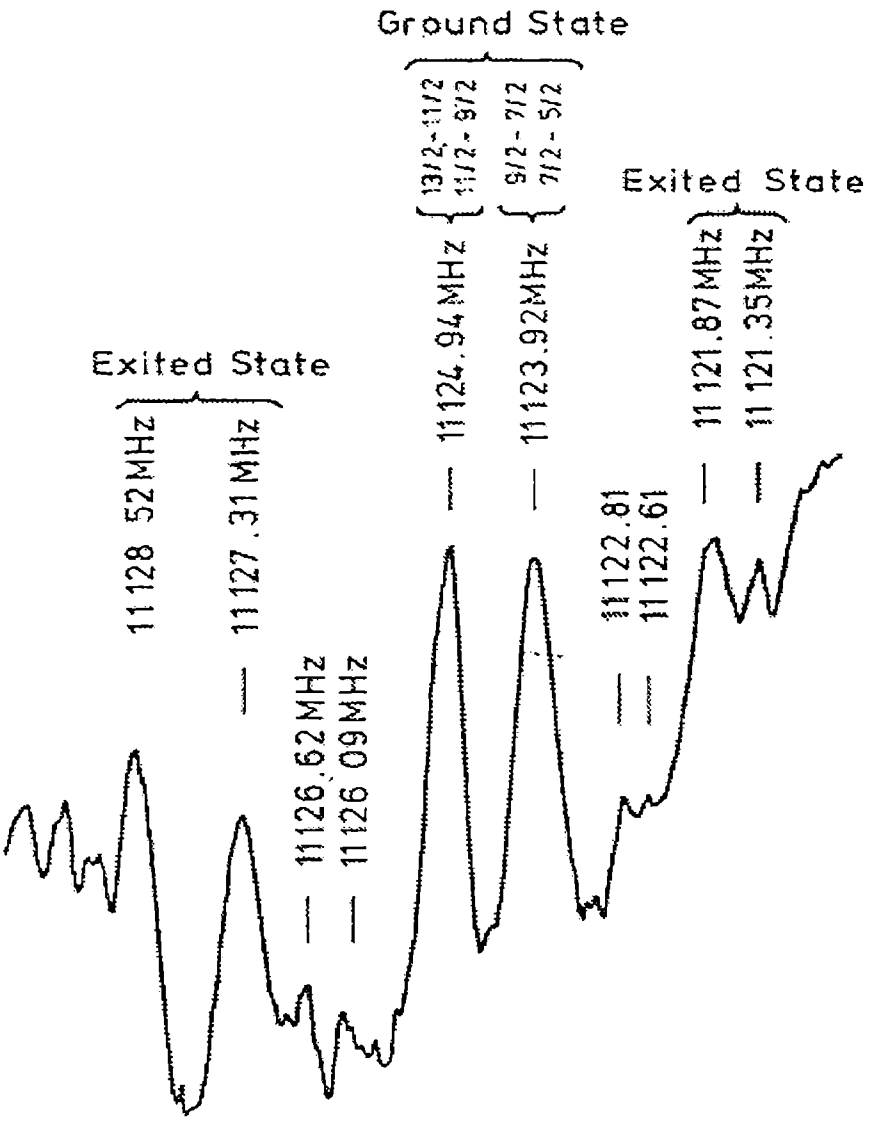

FIG-1· Microwave Spectrum of Orthochlorotoluene ^{35}Cl

$S_{0\ 3}-4_{0\ 4}$ transition Hfs

Table 6.1. Hyperfine frequencies observed in $J = 5_{0\,5} \leftarrow 4_{0\,4}$ transition at different vibrational states $\nu = 0$ to $\nu = 4$ (Frequency in MHz)

Hyperfine components	Vibrational states				
$F' \leftarrow F''$	$\nu = 0$	$\nu = 1$	$\nu = 2$	$\nu = 3$	$\nu = 4$
13/2←11/2	11124.94	11128.52	11121.87	11126.62	11122.81
11/2←9/2	11123.92	11127.31	11121.35	11126.09	11122.61

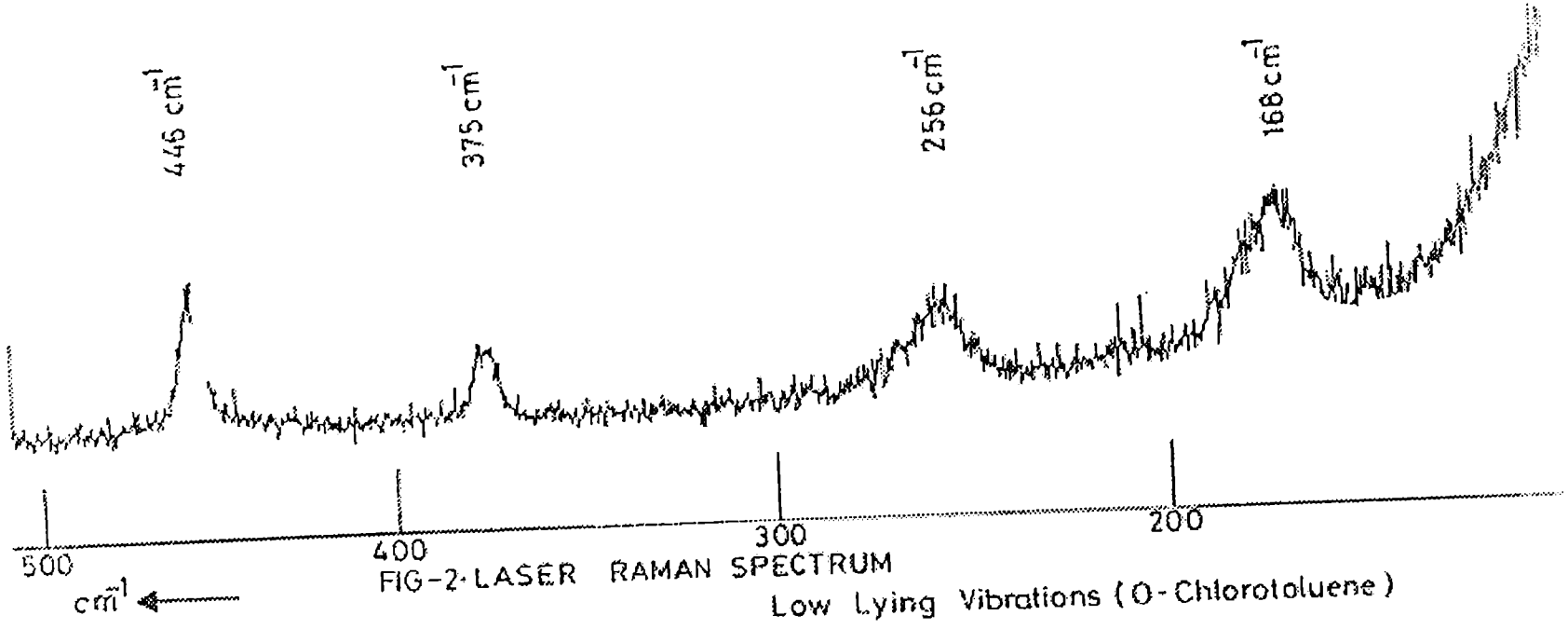

FIG-2-LASER RAMAN SPECTRUM
Low Lying Vibrations (O-Chlorotoluene)

Table 6. 2. Low lying vibrational modes in o-chlorotoluene

Frequency (ν) cm^{-1}	Assignment	
168	CH_3	torsion
256	C-C	o p bending
375	C-Cl	i p bending
446	C-C-C	i p bending

References

1 Nair KPR & Epple K, *Chem Phys Lett*, 166, 146, 1990.

2 Nair KPR, *J Molecular Structure.*, 477, 251, 1999.

3 Richard Erik C, Walker A Robert & James C Weisshaar *J. Chem. Phys*, 104, 4451, 1996.

4 Gordy W & Cook R.L, *Microwave molecular spectra*, (Wiley, New York), 1984.

Summary and conclusions

The major application of Tunable Diode Laser (TDL) is high-resolution recording of vibrational rotational spectra of molecule in the gas phase. Diode lasers have high spectral brightness and are coherent devices. These features allow the use of Tunable Diode Laser for long path length measurements, with high degree of spatial resolution. The most important property of Tunable Diode Laser is the probability of considerable emission frequency tuning with operating conditions changed. In measurements of trace gases by laser absorption spectroscopy, the absorption signal strength is proportional to the product of oscillator strength of the absorption transition and the number of molecules in the path of the laser beam. Hence at very low concentrations, long path length is required for generating detectable absorption signals. The effective path length can be increased by using multi pass cell. The multipass optical system limits the beam divergence and provides large path length and facilitates operation at low pressure and thus broadening of spectral lines can be avoided.

In the present work we have constructed and calibrated successfully a high-resolution spectrometer using tunable diode laser and a long path length cell. The source used in the present setup is a tunable diode laser (Model no.6321, New Focus Inc.) The maximum output power is up to 15 mW The tuning laser tuning range is from 935nm to 975nm. The sample holder is a multipass cell of 36m effective pathlength. The detector used in this set up is Nirvana Model 2017 new Focus Inc. The photo receiver consists of two photodiodes designated as signal and reference. This detector enables traditional balanced detection. In the balance mode the linear output provides a voltage proportional to the difference between the photocurrents of the signal and reference diodes. It also provides auto balance detection with zero DC voltage and noise suppressed AC signal proportional to received signal optical power. In this state the detection automatically balances the photocurrent from signal and reference diodes. The log output at auto-balanced state provides a convenient measurement of absorption

present in the signal path. Using the above setup highly resolved spectrum -OH group of methanol is recorded and the P, Q and R branches were identified.

The near infrared region has been recognized as a prime area for the analysis of overtone and combination bands associated with hydrogenic vibrations. The nature of the individual bond oscillator has been revealed through the study of the near infrared and visible absorption spectra in polyatomic molecules. The X-H (X= C, O, N...) stretching vibrations are anharmonic to a greater extent than the stretching vibrations between two heavy atoms. The local mode model is a powerful tool for the treatment of high energy (> 8000 cm^{-1}) CH stretching overtone spectra. The positions of overtone band maxima, corresponding to a single type of CH bond fit the equation for a diatomic a harmonic CH oscillator. i.e. $\Delta E = w_{CH} V + X_{CH} V^2$ where w_{CH} is the local mode frequency in cm^{-1}, X_{CH} is the diagonal local mode anharmonicity constant, and ΔE is the frequency in cm^{-1}, at the band maximum of the V^{th} overtone. The local mode parameters depict the nature of bond strength and the local physical environment of the CH oscillators. The localized nature of CH stretching overtones indicates that changes relative to a parent molecule reflect the nature of substituent effects

NIR spectra of following compounds were analyzed using local mode approach. ortho and meta chlorotoluene, meta and para fluorotoluene, ortho, meta and para nitrotoluenes, ortho, meta and para hydroxytoluene (cresol) and 1-naphthol.

Local mode parameters, mechanical frequencies and anharmonicity constants of the local oscillators in each molecule were calculated. Additivity of substituent effects in ortho and meta chlorotoluenes were verified using Nakagaki and Hanazaki model.

In nitrotoluene, the methyl group offers steric inhibition to its ortho substituent and consequently the electron withdrawing effect of nitro group is decreased at ortho

position compared to other two isomers. Thus it is confirmed that the steric hindrance offered by the methyl group outweighs the resonance withdrawal by ortho nitro group.

The -OH group is a ring activator and a typical ortho, para director. Alkyl substitution also acts as an electron donor to the ring. It is observed that in cresols the donation by the alkyl group at meta position is lower compared to ortho or para substitution.

The CH oscillators in naphthalene and biphenyl are reported to have a higher mechanical frequency than that of benzene. CH oscillators in α- naphthol is expected to exhibit the same property. However, it is observed that the mechanical frequency decreases from that of benzene. This change in the frequency may be because of the intra-molecular interaction of hydroxyl group and aromatic nucleus in α- naphthol.

Comparative analysis of the microwave and laser Raman spectrum of o-chlorotoluene is done. The microwave spectrum of o-chlorotoluene $C_6H_4CH_3Cl$ shows distinct rotational structures due to four excited vibrational states over and above the ground state spectrum. The vibrational frequency calculated from the relative intensities of the ground and first excited states in the microwave spectra is identified in the laser Raman spectra and is assigned as the first torsional state of the molecule.

List of publications

1. Aryl CH and OH overtone spectra of 1- naphthol. Evidence for the intramolecular interaction in 1-naphthol
   Shibu M.Eappen, S. Shaji, and K.P.R Nair,
   A. J. of Spectroscopy, 2, 2002, 89
2. Microwave and Laser Raman Spectroscopy of o-chlorotoluene
   K.P.R.Nair and Shibu M Eappen
   Indian Journal of Pure and Applied Physics 39, 2001, 750
3. Application of Nakagaki and Hanazaki model in the aryl CH overtone spectra of liquid phase o-chlorotoluene and m-chlorotoluene
   Shibu M.Eappen, R Rekha S. Shaji, T.M.A Rasheed and K.P.R Nair
   Asian Journal of Physics, 11 No1 , 233, 2002
4. Overtone spectrum of cinnemaldehyde in the NIR region-evidence for the indirect lone pair trans effect
   K.K Vijayan, Sunny Kuriakose, S.Shaji, Shibu M.Eappen, K.P.R Nair and T.M.A Rasheed
   A.J. of Spectroscopy 5, 185,2001
5. Overtone spectrum of formamide in the near infrared region-evidence for the inhibition of lone pair trans effect
   Sunny Kuriakose K.K Vijayan, Shibu M. Eappen, S.Shaji, K.P.R Nair and T.M.A Rasheed
   A.J. of Spectroscopy 6, 43,2002
6. TDL high resolution spectrometer instrumentation – highly resolved spectrum of methanol in the transition region $\Delta v=3$
   Shibu M Eappen. S.Shaji, T.M.A Rasheed and K.P.R Nair
   Communicated to *JQSRT*

Seminar

1. High-resolution spectrometer instrumentation- rovibrational spectrum of H_2O in the region $\Delta v=3$

   S.Shaji Shibu M Eappen, T.M.A Rasheed and K.P.R Nair,

   19th Austin Symposium on molecular Structure, Austin Texas, March 2002

2. Application of Nakagaki and Hanazaki model in the aryl CH overtone spectra of liquid phase o-chlorotoluene and m-chlorotoluene.

   Shibu M.Eappen, R Rekha, S. Shaji, T.M.A Rasheed and K.P.R Nair

   National Symposium on Lasers, Spectroscopy and Laser Applications, 27- 30th December 2001 Meerut

3. Aryl CH overtone Spectrum of liquid phase N, methyl aniline and N,N di-methylaniline – A conformational structural analysis using local mode model

   Shibu M.Eappen, Venketeswara Pai. R, S. Shaji, Sunny Kuriakose, K.K Vijayan K.P.R Nair and T.M.A Rasheed

   National symposium on Atomic Molecular Structure, interactions and Laser Spectroscopy, 22-24 February 2002, Banaras Hindu University, Varanasi

4. Tunable diode laser high resolution spectrometer

   K.P.R.Nair, Shibu M Eappen, S. Shaji, T.M. A Rasheed

   Proceedings of the National Symposium on Photonics and Spectroscopy 14- 16th March 2001, Raman School of Physics, Pondicherry University